# NMR STUDIES OF HUMAN AND BEEF TISSUES

By

WALTER HAYWARD LIPKE

Bachelor of Science

University of Tulsa

Tulsa, Oklahoma

1964

Submitted to the Faculty of the Graduate College
of the Oklahoma State University
in partial fulfillment of the requirements
for the Degree of
MASTER OF SCIENCE
July, 1968

# NMR STUDIES OF HUMAN AND BEEF TISSUES

Thesis Approved:

E. C. Kohnke
Thesis Adviser

Thomas L. Hunter

K. D. Berlin

D. D. Durham
Dean of the Graduate College

ACKNOWLEDGMENTS

The author wishes to express his gratitude to Dr. V. L. Pollak for his guidance in the study. Particular thanks is expressed to Dr. T. E. Walters who made possible the supply of beef samples. In expression of appreciation for their contribution to the study is made to Dr. G. W. Newell who supplied the chicken samples and to Dr. R. J. Miller for the fish sample. The author is indebted to Bill Melton for his answering of many questions and especially for his keeping the equipment in good working condition. Gratitude is certainly due those people who volunteered to be the subjects for the human arm measurements. They are: Mary Lou Bravo, Dennis Singer, Nancy Wyhof, James MacInerney, Carolyn Stover, Nancy Roesch, Bill Steckelberg, Patti Goodrich, and Peggy Lipke.

The author is most grateful to Dr. K. D. Berlin, Dr. L. M. Raff, and Dr. E. E. Kohnke for their personal interest and their contribution to the production of the thesis. These three gentlemen took over the responsibilities of the thesis advisors upon Dr. Pollak's departure from O.S.U.

Financial support administered by the American Chemical Society and made available by the Petroleum Research Fund is gratefully acknowledged.

TABLE OF CONTENTS

## LIST OF TABLES

LIST OF FIGURES

LIST OF FIGURES (Continued)

LIST OF FIGURES (Continued)

# CHAPTER I

## INTRODUCTION TO NMR STUDIES OF MUSCLE

As stated by J. A. Jackson and W. H. Langham (1) in their paper, there have been a number of applications of low field NMR to various theoretical and experimental interests, such as measurement of the nuclear polarization of a gas (2), and there have been a number of applications of high-field NMR to biology (3). Apparently though there has been no application of low-field NMR to biology, with the exception of Jackson and Langham's work and the work by T. Ligon (4).

The initial work at Oklahoma State University in this research area was done by Tom Ligon. Ligon made measurements on human arms using the earth's field free precession technique. The measurements made were for the determination of $T_2$ and the field dependence of $T_1$. It was hoped that these experiments would give an indication as to whether the models for the $T_1$ and $T_2$ relaxation[1] presented by Bratton, Hopkins, and Weinberg (5) in their paper, "Nuclear Magnetic Resonance Studies of Living

---

[1] $T_1$ is termed the "longitudinal relaxation time". $T_1$ is proportional to the reciprocal of the rate at which the component of the magnetization parallel to the applied magnetic field approaches its Curie value. $T_2$ is termed the "transverse relaxation time". $T_2$ is proportional to the reciprocal of the rate at which the component of the magnetization perpendicular to the applied field approaches its Curie value (which is ordinarily zero).

Muscle," were adequate for handling the human arm data.

Bratton, Hopkins, and Weinberg proposed a model which described a limited amount of data obtained from the gastrocnemius muscle of the frog. The ideas which are incorporated in this model are the following:

1) Water exists in two states, the bound and the unbound. The bound or solid-like water has a correlation time much longer than the Larmor period. Unbound or liquid-like water has a correlation time much shorter than the Larmor period. The exchange rate between these two phases is hypothesized to occur at a faster rate than the relaxation rates for any given phase; thus, the model will only explain data which is exponential[2].

2) $T_2$ increases when the muscle is isometrically contracted.

3) The increase of $T_2$ plus other experimental data suggest that a fraction of the intracellular water molecules have a restricted rotational freedom and that this fraction decreases when contraction occurs.

4) Part of the bound water appears to be freed reversibly during the isometric contraction and irreversibly in death.

5) $T_2$ has no dependence upon the field in which it is measured.

6) $T_1$ has a field dependence but there is no change in $T_1$ seen due to isometric contraction of the muscle.

---

[2]The term exponential data, or an equivalent term, means that for the $T_2$ measurements the signal amplitude is exponentially dependent upon the decay time, and for the $T_1$ measurements, the difference of the particular signal amplitude corresponding to the Curie value and the signal amplitude for various polarizing times is exponentially dependent upon the polarizing time. Thus, the meaning of the term non-exponential data should be obvious.

7) $T_1$ is greater than $T_2$, at least for the fields at which measurements were made.

Ligon's studies showed that the model of Bratton, Hopkins, and Weinberg was inadequate for describing the human arm data simply because the data plotted was not exponential. Ligon then hypothesized that the non-exponential behavior of the signal is due to the superposition of signals from fat and muscle of the arm. Much of the remainder of his work was pointed toward showing the validity of the argument. The research about to be presented takes up at this point.

In order to clarify the problem of studying proton relaxation in muscle, a broad outline of the environments of water in tissues is given. The two main constituents of muscle are water and protein with water comprising the major portion, approximately 80% by weight. Water may find itself in many environments, but principally there are two, extracellular and intracellular. Intracellular water makes up about 80% of the muscle water with the remaining 20% being extracellular; these composition ratios are kept constant by equilibrium action across a semi-permeable membrane. Summarizing by quoting from the thesis of T. Ligon (4): "The water molecule in muscle may find itself in a homogeneous phase outside of the muscle fibers, inside the cell in an inhomogeneous phase and influenced more or less strongly by association with protein."

The work which follows first had the objective to check the validity of Ligon's explanation for the non-exponential behavior of the signal by performing measurements on beef tissues. Upon observing that muscle and fat tissues, separately, had non-exponential signal characteristics, the problem became, to a large extent, a study of beef round. The study is essentially featured by the desire to demonstrate that the

sum of two exponentials model, which is used to analyze the data, is related in some way to the extracellular and intracellular waters.

## CHAPTER II

## THE MEASUREMENTS

The apparatus which was used for the greatest part of the measurements of $T_1$ and $T_2$ is an earth's field free precession apparatus. This apparatus will hereafter be referred to as an EFP apparatus. The signal from the sample as viewed by this apparatus is just bhe EMF generated in a coil by the precession of the proton magnetization about the earth's field; i.e. a 2.3 KHz decaying sine wave.

Two different techniques are used to obtain $T_1$ and $T_2$ data from the EFP equipment. One is the Sudden Passage technique (abbreviated by S.P.) and the other is the Pedestal Field technique (abbreviated by P.F.). The S.P. technique for the determination of $T_1$ requires magnetically polarizing the sample for a specified time ($t_p$). After the time $t_p$ has elapsed the coil current is suddenly cut off. The amplified EMF signal which represents the transverse component of the relaxing magnetization transverse to the earth's magnetic field may then be viewed after a time $\tau_1$ which is approximately the time for the "ringing" of the coils to decay into the noise level. The desired signal is also decaying during this time $\tau$, therefore, some of the signal for the short decay times is lost. If the signal is always viewed at the same decay time, then the free precession amplitude measured at several polarizing times yields data which allows the calculation of $T_1$ in the particular field

strength depicted by the polarizing current.

The S.P. method for obtaining $T_2$ data is somewhat similar. The free precession amplitude is measured at various time intervals after the coil current cut off. The calculation of the rate of this decay yields $T_2$. $T_2$ can be measured at only one value of the field, the value of the earth's field (about 0.5 gauss).

Whereas the Sudden Passage technique is used to measure $T_1$ in high fields from approximately 200 to 500 gauss, the Pedestal Field, or intermediate field, technique is used to obtain $T_1$ at low fields from approximately 100 gauss down to 1 gauss. This procedure uses two fields before the current to the coil is shut off. The first field is large and is kept on long enough for the magnetization of the sample to have reached its Curie value. This field is then instantaneously removed with a smaller field replacing it. The cut off of this second field yields a signal amplitude from the sample, again, read at some decay time greater than $\tau$, which corresponds to the polarizing time of the smaller field. This polarizing time can be varied and thus other data points can be measured. As in the S.P. experiment, these data allow calculation of $T_1$ for a particular polarizing field.

To explain how values of $T_1$ and $T_2$ are obtained from the data measured by the S.P. and P.F. techniques, the envelope solutions to the Bloch equations (6) are needed. The solutions for the S.P. experiment are:

For longitudinal relaxation, the value of M(t) is given by the equation

1) $M(t) = M_\infty(1-e^{-t_p/T_1})$

where

$M(t)$ = the component of the relaxing magnetization parallel to the applied field,

$M_\infty$ = the Curie value of the magnetization for the particular field,

$T_1$ = the longitudinal relaxation time,

$t_p$ = the polarizing time, the length of time the polarizing field is "on."

For transverse relaxation, the value of $M(t)$ is given by the equation

$$2) \quad M(t) = M_o e^{-t_d/T_2},$$

where

$M(t)$ = the component of the magnetization transverse to the earth's field.

$M_o$ = the component of the magnetization transverse to the earth's field at the instant of coil current cut off.

$t_d$ = the length of time after coil current cut off,

$T_2$ = the transverse relaxation time.

The value of $M_o$ cannot be directly measured on the EFP apparatus; however, it is not needed for the determination of $T_2$.

The solution for longitudinal relaxation for the P.F. experiment is:

$$M(t) = M_\infty + (M_1 - M_\infty)e^{-t_p/T_1},$$

where $M_\infty$ is the Curie value for the pedestal field and $M_1$ is the Curie value of the initial field.

It can thus be seen that the value of $M_\infty$ is needed for the determination of $T_1$. This is done by simply measuring the signal amplitude at a polarizing time ($t_p$) which is much larger than the relaxation time $T_1$. For some low pedestal fields the $M_\infty$ value is so low that it cannot be measured accurately. For these fields the $M_\infty$ value is calculated from a previously measured value for a higher field and the knowledge of the polarizing currents for each case, by the relation:

$$\frac{M_h}{M_1} = \frac{I_h}{I_1}$$

$M_h$ = the $M_\infty$ value measured at a high polarizing field,

$M_1$ = the $M_\infty$ value to be calculated, corresponding to a low polarizing field,

$I_h$ = the value of the current giving rise to the high field,

$I_1$ = the value of the current giving rise to the low field.

This may be done because by the Curie law the equilibrium magnetization is proportional to the applied field, and in turn for the coils used, the applied field is proportional to the coil current.

The data for all the experiments are reported in the form of semi-log plots. The S.P. determination of $T_1$ is the plot of $\log[M_\infty - M(t)]$ vs $t_p$ and for the P.F. method the plot is the $\log[M(t) - M_\infty]$ vs $t_p$. For the S.P. determination of $T_2$ the graph is $\log M(t)$ vs $t_d$. By manipulating algebraically the envelope equations given previously, it can

easily be seen that the slopes of these curves are related respectively to $T_1$ and $T_2$.

The methods described here are very general to the bulk of the measurements made. Additional methods which were employed will be discussed in the next chapter as the discussion of particular experiments arises; they will either be written into the context or will be written up as an Appendix.

# CHAPTER III

# THE EXPERIMENTS AND EXPERIMENTAL TECHNIQUES

## Initial Experiments

The treatment for all of the beef samples was essentially the same. The samples were obtained from the Oklahoma State University Meat Laboratories approximately 10 days after slaughter. The meat had been chilled and stored for these 10 days at -4.4°C; this is standard procedure for meat suppliers.

The samples were chunks of tissues which were placed in 500 ml Nalgene containers and sealed. When the samples were not in use, they were stored at 4°C. It was felt that storage at low temperatures would inhibit bacteria growth and any aging effects which might occur. Non-freezing temperatures were used because it was not known if there would be some additional affects introduced by freezing and thawing.

The first experiments were those on beef round, fat, and liver. $T_2$ measurements in the earth's field and $T_1$ measurements for various polarizing fields in the range from 1 through 500 gauss were made on each sample. These measurements were all taken using a set of coils which will be referred to as Coils #1.

The property Coils #1 has in preference to an alternate set, referred to as Coils #2, is that the initial transient which masks the wanted signal fades into the level of the system's noise at an earlier

time than does the transient when Coils #2 is used. This was deemed a necessary requirement for the $T_2$ decay so that the data for short decay times could be obtained[1].

The temperature was not controlled for the measurements on the first samples. Because of this and because of the amount of scatter in the data for the first samples, the $T_1$ field dependence and $T_2$ measurements were repeated using freshly obtained samples of beef round. The temperature for these experiments was kept at $25 \pm 2^{\circ}C$.

Some additional experimental technqiues were employed for these measurements so that a greater number of points could be obtained for each graph of the $T_1$ and $T_2$ data. Only Coils #2 in its high Q state was used to make the $T_1$ measurements. Coils #1, and Coils #2 (in both its high and low Q states) were used to obtain the $T_2$ decay. Coils #1, and Coils #2 (low Q) were used to obtain the "initial" portion of the decay,

---

[1]The paragraph needs further clarification because of the construction of Coils #2. The tuning box for Coils #2 (each set of coils has its own tuning box) has a switch which connects and disconnects a resistor in parallel with the coils, thus making possible the option of having Coils #2 in a high or low gain state, i.e., high or low Q. The previous discussion of Coils #1 and #2 is valid only when the Coils #2 is used in its high Q switch position. When Coils #2 is in its low Q state, it has virtually the same properties that Coils #1 has, except that Coils #1 has a slightly larger signal-to-noise ratio due to a higher polarizing field.

while Coils #2, with its added gain in the high Q state, was used for the "tail" portion of the decay.

To construct a composite graph of the $T_2$ data from the three coil configurations requires a method of correlating all of the data. A treatment explaining how this was accomplished is given in Appendix C.

Another technique will now be explained regarding the determination of the signal amplitude for the $T_2$ decay at the decay time equal to zero. The method uses both a high resolution NMR apparatus, the Varian A-60, and the earth's field free precession apparatus. The high resolution apparatus is used to determine the value of the water equivalence of the sample. The water equivalence is defined to be the ratio of the signal amplitude from a meat sample to the signal amplitude of a water sample at the decay time equal to zero, when the two samples have equal volumes. That is, the water equivalence, E, is:

$$E = \frac{(A_s^v/V_s^v)}{(A_w^v/V_w^v)} = \left(\frac{A_s^v}{A_w^v}\right)\left(\frac{V_w^v}{V_s^v}\right).$$

The symbol A is the value of the spectrum integral from the Varian A-60, the symbol V is the volume of sample in the Varian tube, the superscript v refers to the measurements associated with the Varian A-60, the subscript s refers to the meat sample, and the subscript w refers to the water sample. The same symbols will occur at a later time except with the superscript e which refers to measurements associated with the EFP apparatus. The symbols will have the same meanings as described above, except for the A which will mean the amplitude at t = 0.

The ratio A/V is proportional to the number of signal-giving protons per unit volume and has a characteristic value for each kind of

sample. This value for water is determined using the EFP apparatus by simply measuring the volume of the water and finding the initial amplitude of the signal by extrapolating the $T_2$ decay curve to t = 0. Thus, if the volume of the meat sample can be measured, then its signal amplitude at the decay time equal to zero can be calculated by using the following equation:

$$A_s^e = E\left[\frac{A_w^e}{V_w^e}\right]V_s^e .$$

There are some experimental difficulties in this method of determination of $A_s^e$ which need to be described. First, E is not easily determined because of the difficulty of inserting a meat sample into a Varian A-60 sample tube without either "packing" the sample specimen or leaving air spaces. This difficulty is circumvented by using a "coring" method described by Sussman and Chin (7).

A second problem is determining the value of $V_s^e$. There is some skepticism about whether this can be done accurately or not. A way to eliminate this measurement is to multiply through the equation for $A_s^e$ by the unity factor $(\rho_w\rho_s/\rho_w\rho_s)$, where $\rho_w$ is the density of water and $\rho_s$ is the density of the meat sample. This yields the equation:

$$A_s^e = E\,\frac{\rho_w}{\rho_s}\,\frac{A_w^e}{V_w^e\,w}\,V_s^e\,\rho_s$$

or,

$$A_s^e = E^*\,\frac{A_w^e}{W_w^e}\,W_s^e,$$

where the symbol W means weight. E* is the water equivalence by weight, which is given by the equation

$$E^* = E\frac{\rho_w}{\rho_s} = \frac{A_s^v}{A_w^v}\frac{V_w^v \rho_w}{A_s^w \rho_s}$$

$$E^* = \frac{A_s^v}{A_w^v}\frac{W_w^v}{W_s^v}.$$

From this alternate form for $A_s^e$ it is seen that, besides the various amplitude terms, only the weights of the sample need to be measured. This can be performed easily with good precision.

Using the previously described method to find the signal amplitude at $t_d = 0$ was thought to be a necessity because of the non-exponential behavior of the observed signal. In other words, it is not certain that the semi-log graphical plot of the non-exponential data could be simply extrapolated back to $t = 0$ because the behavior of the signal in the period of time $\underline{t}$ during which the signal is masked by the switching transient is not known.

After experiments on the second beef round sample were performed, the measurements of the $T_1$ and $T_2$ data were repeated with the exception of the $t = 0$ point for the $T_2$ decay. The experiments on sample #2. The sample during this interim period between measurements, was stored at $4^oC$.

The purpose of the repeated experiments was to investigate the accuracy and reproducibility of the various measurements. The seeming scatter in the previous measurements was always large regardless of the

coil technique used. It was hoped that the additional effect of aging would not complicate the analysis of these data.

## Separated Liquid and Solid Samples

It had been observed for some time that fluid separated from the solid portion of the muscle samples. Therefore, it was thought that the signal components which make up the non-exponential graphical results are: 1. The protons in the separation fluid, and 2, the protons in the actually bound water of the solid portion of the sample.

To test this hypothesis the following experiment was performed. The liquid and solid portions of two different samples of beef round (sample #2) were separated. This was accomplished by allowing the sample to sit in covered breakers at room temperature for approximately 48 hours; the fluid which formed was drained out. Then, for each of these samples, measurements were made for the determination of $T_2$ and the construction of the graph of the dependence of $T_1$ on the field. It was anticipated that the relaxation times obtained from these separated samples would compare favorably with the relaxation times for the initial and tail portions of the semi-log plots for the last experiments performed on sample #2 in its whole state.

## Aging Experiments

The effect of the aging of the samples had not been specifically studied, but the effects had been deduced via some comparisons. It was noticed that after a period of storage time the graphical results of an experiment, either $T_1$ or $T_2$, showed that data could be obtained over a

larger range of polarizing and decay times then when the measurements on the samples were first made.

To check this observation, it was decided to make measurements to determine if an aging effect existed. First, beef round from a freshly slaughtered animal was obtained. The meat was allowed to cool down to 25°C and the measurements were begun. The measurements taken at various intervals after slaughter were $T_1$ measurements at B equal to 265 gauss and $T_2$ in the earth's field. During the periods of time between measurements the sample was allowed to remain at room temperature. It was thought that aging would occur more rapidly at room temperature and that as a result the effects would be more noticeable. Again, the sample was kept in a sealed container.

## High Field Experiments

The experiment to determine the water equivalence of beef round has been discussed previously. It will be recalled from the experiment involving the Varian A-60 apparatus. Besides the integrals, the absorption curve for beef round was also measured. The spectrum obtained (Figure 19) is a single symmetrical peak which looked as if it could be Lorentzian in shape. If the spectrum does have a Lorentzian shape, this would indicate that there is a single relaxation time in this high field strenght[2].

To determine if the curve was Lorentzian or not, a method was devised to construct a Lorentzian curve of the proper size. It was

---

[2] $\nu = \gamma H$, where $\gamma$ is the gyromagnetic ratio for protons. $\gamma$ is equal to 4.3 kilocycles/sec per gauss. Therefore, since $\nu = 60 \times 10^6$ cycles/sec., then $H = \nu / \gamma$, which is approximately 14,000 gauss.

reasoned that if the calculated points from this constructed equation overlayed the actual absorption curve, then the absorption curve could be considered Lorentzian shaped. The method for constructing the curve is given in Appendix D.

Independently, measurements on beef round were made using a spin-echo apparatus to determine if at high fields (14,000 gauss) there is a single relaxation time. The spin-echo apparatus uses small samples, which like the Varian A-60, are placed in tubes. The "coring" technique (7) referenced earlier was again used to insert the beef round into the sample tubes.

The samples for the spin-echo measurements were handled, by necessity, somewhat differently than the one used for the Varian measurements. The spin-echo sample was packed in an ice bath in a thermos and was shipped to Cleveland, Ohio, for measurements, whereas the Varian sample was measured immediately after it was obtained. Dr. V. L. Pollak at Case-Western Reserve University made the measurements.

## Human Arm Experiments

Nine persons volunteered for the experiments; all were in the age group of from 20 to 26 years. Six are female and three are male. The nine subjects were selected by their arm size. The coils have an inner diameter of only 3 inches; this is a fairly strict requirement, especially when selecting a male subject. Thus, the greater number of female subjects is explained.

Two subjects, #1 and #9, were used to obtain data for the field dependence of $T_1$, and all were used for the $T_2$ measurements. Many of the same techniques and methods were used to make the measurements as

had been used for the previously described beef experiments. However, before the measurements could begin, two experimental problems required solution. One was the problem of insulating the forearm from the coil, and the other was the problem concerning the increased noise level when the arm was in the coil. Both of these problems had extremely simple solutions. Insulating the arm from the coil was accomplished by having the subject wear a shoulder length rubber sleeve. The noise problem caused by the arm is nearly eliminated by grounding the person's arm while it is in the coil.

# CHAPTER IV

## ANALYSIS AND RESULTS

The data for all the experiments about to be discussed were analyzed in the same way. The exponential data were analyzed by the methods described in Chapter II. The non-exponential data were treated somewhat differently. The model chosen to analyze these non-exponentials graphs is a simple one. It has two signal-yielding components. The assumption is made that no exchange of protons occurs between proton sites which yield the components. The mathematical model is then represented as the sum of two exponentials. This model has the advantage over some others in that it is able to describe the graphical results completely, yet it has only four undetermined quantities which can be obtained by a graphical analysis. This graphical method rather than being discussed here is given in Appendix A. An adjoining appendix, Appendix B, is written to discuss the errors caused by the graphical method.

Two additional items should be mentioned. The graphical results to be presented will have the following form. The data points will be represented by a symbol, generally a small circle, and a curve is drawn through these points. The two exponentials which fit the non-exponential data curve are also drawn on the graph. They will be, simply, two straight lines which have no data points represented. The symbolism used to indicate the four fitting parameters is the following: $^{1}T_{1}$,

${}^{s}T_1$, ${}^{l}T_2$, ${}^{s}T_2$, $f_l$, $f_s$. The symbols $T_1$ and $T_2$ (longitudinal and transverse relaxation times) have been defined previously and retain those definitions. The symbol f is defined to be a fraction of the total signal at $t_d$ or $t_p$ equal to zero. The small letters, l and s, which are used as both superscripts and subscripts have these meanings: l refers to the exponential having the longer relaxation time and s refers to the exponential having the shorter relaxation time.

## Initial Experiments

The first measurements made were those on beef samples. The samples chosen were beef round, fat, and liver. It was speculated that experiments on these samples could further bolster Ligon's statement (4) that the non-exponential behavior exhibited by the signal from human tissues was due to the superposition of signals from the muscle and fat portions of the arm. If what Ligon said was actually true, then each of the signal components, fat and lean, should yield a signal which has an exponential behavior.

However, there is an alternate solution. The non-exponential behavior for the signal from human arms could also be due to the fact that the behavior of each anatomically contributing component is non-exponential. This, for some cases, is what was actually found when measurements were performed on the beef samples.

For beef fat, data for measuring $T_1$, when graphed, was definitely seen to be non-exponential for all fields, as illustrated by Figures 1a, 1b, and 1c. And for data for the measurement of $T_2$, the graphed curve, Figure 1d, appeared to be exponential with quite a large amount

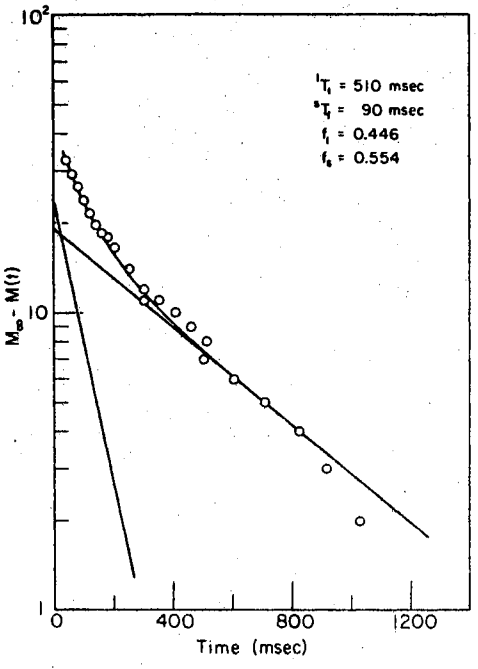


(a) $T_1$ Data @ 354 Gauss

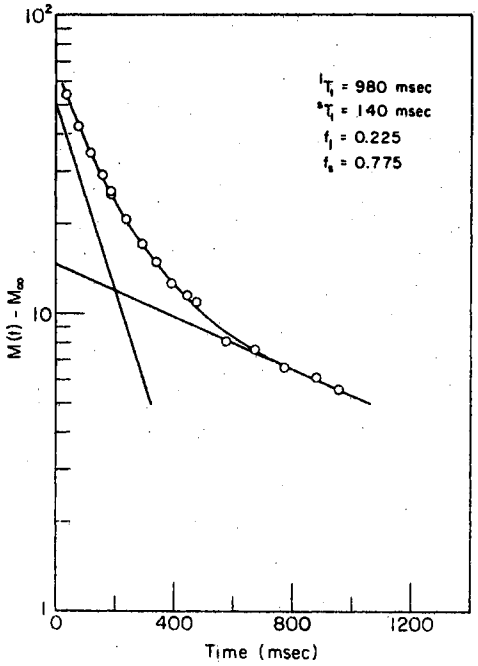


(b) $T_1$ Data @ 35.7 Gauss

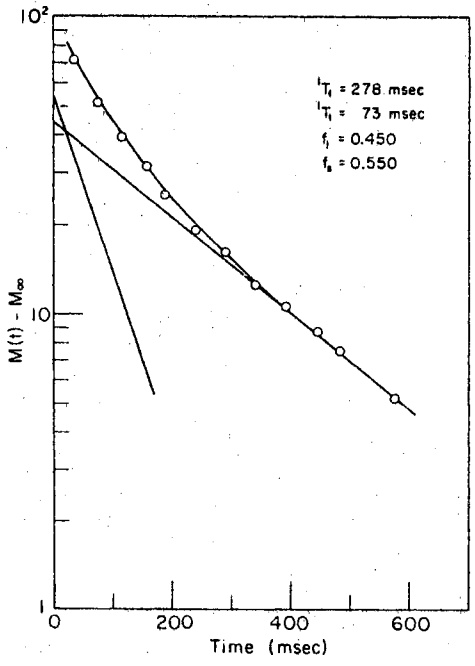


(c) $T_1$ Data @ 4 Gauss

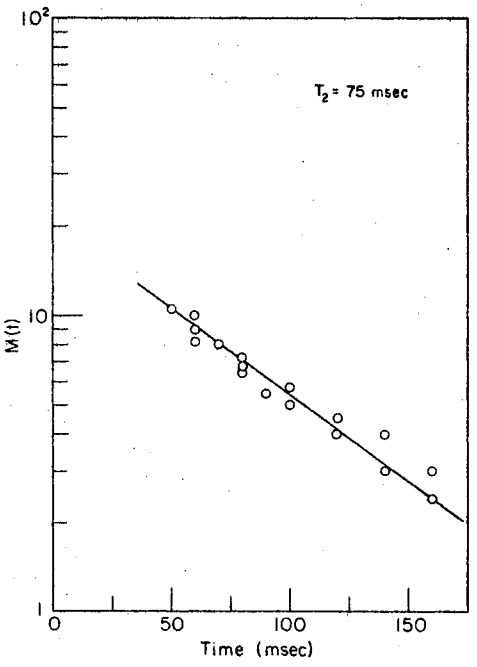


(d) $T_2$ Data

Figure 1. Typical Graphs of the $T_{1,2}$ Data for Beef Fat

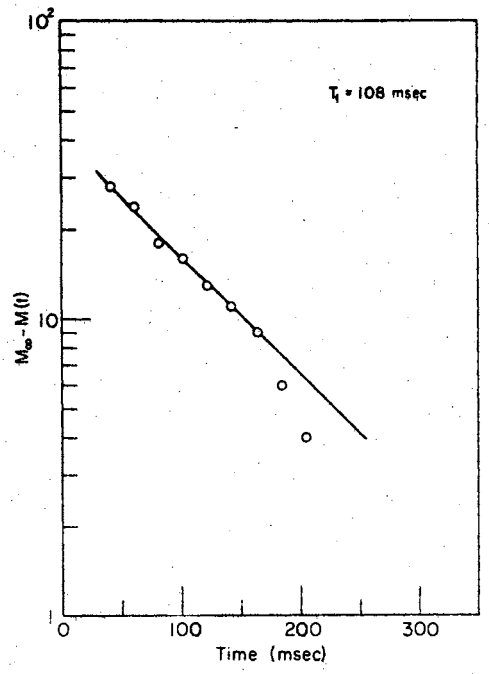


(a) $T_1$ Data @ 547 Gauss

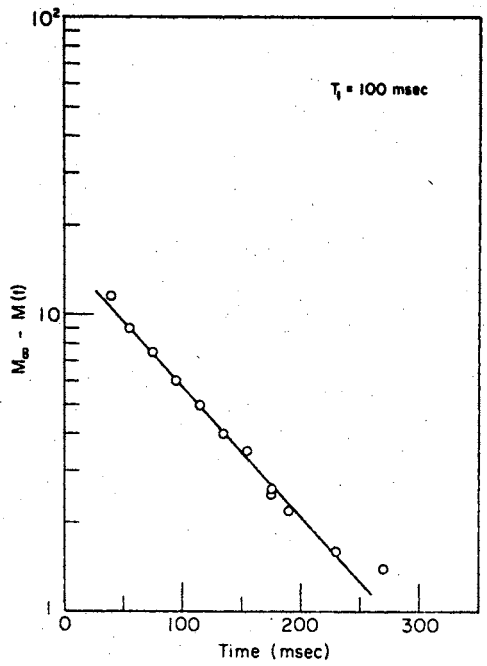


(b) $T_1$ Data @ 156 Gauss

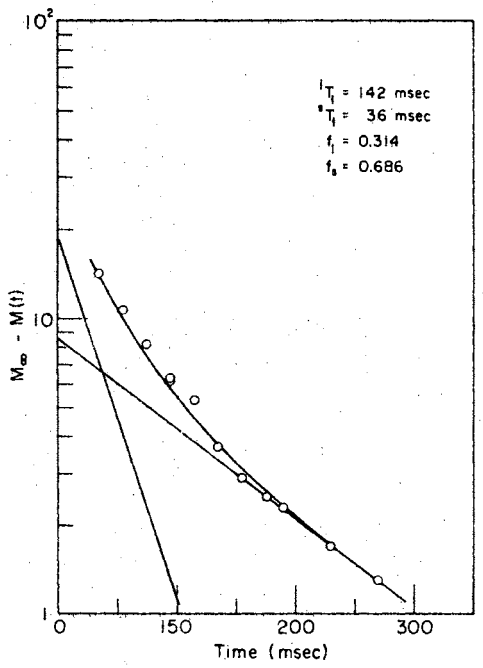


(c) $T_1$ Data @ 81.6 Gauss

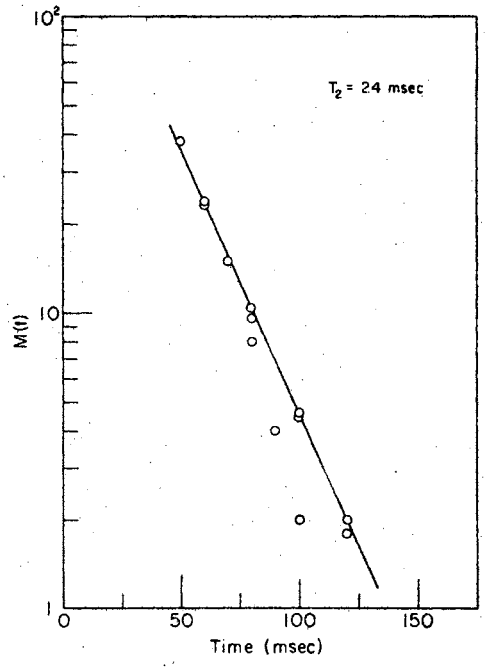


(d) $T_2$ Data

Figure 2. Typical Graphs of the $T_{1,2}$ Data for Beef Liver

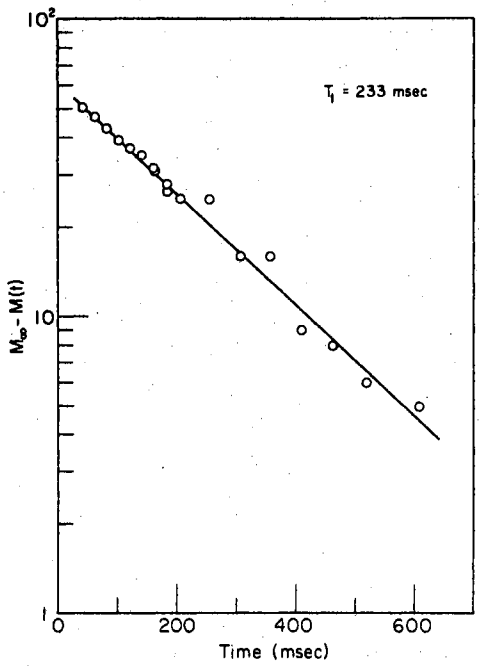


(a) $T_1$ Data @ 547 Gauss

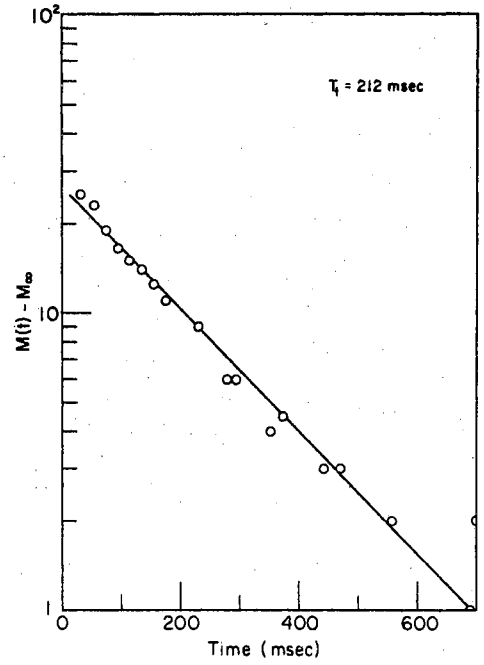


(b) $T_1$ Data @ 170.4 Gauss

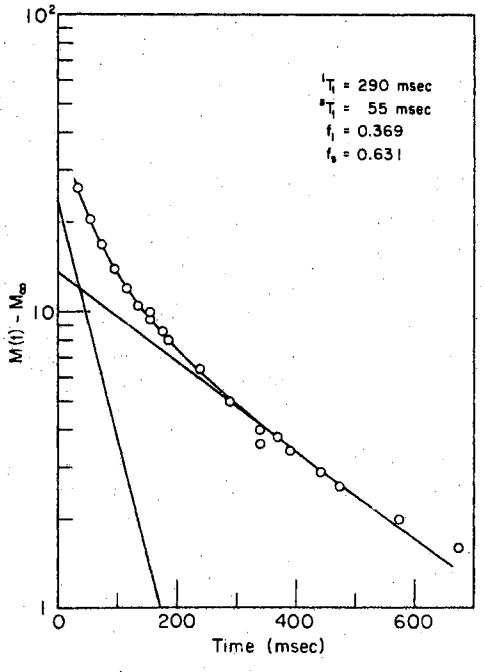


(c) $T_1$ Data @ 1 Gauss

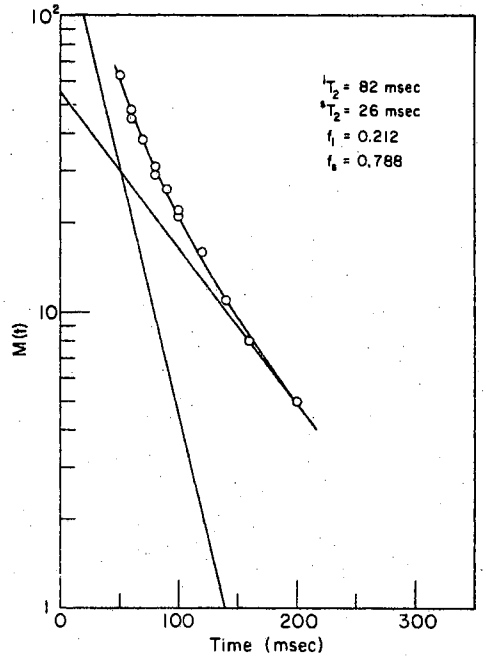


(d) $T_2$ Data

Figure 3. Typical Graphs of the $T_{1,2}$ Data for Beef Round

of scatter. The scatter is easily accounted for by the small signal to noise ratio obtained from fat, approximately one-fourth that obtained for an equal volume of water.

The graphical plots of the $T_1$ data, Figures 2a, 2b, 2c, for beef liver seemed to indicate that there is a transition from exponential to non-exponential behavior as the polarizing field is decreased. The graphs for polarizing fields larger than 156 gauss all appear as exponentials, and all graphs for B-fields less than 82 gauss look to be non-exponential. The graph of the $T_2$ data, Figure 2d, appeared to plot exponentially. There is, as for the fat, a large amount of scatter in the $T_2$ data.

The beef round data appears to have the same general characteristics as that for the beef liver. The beef round data, like the data for beef line, shows the exponential plots of $T_1$ data at high fields and the non-exponential graphs at low fields. The $T_2$ data graphs are non-exponential, which distinguishes the beef round from either the beef liver or fat. These data plots are given in Figures 3a, 3b, 3c, and 3d. One other distinguishing feature of the $T_2$ graph for beef round is that it is a smooth curve with seemingly very little scatter in the points.

The results obtained by the application of the "best fit" analysis to these first samples are summarized by Log $T_{1,2}$ vs Log B plots, Figures 4, 5, and 6, and by Tables I, II, and III, which list the values of the fitting parameters obtained for the sample when measured in a particular field strength. Figure 4 and Table I, which are information about beef liver, show that the ${}^{s}T_1$ and $f_1$ are fairly constant at ${}^{s}T_1 \approx 34$ msec and $f_1 \approx 0.35$ over the range of fields for which measurements were

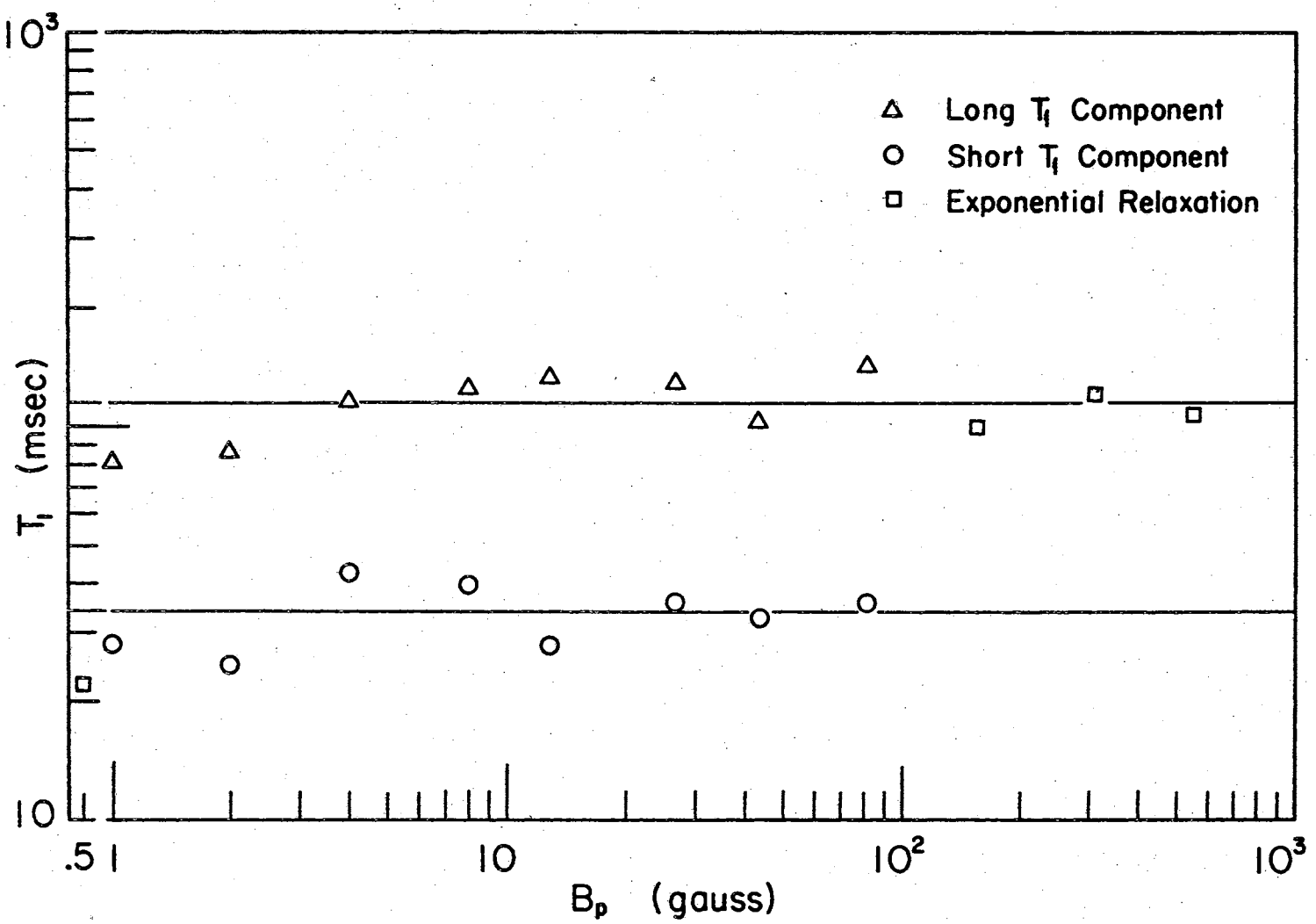


Figure 4. Log $T_{1,2}$ Versus Log B for Beef Liver

taken. The $^{l}T_{1}$ values have a somewhat greater variance than $^{s}T_{1}$ and $f_{l}$; the average $^{l}T_{1}$ value is approximately 115 msec.

TABLE I

FITTING PARAMETER VALUES FOR BEEF LIVER

| Field (gauss) | $^{l}T_{1}$ (msec) | $^{s}T_{1}$ (msec) | $f_{l}$ | $f_{s}$ |
|---|---|---|---|---|
| 547 | 108* | — | 1* | — |
| 312 | 122* | — | 1* | — |
| 156 | 100* | — | 1* | — |
| 82 | 142 | 36 | 0.314 | 0.686 |
| 44 | 102 | 33 | 0.569 | 0.431 |
| 27 | 128 | 36 | 0.327 | 0.673 |
| 13 | 133 | 28 | 0.332 | 0.668 |
| 8 | 126 | 40 | 0.372 | 0.628 |
| 4 | 115 | 43 | 0.359 | 0.641 |
| 2 | 87 | 25 | 0.233 | 0.767 |
| 1 | 82 | 28 | 0.493 | 0.507 |
| $T_{2}$ Data @ ½ gauss | 24* | — | 1* | — |

* : Exponential data plots were observed.

The parameters obtained for beef round show some variation from what was obtained for beef liver. The variation of the parameters for beef round with the magnetic field strength is given in Figure 5 and Table II. For the plot of Log $T_{1}$ vs Log B there seems to be a great

amount of scatter in the $^{l}T_1$, $^{s}T_1$, $^{l}T_2$, $^{s}T_2$ values. $^{l}T_1$ values appears to hover about the approximate value of 240 msec., while the $^{s}T_1$ value is fairly constant over the range of 1 to 30 gauss fields and then increases with the increase of field value. Looking at the lines which are drawn to fit most of the data points in Figure 5, it is seen that at the highest field for which measurements were made, the $^{l}T_1$ and $^{s}T_1$ values found from the lines which were drawn to fit the points of the graph are about equal. The point to be made is if $^{l}T_1$ and $^{s}T_1$ are actually close to being equal, the two components would be unreasolvable and would appear as a single exponential which is what was observed.

If the beef round data were the only data, then the above argument might be valid, but it is not the only data. The beef liver data contradicts the argument because for the non-exponentials observed the relaxation times for the two components appear for the beef liver to be fairly invariant over the range of fields.

One other unusual feature of the beef round data is that the values obtained for $^{l}T_2$ and $^{s}T_2$ are so much below those values found for low field $^{l}T_1$ and $^{s}T_1$. Theoretically, the low field values of $T_1$ should approximate the values obtained for $T_2$. The fact that $^{l}T_2$ , $^{l}T_1$ and $^{s}T_2$ , $^{s}T_1$ may possibly be explained by the imprecise method of making the measurements. The measurements of $T_2$ data were made at approximately room temperature, and then six days later the field dependence measurements of $T_1$ were obtained. The sample during this period of time was kept at 4°C, but still there may have been some effect due to the "aging" of the sample. When the field dependence measurements were

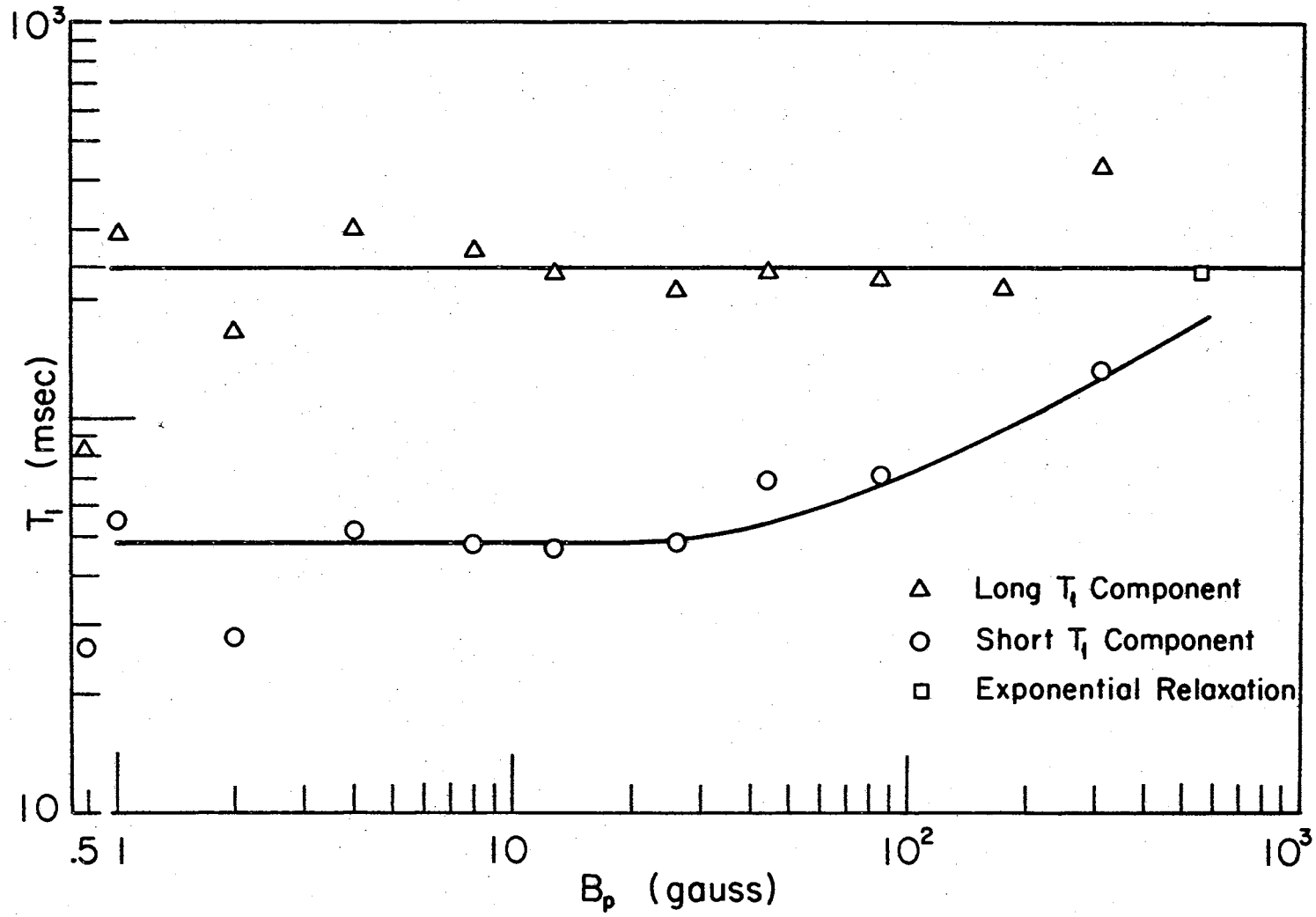


Figure 5. Log $T_{1,2}$ Versus Log B for Beef Round, Sample #1

made, the sample, after reaching room temperature, was simply placed in the coil and left until the measurements were finished. Effectively what is estimated to have happened is that the sample's temperature rose steadily from about 25°C to approximately 35°C.

From Table II it is observed that as the field is varied, there is seemingly a general trend towards lower values of $f_1$ as the field becomes smaller. At high fields the value of $f_1$ is approximately 0.5 and at low fields $f_1$ is approximately 0.3. There is scatter in this observation which was thought to probably be related to the measurements procedure discussed in the preceeding paragraph.

TABLE II

FITTING PARAMETER VALUES FOR BEEF ROUND (SAMPLE #1)

| Field (gauss) | $^1T_1$ (msec) | $^sT_1$ (msec) | $f_1$ | $f_s$ |
|---|---|---|---|---|
| 547 | 233* | — | 1* | — |
| 320 | 443 | 133 | 0.532 | 0.468 |
| 170 | 212* | — | 1* | — |
| 85 | 225 | 72 | 0.608 | 0.392 |
| 44 | 233 | 70 | 0.475 | 0.525 |
| 26 | 210 | 49 | 0.527 | 0.473 |
| 13 | 233 | 47 | 0.471 | 0.529 |
| 8 | 262 | 48 | 0.313 | 0.687 |
| 4 | 300 | 52 | 0.312 | 0.688 |
| 2 | 165 | 28 | 0.465 | 0.535 |
| 1 | 290 | 55 | 0.369 | 0.631 |

TABLE II (Continued)

| | | | | | |
|---|---|---|---|---|---|
| ($T_2$ Data) | 0.5 gauss | 82 | 26 | 0.212 | 0.788 |

* : Exponential data plots were observed.

The fitting parameters for the measurements on beef fat are illustrated by Figure 6 and Table III. From Figure 6 it is seen that both $^{l}T_1$ and $^{s}T_1$ increase slightly with increasing field. For $^{l}T_1$ the value appears to be constant at 300 msec. over the low field range up to about 10 gauss and then increases with a very large amount of scatter as the field increases. The $^{s}T_1$ values appear to be fairly constant, about 80 msec. over the same range of fields as were the $^{l}T_1$ values and then increase very slightly with a large amount of scatter as the field is increased. Table III shows the $f_1$ value to be fairly constant over the entire range of fields; $f_1$ is about 0.45.

TABLE III

FITTING PARAMETER VALUES FOR BEEF FAT

| Field (gauss) | $^{l}T_1$ (msec) | $^{s}T_1$ (msec) | $f_1$ | $f_s$ |
|---|---|---|---|---|
| 354 | 510 | 90 | 0.446 | 0.554 |
| 236 | 550 | 115 | 0.435 | 0.565 |
| 109 | 715 | 95 | 0.475 | 0.525 |
| 36 | 980 | 140 | 0.225 | 0.775 |
| 22 | 400 | 90 | 0.448 | 0.552 |

TABLE III (Continued)

| | | | | |
|---|---|---|---|---|
| 10 | 305 | 80 | 0.512 | 0.988 |
| 65 | 330 | 87 | 0.402 | 0.598 |
| 4 | 278 | 73 | 0.450 | 0.550 |
| 2 | 305 | 75 | 0.385 | 0.615 |
| 1 | 310 | 88 | 0.377 | 0.623 |
| ($T_2$ Data) at 0.5 Gauss | 75* | — | 1* | — |

* = exponential observed.

The $T_1$ and $T_2$ measurements on a freshly obtained sample of beef round were made. For these measurements the temperature was controlled and kept constant at 25 $\pm$ 2°C. Some additional techniques were used for these measurements, including the use of two sets of coils to obtain the $T_2$ decay and the use of the Varian A-60 apparatus in conjunction with the EFP apparatus to obtain the signal amplitude for the $T_2$ decay of the beef round sample at $t_d = 0$. These techniques have been discussed in some detail in Chapter III.

The data compiled for beef round-Sample #2 using these additional methods are illustrated by Figures 7, 8a, and 8b and Table IV. Figures 8a and 8b typify the plots of the data; most of the graphs seem to have the abrupt change in slope shown by these two. The reason for this abrupt change in slope is not known and is somewhat bothersome since it was not observed for Sample #1 of beef round. Sample #2 was not treated differently from Sample #1 in that it was kept in a sealed Nalgene container and stored when not in use at 4°C. The methods for making the measurements used for the two samples, with the exception of controlling

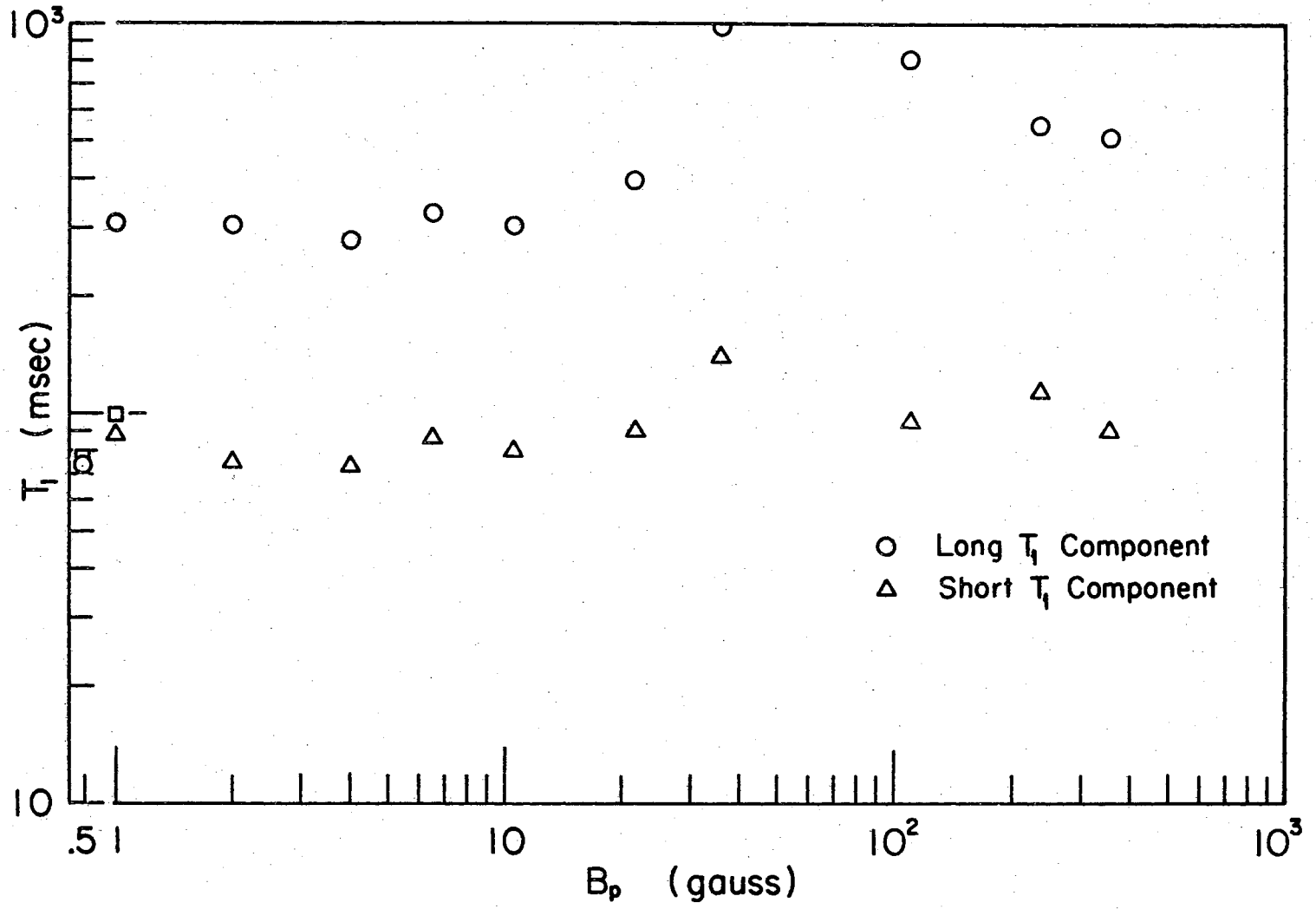


Figure 6. Log $T_{1,2}$ Versus Log B for Beef Fat

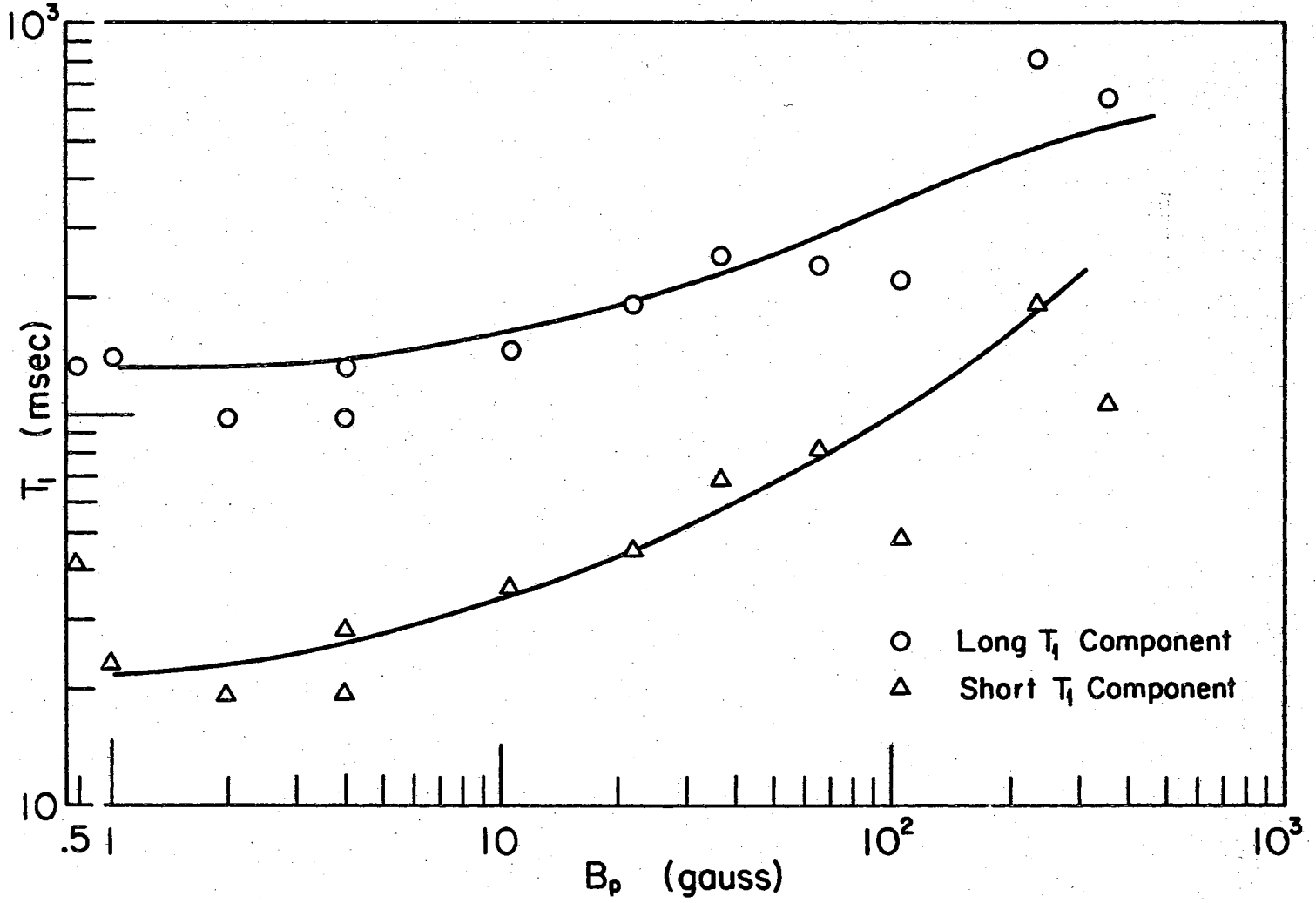


Figure 7. Log $T_{1,2}$ Versus Log B for Beef Round, Sample #2, Fresh

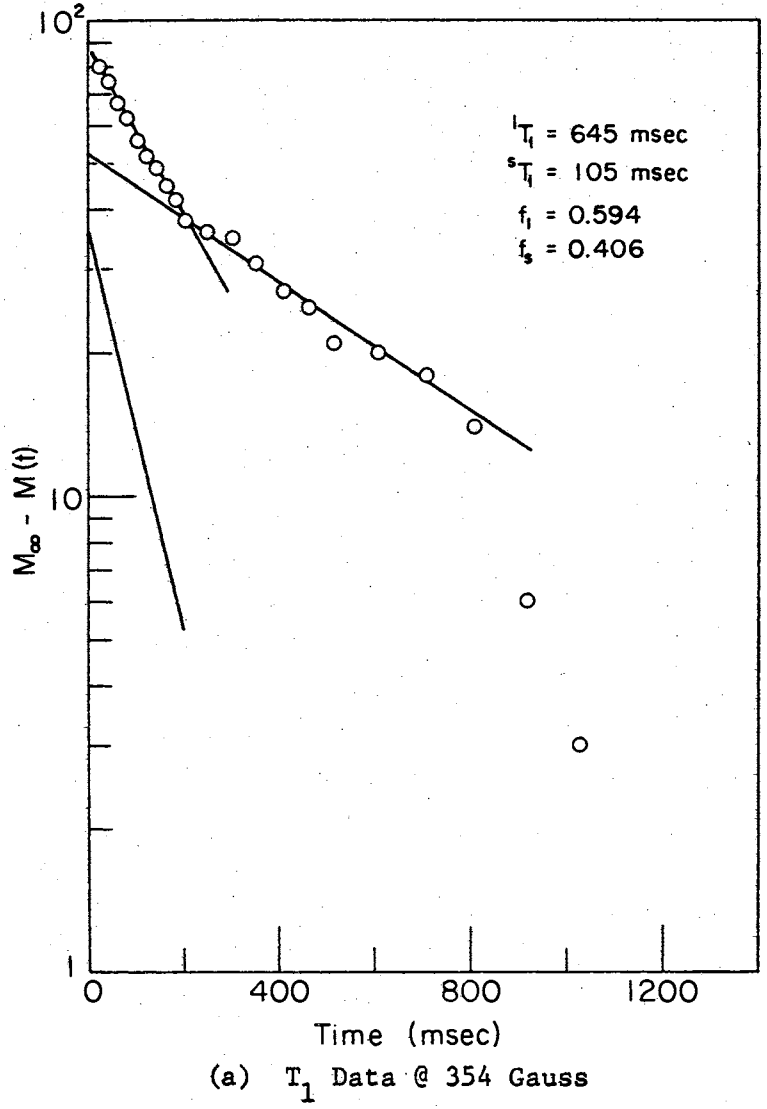


(a) $T_1$ Data @ 354 Gauss

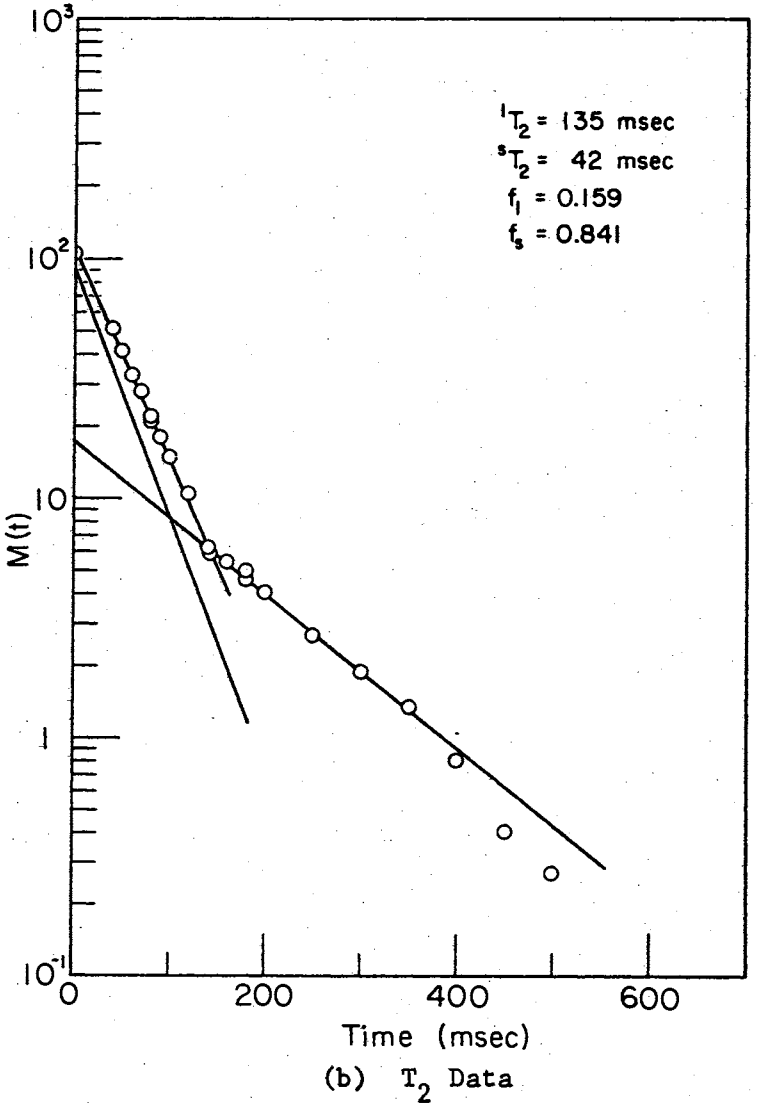


(b) $T_2$ Data

Figure 8. Typical $T_1$ and $T_2$ Plots for Beef Round, Sample #2, Fresh

the temperature for Sample #2, were identical also.

Figure 7 shows more of a variance for $T_1$ values over the range of fields than does Figure 5. As a general statement comparing the two $T_1$ field dependence graphs, $T_1$'s are larger at high fields and lower at low fields for Figure 7 than are the corresponding $T_1$ values for Figure 5. Also, for Sample #2 there does not seem to be a range of fields over which $T_1$ has a constant value as was observed for Sample #1. Possibly, these differences could have been caused by the fact that for the first sample the temperature varied. For high fields, the lowest temperature recorded was about 25°C, and for the low fields, the highest temperature found was about 35°C.

One thing noted is that even with the higher Q coils used for these measurements the scatter that is seen is still large. There are many reasons for this. Among them are:

1) The distinct possibility that the method of analysis, the model of the sum of two exponentials, for the observed data is totally incorrect,

2) The inaccurate graphical technique used to fit the curve; probably a computer fit would give a much better picture of the dependence of the parameters upon the field.

3) The inaccuracy with which $M_\infty$ can be determined; this accuracy is especially poor for the middle range of fields.

Again, as for Sample #1, the $T_2$ values for Sample #2 do not compare favorably with the low field values of $T_1$. $^1T_2$ is in good agreement with $^1T_1$ at one gauss, but $^sT_2$ is about 20 msec. longer than $^sT_1$ at one

gauss. Also, there was no single exponential behavior seen at high fields as there had been for the previous measurements.

The $f_1$ values shown in Table IV behave very differently than the $f_1$ values obtained previously. Whereas the $f_1$ values for Sample #1 show a trend toward decreasing as the field decreases, the $f_1$ values for Sample #2 have a trend toward being constant over the entire range of fields. Eight of the twelve values obtained from the $T_1$ data lie within a range of $0.6 \pm 0.1$. This high value for $f_1$ is also markedly different from those obtained previously. In fact, there were only three values of $f_1$ greater than 0.5 obtained for Sample #1.

TABLE IV

FITTING PARAMETERS VALUES FOR BEEF ROUND (SAMPLE #2)

| Field (gauss) | $^1T_1$ (msec) | $^sT_1$ (msec) | $f_1$ | $f_s$ |
|---|---|---|---|---|
| 354 | 645 | 105 | 0.594 | 0.406 |
| 236 | 810 | 190 | 0.729 | 0.271 |
| 106 | 223 | 48 | 0.644 | 0.356 |
| 65 | 242 | 81 | 0.346 | 0.654 |
| 36 | 256 | 68 | 0.296 | 0.704 |
| 22 | 191 | 45 | 0.550 | 0.450 |
| 11 | 148 | 36 | 0.547 | 0.453 |
| 6.5 | 95* | — | 1* | — |
| 4 | 98 | 19 | 0.660 | 0.340 |
| 4 | 132 | 28 | 0.599 | 0.401 |
| 2 | 98 | 19 | 0.641 | 0.359 |
| 1 | 140 | 23 | 0.548 | 0.452 |
| ($T_2$ Data) at 0.5 gauss | 135 | 42 | 0.159 | 0.841 |

*The graph obtained had a very slight curvature.

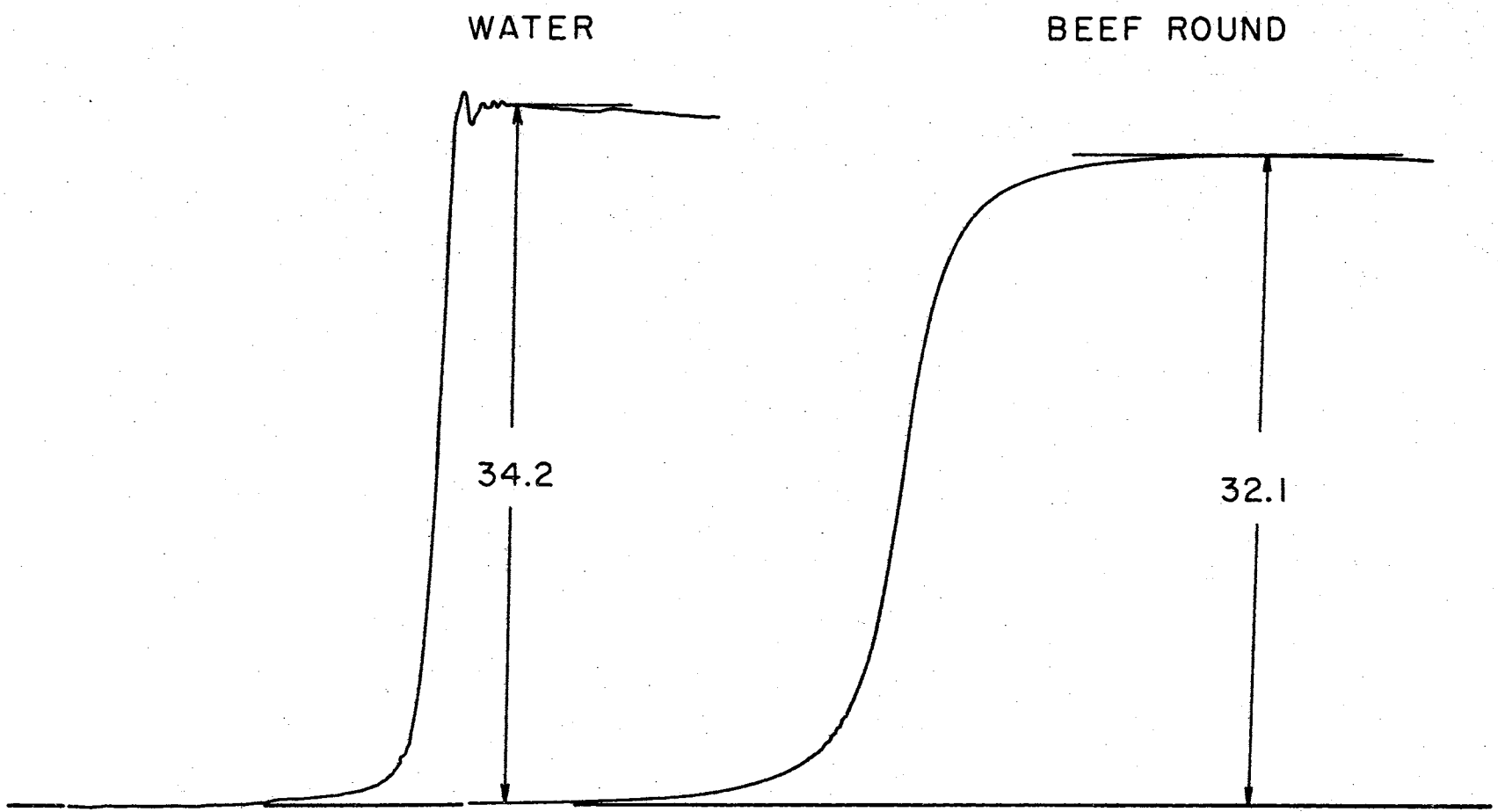


Figure 9. Integrals of Absorbtion Curves for Water and Beef Round Using the Varian A-60. (Amplitude Units are Arbitrary.)

Figure 8b is the compilation of data from the three coil configurations plus the point at t = 0. The $T_2$ decay data has been adjusted by the correlation terms explained in Appendix C, to the scale of the data obtained from Coils #1. The data point at the decay time equal to zero certainly seems to fit the data curve.

The calculation of the data point $A_s^e$ is given here. First, E* was calculated from the weights of the samples in the Varian tubes and the amplitudes of the spectrum integral for each sample. From Figure 9, $A_s^v = 32.1$, $A_w^v = 34.2$, and the weights obtained were $W_s^v = 0.810$ gm., and $W_w^v = 0.480$ gms. Thus E* is calculated using the equation given in Chapter III:

$$E^* = \frac{(32.1/0.810 \text{ gms.})}{(34.2/0.480 \text{ gms.})} = 0.556^{1}.$$

The value of $A_w^e$ (2) was determined to be $157.5^{2}$. The value of $W_w^e$ was 484 gms. The value of the weight of the beef round sample, $W_s^e$, was 591.7 gms. Thus, with all the quantities determined the calculation is simply:

---

[1]At a later time a measurement to determine the density of beef round was made. $\rho_s$ was found to be 1.08 gms/cm$^3$. Thus, E can be calculated:

$$E = E^* \frac{\rho_s}{\rho_w} = (0.556)(1.08)$$

$$E = 0.600$$

[2]The data for this determination was taken using Coils #1 because all the other data had been correlated to the scale for Coils #1.

$$A_s^e = E^* \frac{A_w^e}{W_w^e} W_s^e = (0.556) \frac{157.5}{484 \text{ gms.}} (591.7 \text{ gms.})$$

$$A_s^e = 107.$$

The units for the above calculation are arbitrary but correspond to the scale of the other data.

After a period of time of approximately seven weeks, the $T_1$ and $T_2$ experiments were repeated, with exception of the determination of the signal amplitude at $t_d = 0$ for the $T_2$ decay. The purpose of these experiments was to see if the same values of the fitting parameters could be obtained as had been obtained in the previous experiments using beef round Sample #2.

The results of these repeated measurements for Sample #2 may be summarized by Figures 10, 11a and 11b and Table V. Figures 11a and 11b typify the data by their smooth curves, a really direct contrast to what had been obtained previously for this same sample. Comparing Figures 10 and 7 it is seen that the field dependence of the $^1T_1$ component is approximately the same for each curve. $^1T_1$ appears to be slightly longer at low fields for Figure 10 than for Figure 9, but it is difficult to judge because of the scatter in the data; note the measurements at four gauss for each of the graphs.

Unlike the similar appearance of the $^1T_1$ dependence on B for the curves, the $^sT_1$ curves are somewhat dissimilar. With B equal to 10 gauss or less, $^sT_1$ from Figure 10 exceeds $^sT_1$ from Figure 7 by ten to

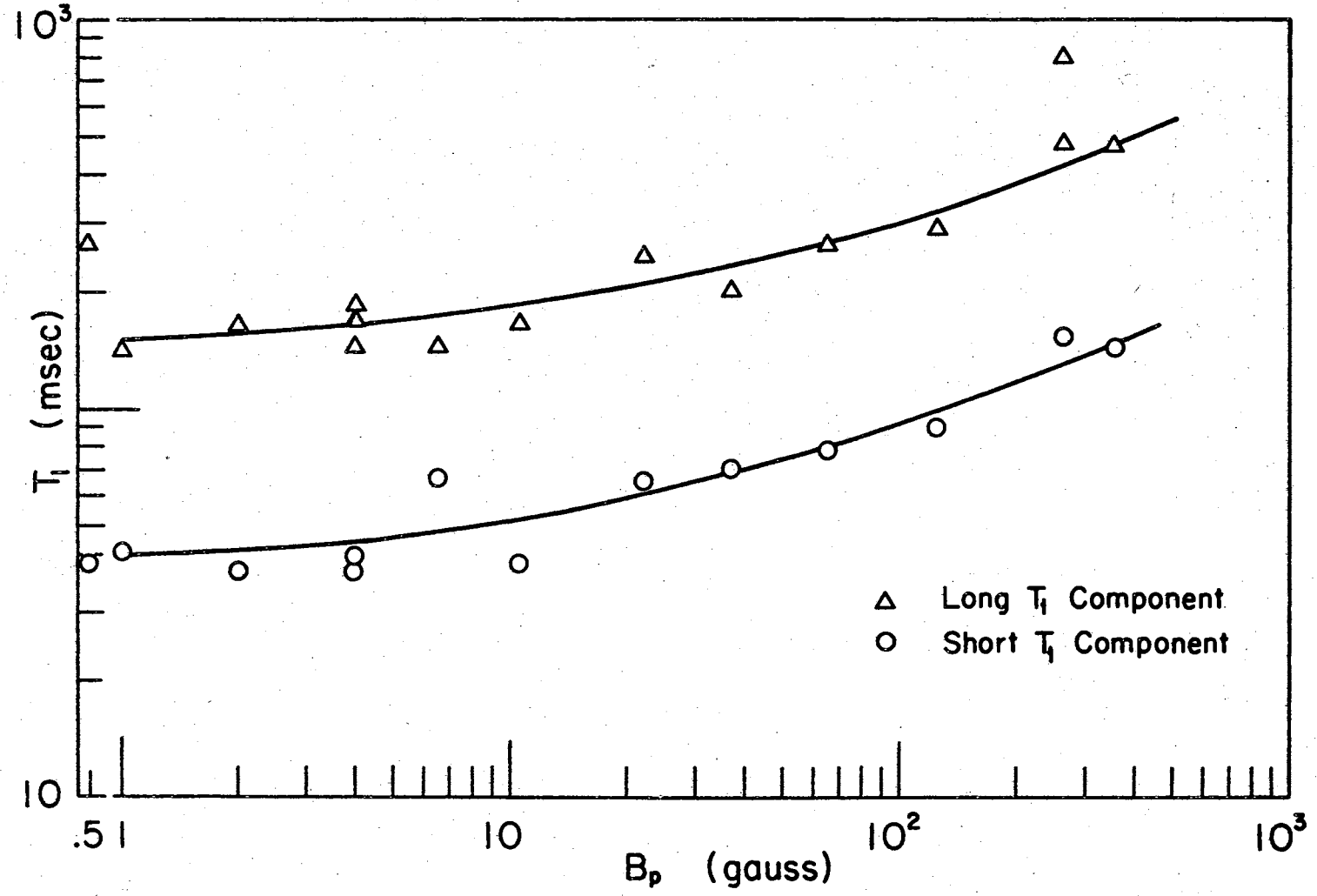


Figure 10. Log $T_{1,2}$ Versus Log B for Beef Round, Sample #2, Aged 7 Weeks at 5°C

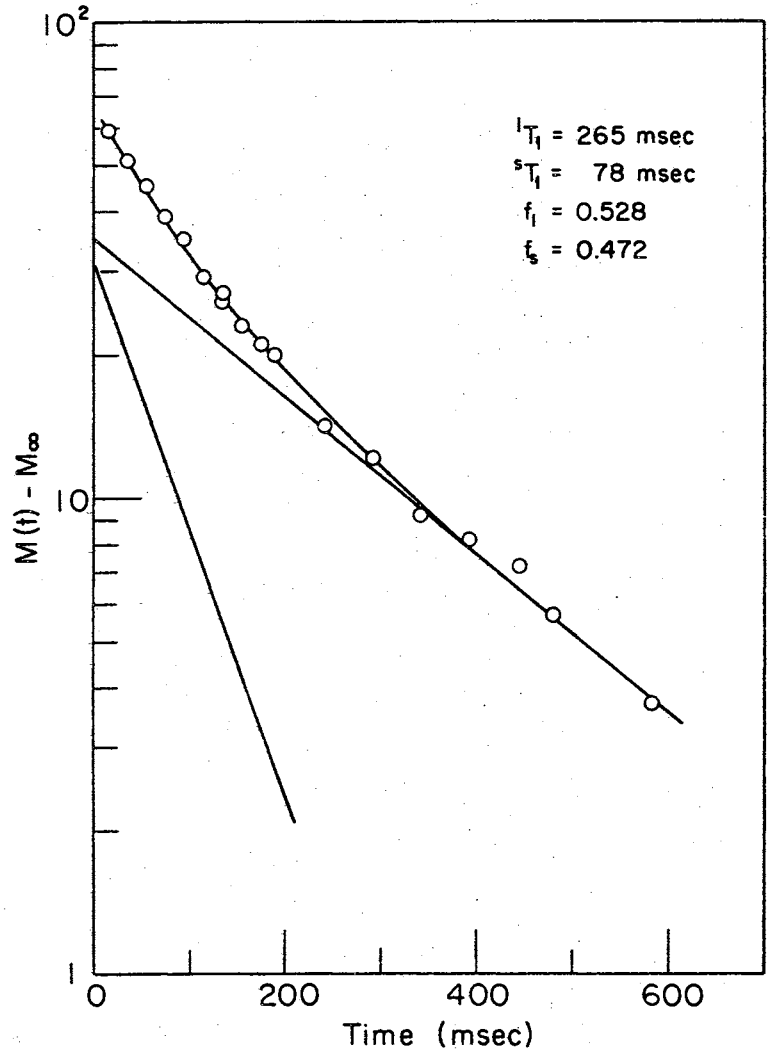


(a) $T_1$ Data @ 64.9 Gauss

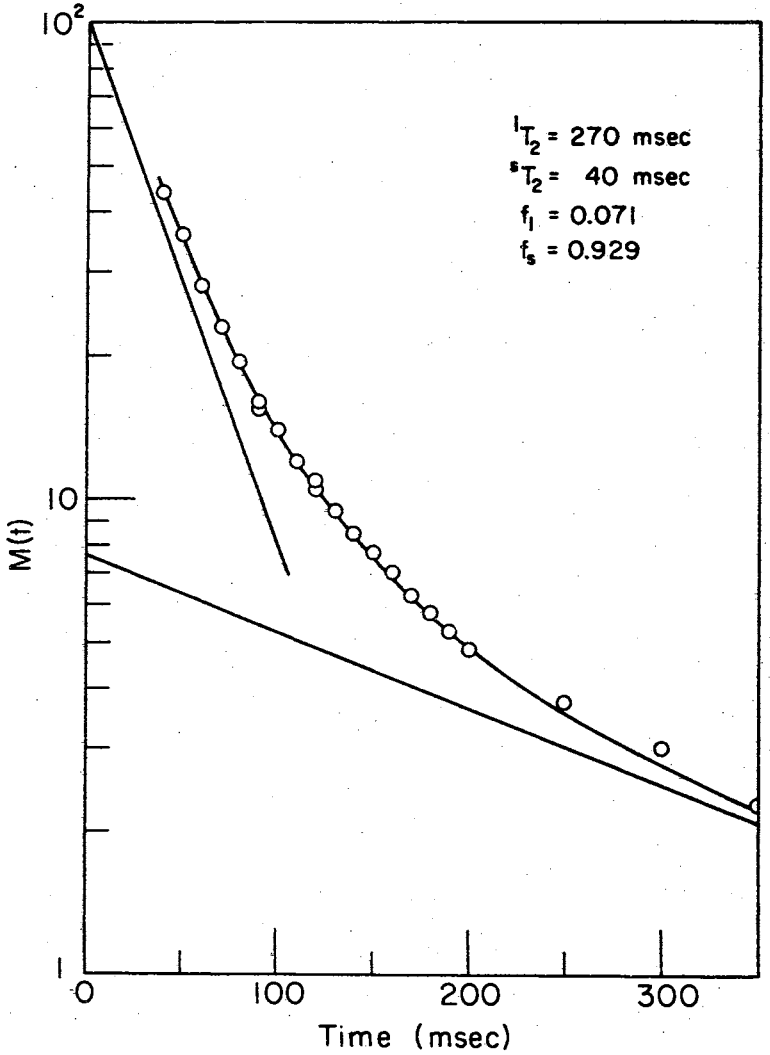


(b) $T_2$ Data

Figure 11. Typical $T_1$ and $T_2$ Plots for Beef Round, Sample #2, Aged 7 Weeks at 5°C

twenty milliseconds. The field dependence of the $^{s}T_1$ component in Figure 10 appears to be less, i.e., the curve has a flatter appearance than does the Figure 7 curve.

The $^{s}T_2$ values are approximately the same for both curves at 40 msec., whereas $^{l}T_2$ ($\approx$ 270 msec.) for Figure 10 is about twice $^{l}T_2$ ($\approx$ 135 msec.) from Figure 7. The $f_1$ values from Table V are noted to behave somewhat like the $f_1$ values in Table IV. As for Table IV, there is so much scatter in the $f_1$ values in Table V that any trend with respect to the varying field is very difficult to detect. The values do seem to collect about the point $f_1 = 0.5$, i.e., $f_1$ is possibly constant over the range of fields. This is the same characteristic seen from the previous measurements of this sample except that the value of $f_1$ was thought to be about 0.6

TABLE V

FITTING PARAMETER VALUES FOR BEEF ROUND, SAMPLE #2
(AGED 7 WKS @ 5°C)

| Field (gauss) | $^{l}T_1$ (msec) | $^{s}T_1$ (msec) | $f_1$ | $f_2$ |
|---|---|---|---|---|
| 354 | 470 | 145 | 0.591 | 0.909 |
| 265 | 475 | 155 | 0.375 | 0.625 |
| 265 | 808 | 155 | 0.326 | 0.674 |
| 124 | 289 | 90 | 0.710 | 0.290 |
| 65 | 265 | 78 | 0.528 | 0.472 |
| 37 | 200 | 70 | 0.644 | 0.356 |
| 22 | 248 | 65 | 0.536 | 0.464 |
| 11 | 165 | 40 | 0.635 | 0.365 |

TABLE V (Continued)

| | | | | |
|---|---|---|---|---|
| 6.5 | 143 | 67 | 0.573 | 0.427 |
| 4 | 144 | 38 | 0.563 | 0.437 |
| 4 | 168 | 38 | 0.512 | 0.488 |
| 4 | 185 | 42 | 0.449 | 0.551 |
| 2 | 165 | 38 | 0.392 | 0.608 |
| 1 | 140 | 43 | 0.565 | 0.935 |
| ($T_2$ Data) at 0.5 gauss | 270 | 40 | .071 | 0.929 |

From these repeated measurements it may be concluded, that:

1) The sample, as far as the signal observed from the EFP apparatus is concerned, is not appreciably affected by extended periods of storage at cool, not freezing, temperatures.

2) The scatter of the data is large, probably because of a combination of the inaccurate method by which the parameters are obtained and the low signal observed from beef samples. In turn, because of the low signal and somewhat rapid relaxation times, the scatter of the parameter values could be attributed to the short range over which reliable data may be taken.

## Separated Liquid and Solid Samples

Some interesting observations can be made from the preceeding data for beef tissues. One, especially, is that the hypothesis made by Ligon (4) cannot be true because non-exponentials are obtained for signals from beef fat and beef round separately.

Since it had been observed that fluid separated from the solid

portion of the sample it was postulated that the two components of the signal could be attributed to the protons in the separated fluid and the protons in the solid portion of the sample. This idea was tested by making measurements on the liquid and solid portions separately and comparing these results with the previous results for the unseparated sample.

The data for the solid and liquid samples are given in Figures 12 through 16. Looking at Figures 14a, 14b, and 14d (graphs for the determination of $T_2$ for the solid sample) it is seen in Figure 14a and 14d that the signal behaves exponentially whereas in Figure 14b the signal appears to be non-exponential. However, the non-exponential signal does have some things in common with the others. Drawing a slope to fit the initial portion of the curve yields a value of $T_2$ from Figure 16b which approximates $T_2$ found from Figure 14a. The initial $T_2$ = 42 msec. from Figure 14b and $T_2$ = 47 msec. from 14a. Performing the same operation on the "tail" of the curve yields the value found in Figure 14d. The tail value for $T_2$ from Figure 14b is 67 msec. and $T_2$ = 65 msec. from Figure 14d. Figure 14d should be an approximation for the "tail" of the signal because of the range of decay times in which data was taken.

Fitting the data of Figure 14b by the "best fit" method, shown in Figure 14c the following values were obtained: $f_1 = 0.189$, $f_s = 0.816$, ${}^{l}T_2$ = 69 msec., and ${}^{s}T_2$ = 23 msec. When compared to the most recent data which had been taken on the unseparated samples, i.e., the $T_2$ data obtained for the aged beef round Sample #2, Figure 11b, it is seen that the values of $f_1$, $f_s$, ${}^{l}T_2$, and ${}^{s}T_2$ are not too comparable. But, the $T_2$ value obtained for the solid-separation sample in Figure 14a is approxi-

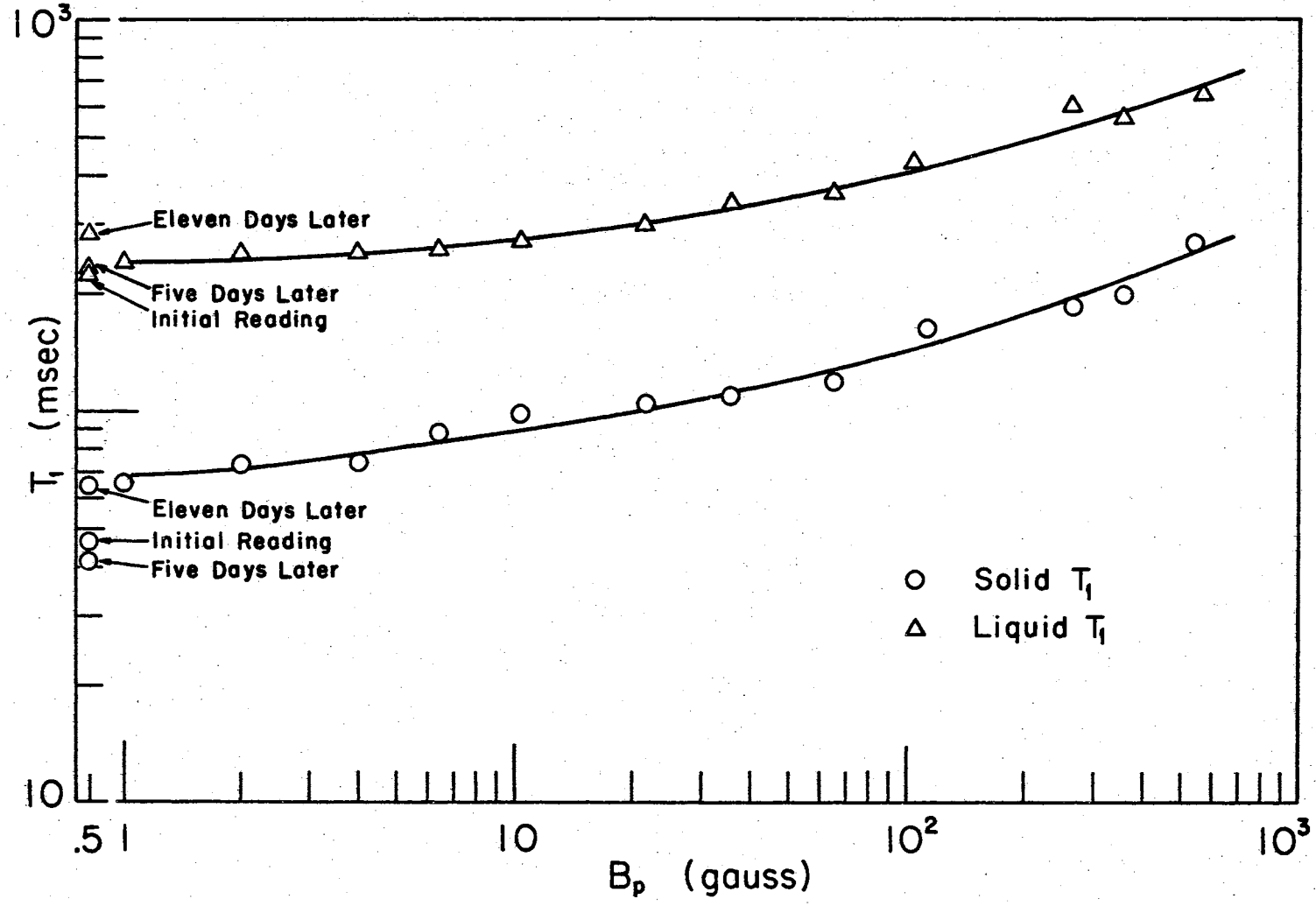


Figure 12. Log $T_{1,2}$ Versus B for Beef Round (Sample #2) Separations, Solid and Liquid.

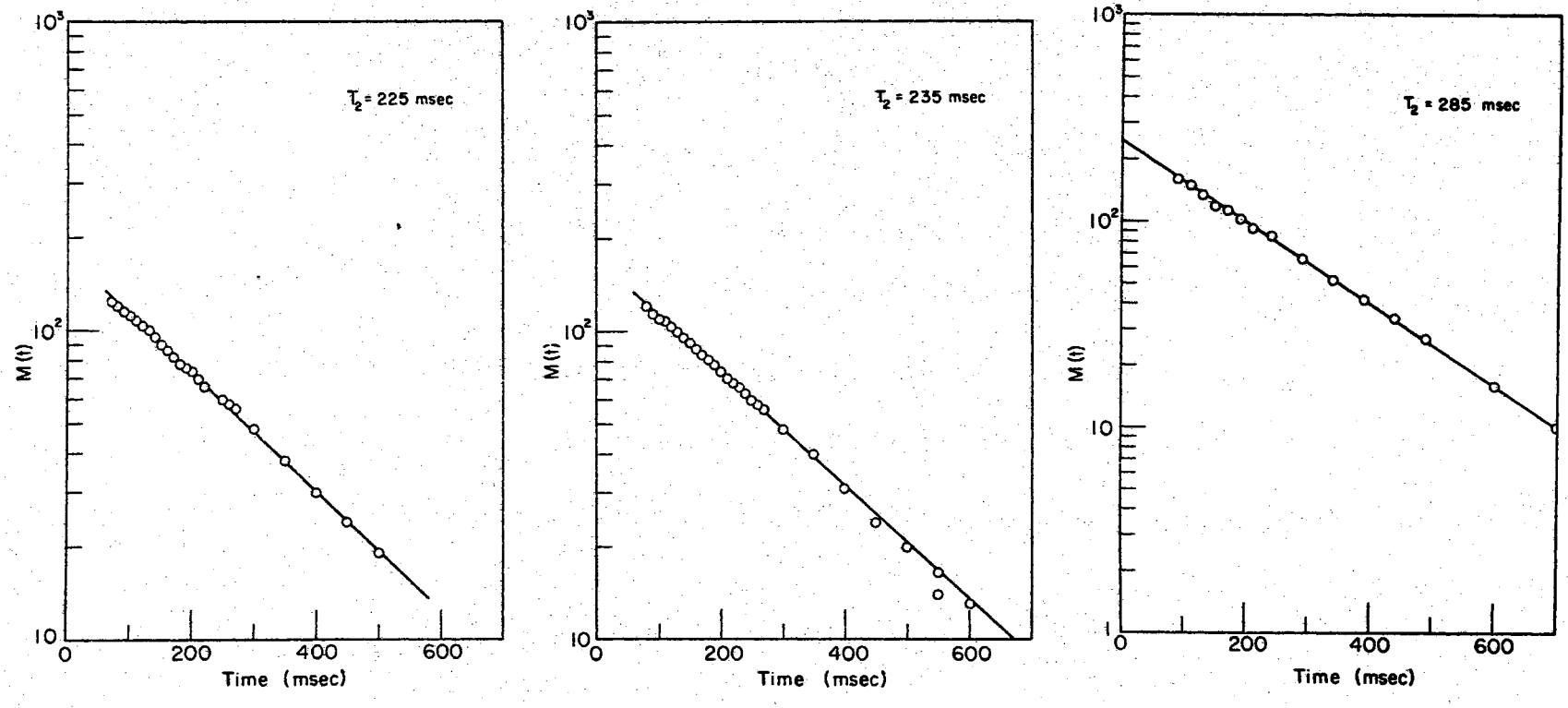


(a) Initial Measurement (b) After 5 Days (c) After 11 Days

Figure 13. $T_2$ Data Plots for Separation Fluid

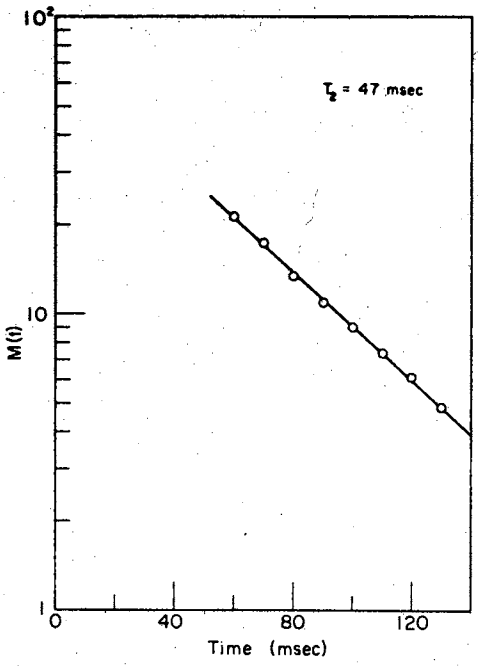


(a) Initial Measurement

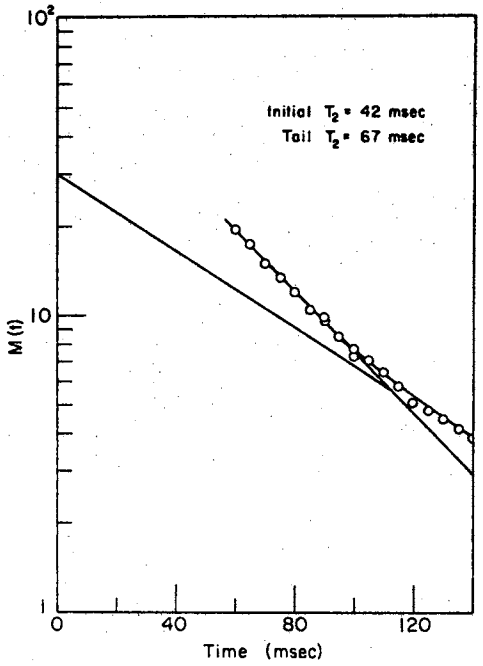


(b) After 5 Days

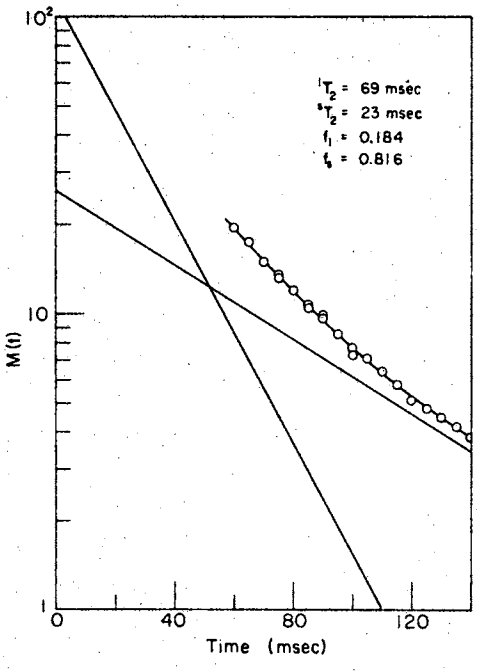


(c) After 5 Days

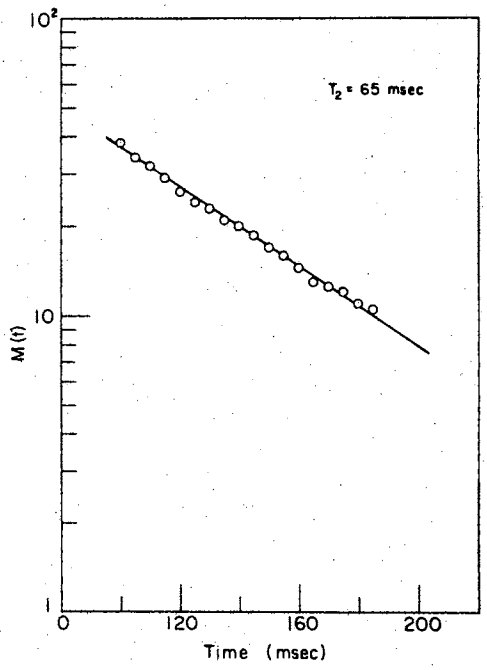


(d) After 11 Days

Figure 14. $T_2$ Data Plots for Separation Solid

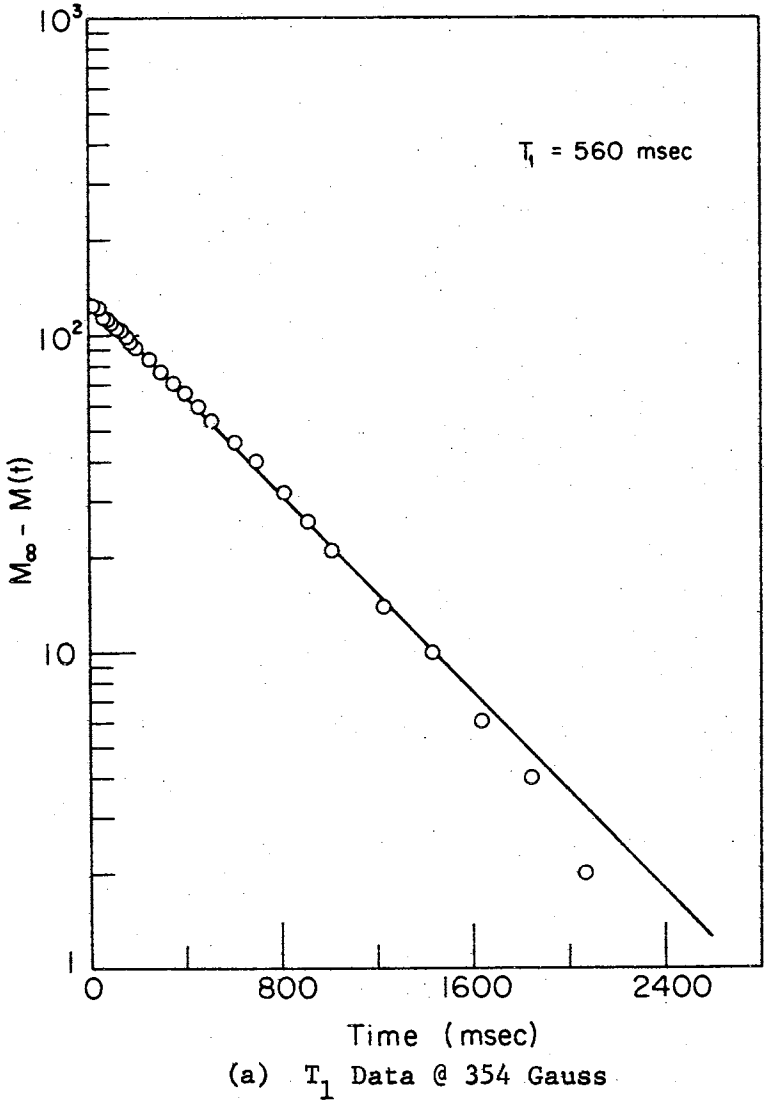


(a) $T_1$ Data @ 354 Gauss

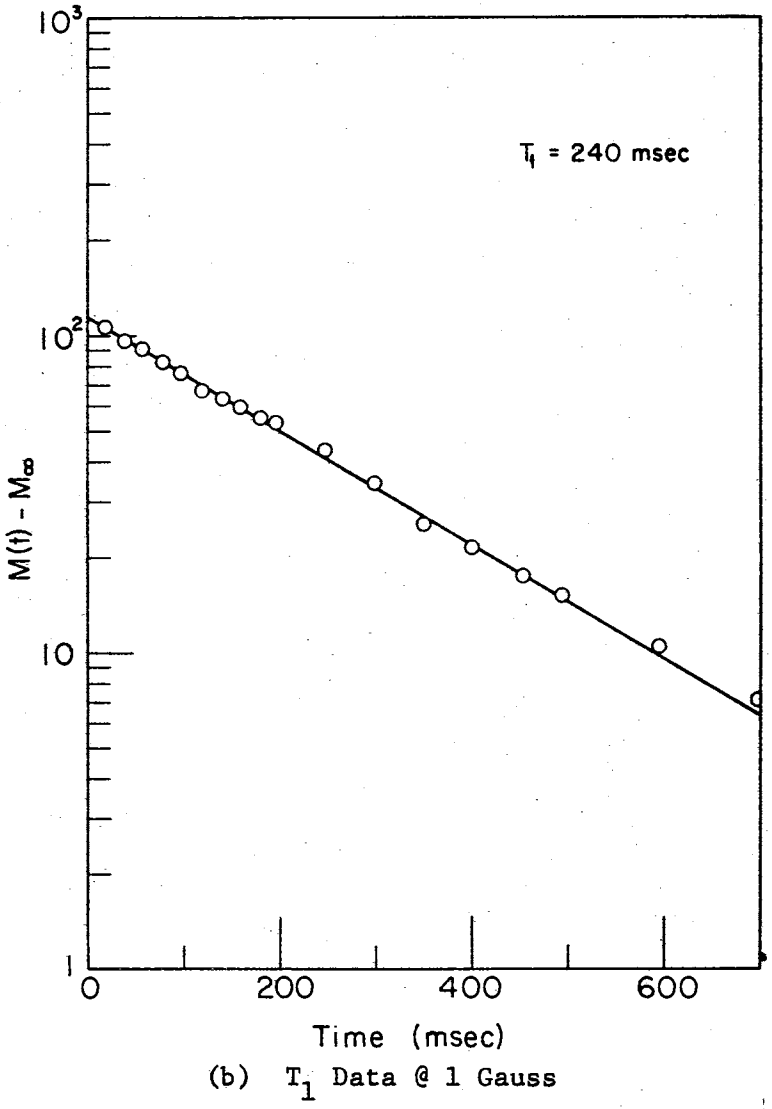


(b) $T_1$ Data @ 1 Gauss

Figure 15. Typical $T_1$ Data Plots for Separation Fluid

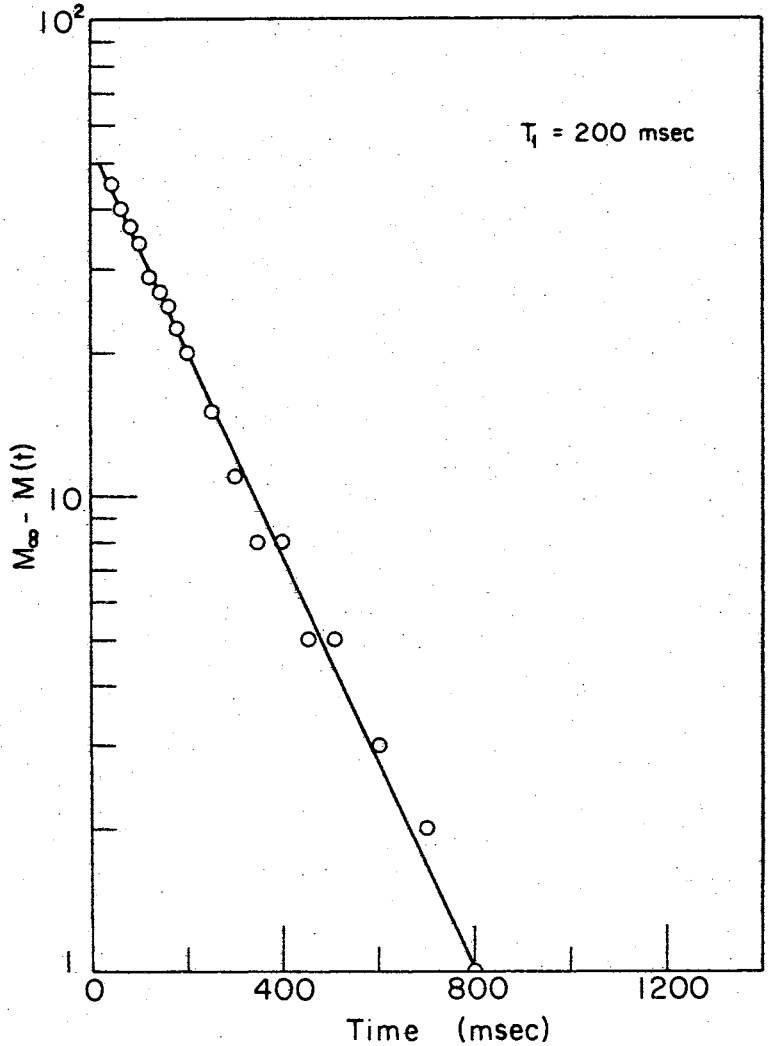


(a) $T_1$ Data @ 354 Gauss

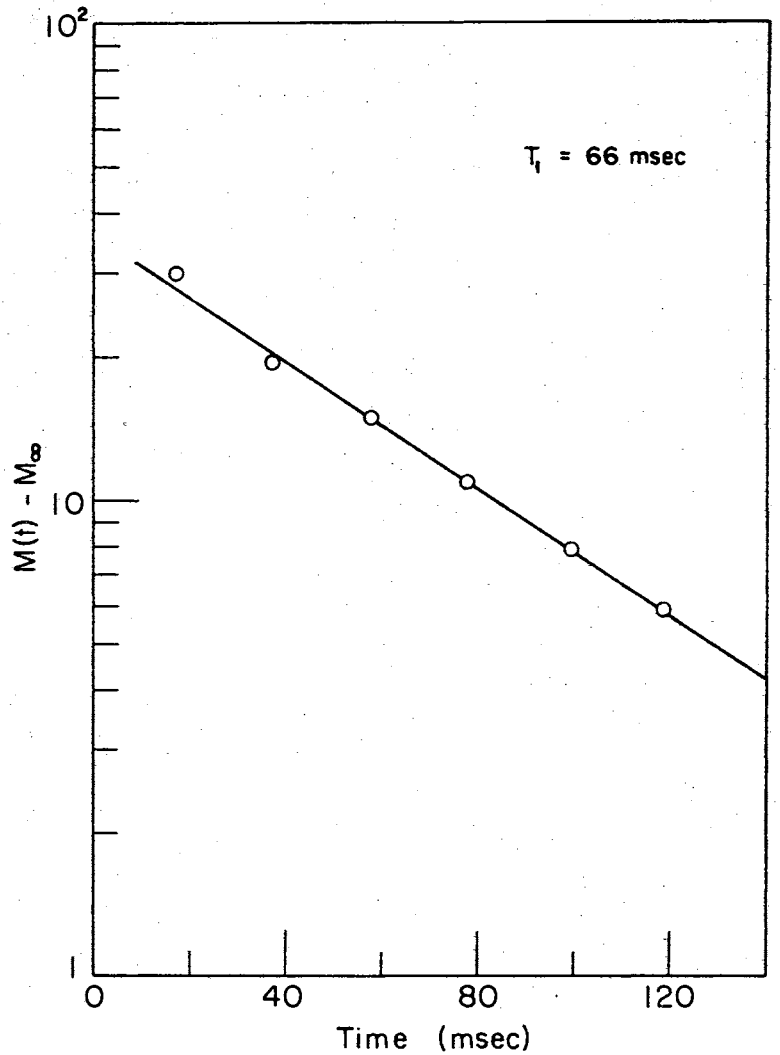


(b) $T_1$ Data @ 1 Gauss

Figure 16. Typical $T_1$ Data Plots for Separation Solid

mately equal to the $^{s}T_2$ value obtained in Figure 11b. $T_2$ from Figure 14a equals 47 msec. and $^{s}T_2$ from Figure 11b equals 40 msec. This comparison gives some credence to the idea that one portion of the signal comes from the protons of the solid portion of the sample.

However, these results may be a function of time after the original system was separated in liquid and solid portions. The data for Figure 14a was taken just after the separation was completed. The data for Figure 14b was taken five days later, and at this time some fluid was visible in thecontainer. The data obtained for Figure 14c was taken about 11 days after the separation process. These data were recorded after the fluid which had drained from the sample was again separated from it, thus, visibly, only the solid portion remained.

The remainder of the data obtained for the solid-separation sample is shown in Figure 12, log $T_1$ vs log B, and in Figures 16a and 16b. Figures 16a and 16b just represent a sampling of the data obtained for the determination of $T_1$ at a particular magnetic field strength. As can be seen, the data plots appear to have an exponential behavior as do all the others which have not been shown.

The log $T_1$ vs log B graph, Figure 12, for the solid-separation sample compares fairly well in general form with the log $^{s}T_1$ vs B curve for the aged Sample #2, Figure 10. The values of $^{s}T_1$ and $^{s}T_2$ for the beef round are all somewhat smaller than those found for the solid-separation sample. This discrepancy, if it is a discrepancy, i.e., it has not been shown that there is a correlation between these two quantities, may be due to either of two things or, more likely, both:

1) The longer relaxation times found for the separation-solid,

when compared to the short-time relaxation component, $^{s}T_1$ and $^{s}T_2$ of the beef round, could be due to an aging effect. The data taken on the separation-solid was taken approximately one month after that for the whole sample of beef round. The beef round sample was kept, as before, at 5°C during this time between measurements.

2) The shorter relaxation times observed for the beef round may possibly be due to the error which is induced by applying the "best fit" technique. The effect of this analysis has been discussed previously and it was shown that, effectively, shorter than actual values were obtained using the method.

The data for the determination of $T_2$ from the liquid sample which was obtained by the separation process is shown in Figures 13a, 13b, and 13c. All three curves are observed to have an exponential behavior. Also, another phenomenon can be noted. $T_2$ increases from Figure 13a, $T_2$ = 225 msec., to 13b, $T_2$ = 235 msec., and from Figure 13b to 13c, $T_2$ = 285 msec. With respect to Figure 13a the sample was 5 days older when data was taken for Figure 13b and 11 days older when measurements were made for Figure 13c. This possibly then means that the relaxation time, $T_2$, for the separation-liquid increases with time after separation or aging of the sample.

The $T_2$ values of the separation liquid compared with the $^{1}T_2$ value of 270 msec. for beef round from Figure 11b are very nearly equal to each other. Further, in comparing the log $T_1$ vs log B graphs of the two samples, Figure 12 and Figure 10 virtually the same conclusions can be stated that were given in the comparison of the solid-separation $T_1$

values to the $^{s}T_1$ values of the unseparated beef round samples. The $^{l}T_1$ values of the unseparated beef round sample are shorter than those obtained for the separation liquid sample. The reasons for this, the same ones given for the separation-solid sample, are: one, the error induced by the "best fit" analysis, and two, the aging of the beef sample.

Some important possibilities for explaining the behavior of the signal from beef round are seen from these solid and liquid-separation experiments. It is believed that they are important enough to be summarily repeated here as follows:

1) The data for the solid and liquid separations indicates that they may be the individual components which make up the signal. This is based on the comparison of separation-sample data with the most recent studies of the unseparated beef round samples. The unseparated beef round samples used in the comparison were the ones later separated to make the solid and liquid samples.

2) Data from these experiments are exponential.

3) The $T_2$ relaxation times increased with age for both the liquid and solid separation samples.

As a matter of interest the field dependence of the separation-fluid for beef round was measured at other temperatures (3°, 15°, 25°, 35°, and 45°C) than that discussed previously for 25°C. For all temperatures and all fields, the signal behaved exponentially for both $T_1$ and $T_2$ experiments. The field dependence curves, log $T_1$ vs B, Figure 17, are all seen to be somewhat similar. As is detected from the graphs,

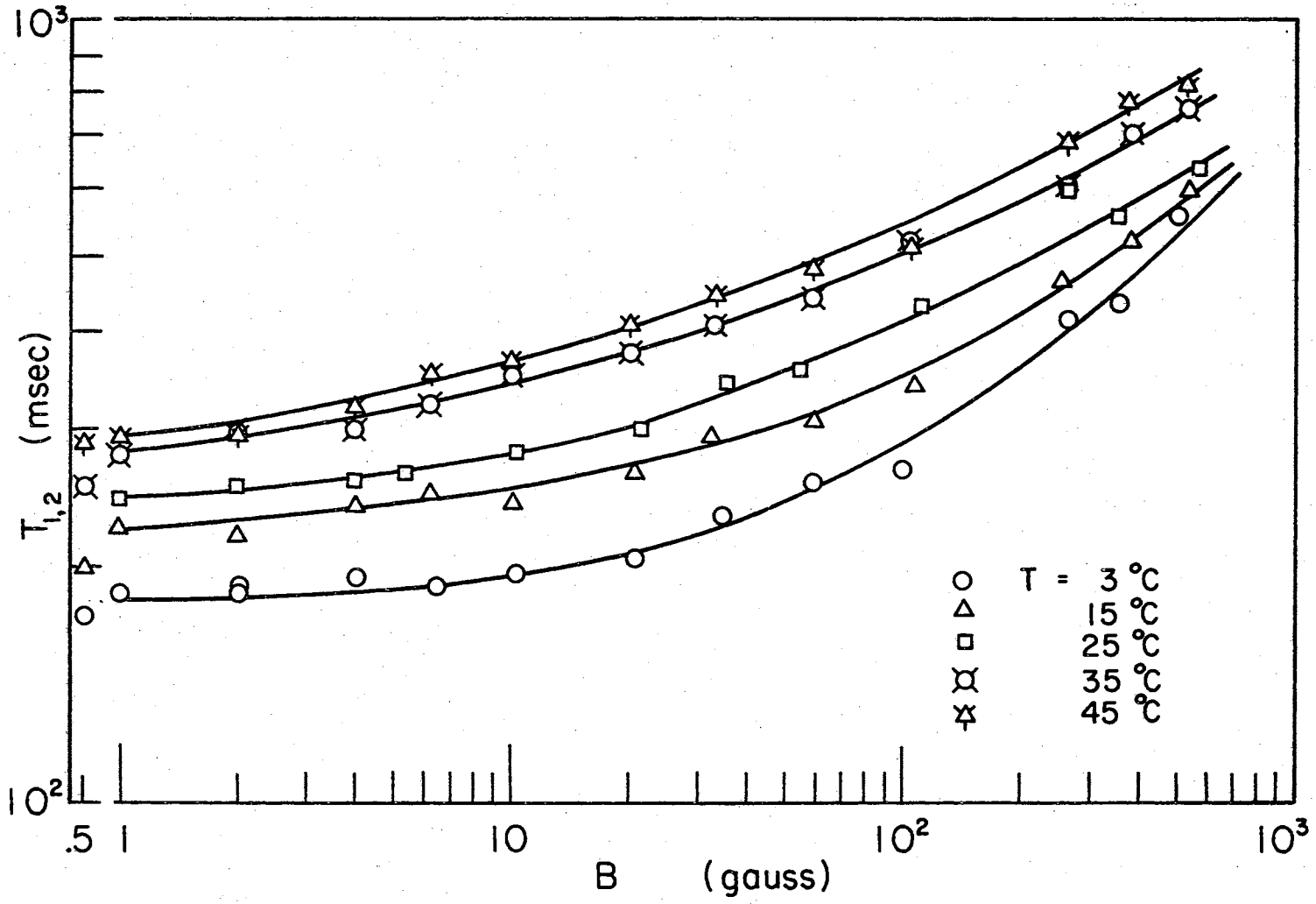


Figure 17. Log $T_{1,2}$ Versus Log B for Separation Fluid at 3°C, 15°C, 25°C, 35°C, 45°C.

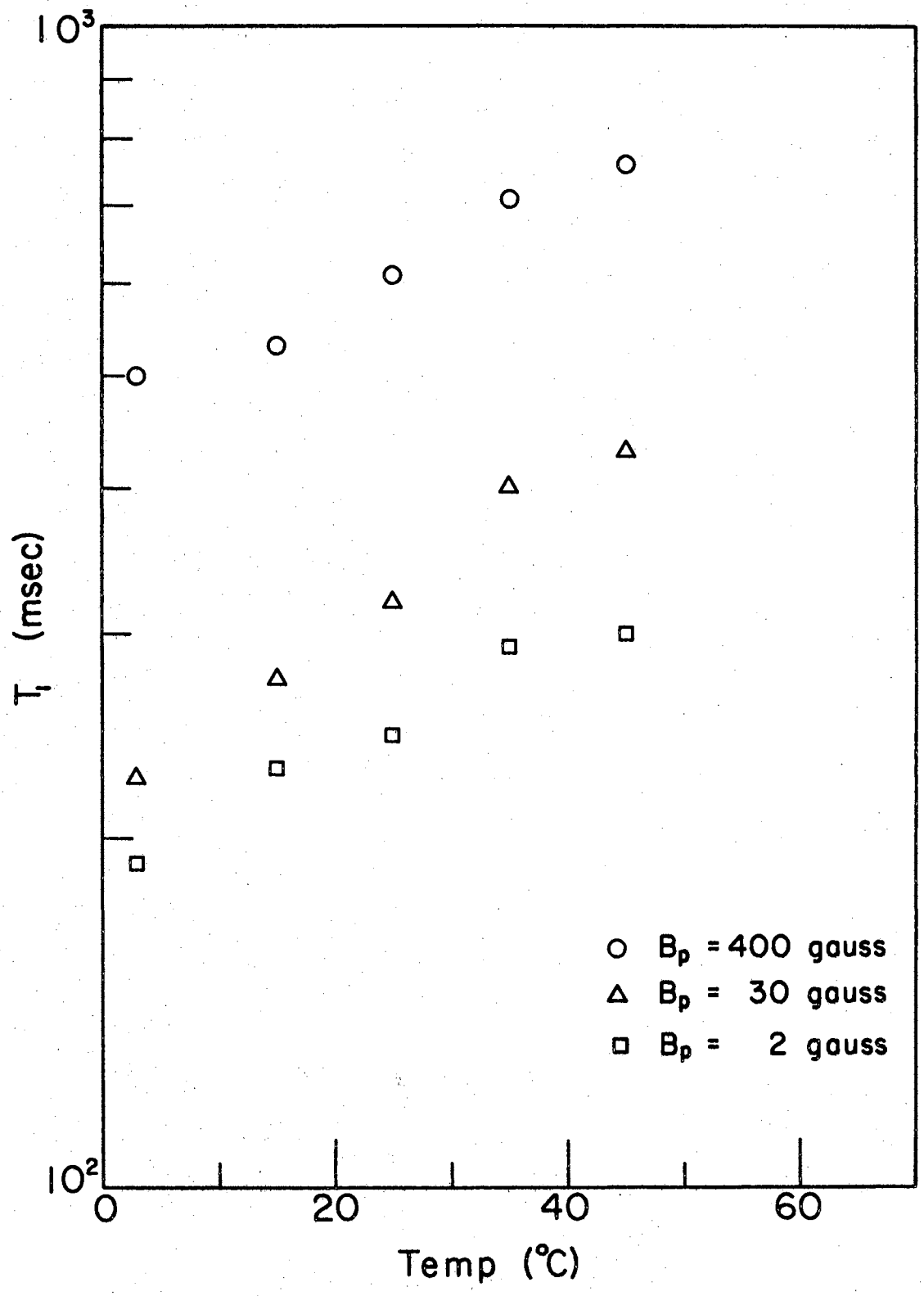


Figure 18. Log $T_1$ Versus Temperature for Separation Fluid

the log-log curve of the $T_1$ dependence on the polarizing field progressively gets steeper for the lower values of the field, one gauss through about 20 gauss, as the temperature is increased.

Also, the relaxation times are seen to increase as the temperature is increased. This can most easily be shown by Figure 18. Figure 18 is a graph of the logarithm of $T_1$ vs the temperature in degrees centigrade for three different fields of the field dependence curves.

## Aging Experiments

To check the conclusion reached, via some comparisons, that the relaxation times increase with aging of the sample, measurements at various intervals of time were made to determine $T_1$ at 265 gauss and $T_2$ in the earth's field. The simple for this experiment was obtained from a freshly slaughtered animal.

The compilation of the $T_1$, $^1T_2$, $^sT_2$, and $f_1$ values obtained for $T_2$ experiments are given in Table VI. Generally, what is shown is that the relaxation times for both $T_1$ and $T_2$ become longer with the increase of time after slaughter. The $f_1$ values show a great amount of scatter but are thought to be constant; there is no general trend shown as there had been before. This could arise because Sample #2 had aged much longer than this sample; i.e., the effect for $f_1$ could be very slow with time.

An unexplainable occurrence for the $T_1$ data is that all the data, with one exception, plotted as exponentials. The only conjecture that can be made from this is that keeping the sample at sub-freezing temperatures, $-4.4^oC$, for periods of time of approximately two weeks after

TABLE VI

AGING EFFECTS FOR BEEF ROUND (SAMPLE #3, OBTAINED FROM A FRESHLY SLAUGHTERED ANIMAL)

| Time (hrs.) (since time of slaughter) | $T_1$ @ 265 gauss | $l_{T_2}$ | $s_{T_2}$ | $f_1$ (For $T_2$ Measurements only) |
|---|---|---|---|---|
| 3 | 158 | 53 | 21 | 0.146 |
| 50 | 175 | 64 | 21 | 0.164 |
| 96 | 190 | 62 | 22 | 0.230 |
| 121 | 201 | 71 | 19 | 0.109 |
| 172 | 260* | 106 | 24 | 0.122 |
| 270 | 238 | 165 | 31 | 0.133 |
| 434 | 330 | 154 | 24 | 0.165 |

*Seemingly non-exponential obtained for this measurement of $T_1$. The point was determined by a best-straight line fit. All measurements at 25°C. Aging took place at temperatures ranging from +20 to +27°C.

slaughter has an effect upon the $T_1$ relaxation. The reason for this statement is that all the beef round samples had been treated in this manner until the time they were obtained from the meat laboratories, except for the last sample which was obtained from a freshly slaughtered animal.

## High Field Experiments

Basically, these experiments were to determine if there is a single relaxation time at high fields. A single seemingly Lorentzian line shape had been obtained for the spectrum from the beef round sample when the water equivalence measurements were made. If the spectrum shape is Lorentzian, then, of course, there is only one relaxation time at high

fields. To make this determination, two things were done:

1) The spectrum shape was fitted with an actual Lorentzian shape.

2) Independent measurements were made using spin-echo equipment at 14,000 gauss.

The calculated results of the method of Appendix D for fitting a Lorentzian shape are given in Table VII and Figure 19. To show how well the actual absorption curve compares with the calculated Lorentzian shape, F(w) is plotted on Figure 19 by just the calculated points; the solid line is the absorption curve obtained from the A-60. The fit is remarkably good as can be seen.

TABLE VII

VALUES FOR THE CALCULATED LORENTZIAN CURVE

| F(w) | $0.215 + w^2$ | $w'$ | $w = w' \times 0.135$ | $w^2$ |
|---|---|---|---|---|
| 54.6 | 0.215 | 0 | 0 | 0 |
| 50.4 | 0.2332 | 1 | 0.135 | 0.0182 |
| 40.8 | 0.288 | 2 | 0.270 | 0.0729 |
| 31.0 | 0.379 | 3 | 0.405 | 0.164 |
| 23.2 | 0.507 | 4 | 0.540 | 0.292 |
| 17.98 | 0.654 | 5 | 0.663 | 0.439 |
| 13.49 | 0.872 | 6 | 0.810 | 0.657 |
| 8.50 | 1.382 | 8 | 1.080 | 1.167 |
| 5.775 | 2.035 | 10 | 1.35 | 1.82 |
| 4.14 | 2.835 | 12 | 1.62 | 2.62 |
| 2.82 | 4.165 | 15 | 1.99 | 3.95 |
| 1.625 | 7.235 | 20 | 2.65 | 7.02 |
| 1.052 | 11.165 | 25 | 3.31 | 10.95 |
| 0.732 | 16.045 | 30 | 3.975 | 15.83 |

Thus, with some assurance that the absorption curve is Lorentzian,

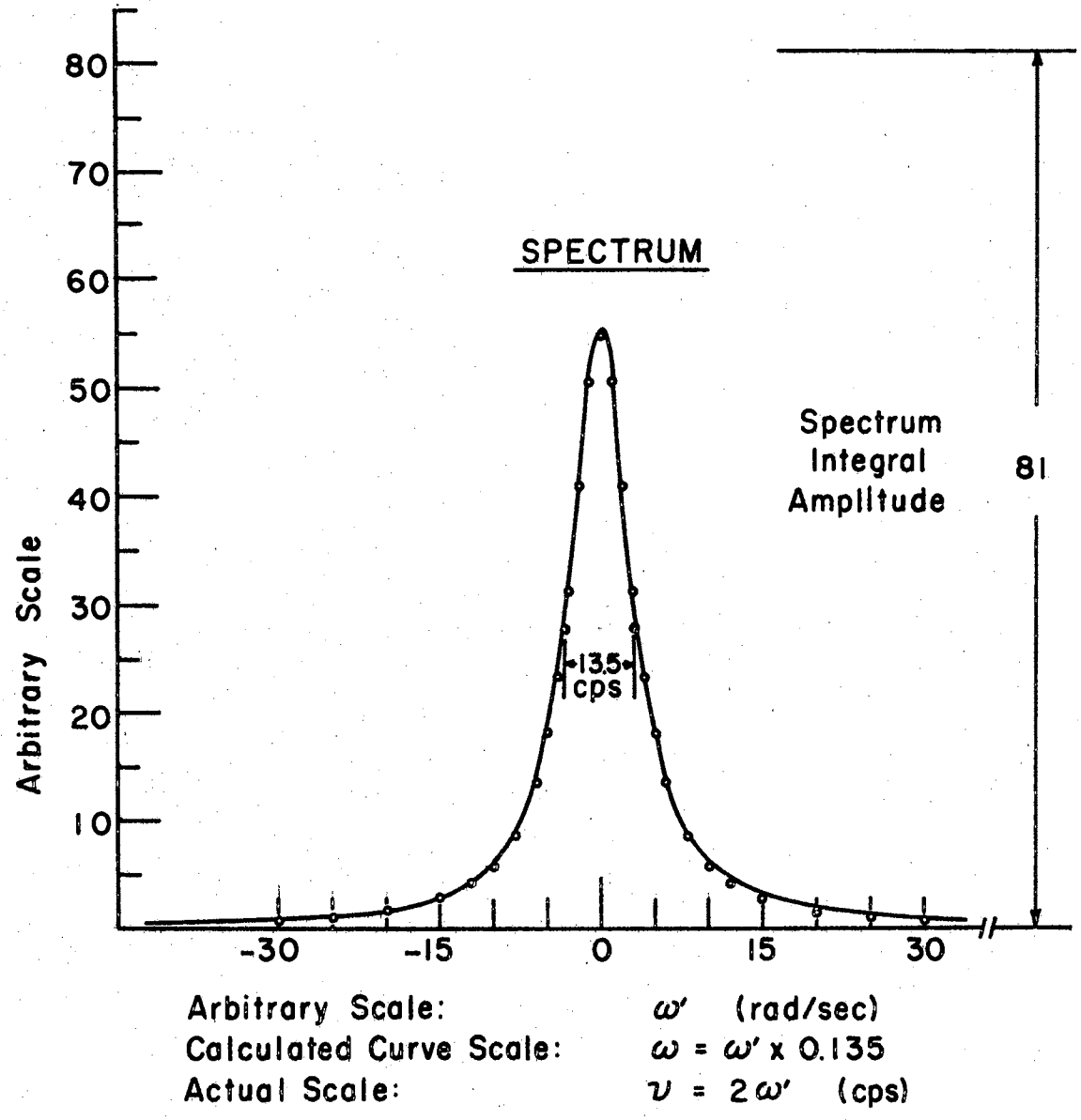


Figure 19. Absorbtion Curve for Beef Round from Varian A-60

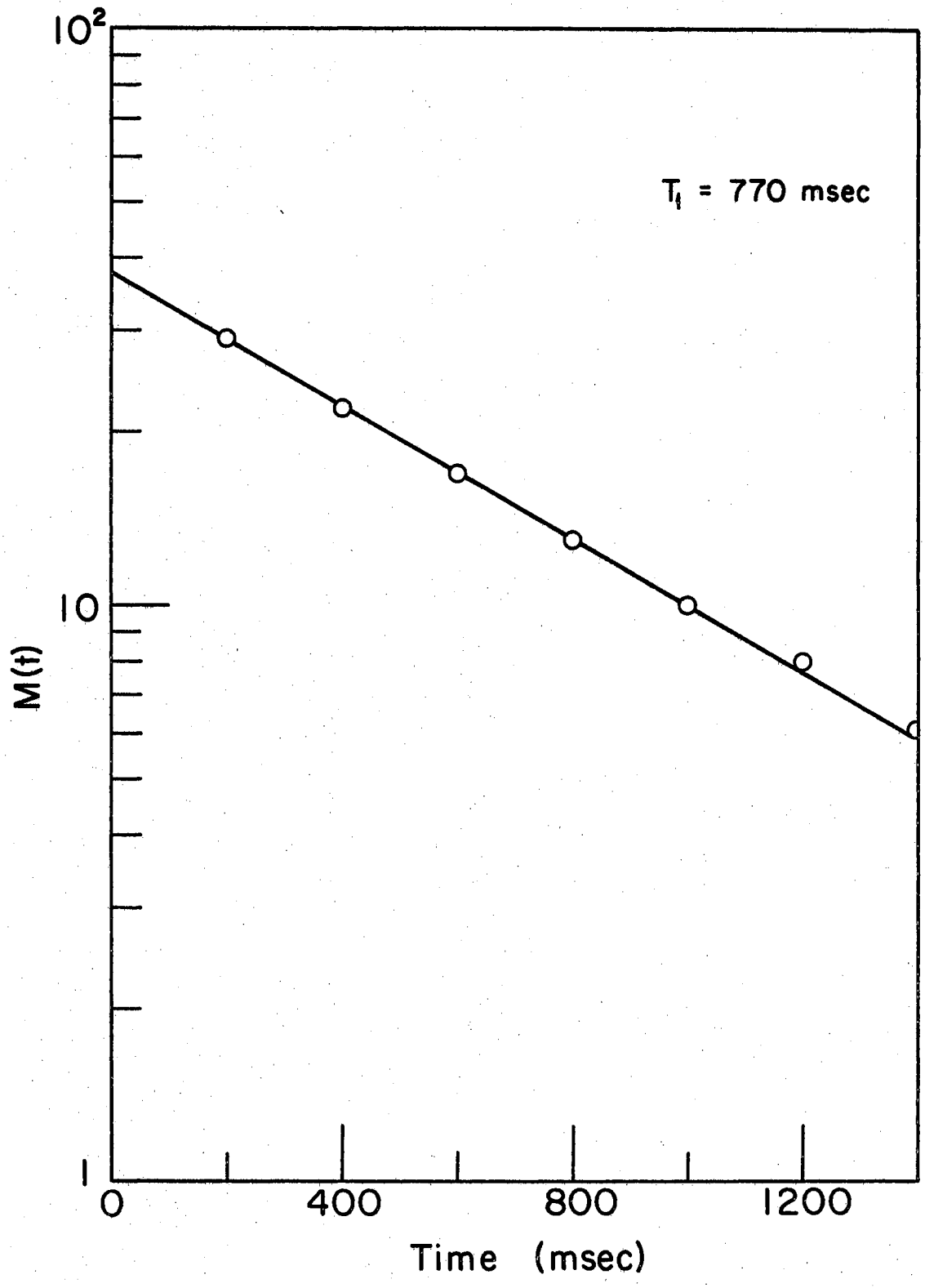


Figure 20. Spin-Echo Data for $T_1$ Determination of Beef Round

a transverse relaxation time, $T_2$, can be calculated from the width at half maximum by the equation (6):

$$T_2 = \frac{2}{(\Delta w)_{\frac{1}{2}}}$$

where $(\Delta w)_{\frac{1}{2}}$ = total frequency width in rad/sec at half maximum. The value of $(\Delta w)_{\frac{1}{2}}$ can be read directly from the absorption curve to be 2 (13.5 cps). Thus, $T_2$ is found to be 23.6 msec. at 60 megacycles and at room temperature.

However, the above equation for $T_2$ is only valid if the saturation factor (8), $1 + \gamma^2 H_1^2 T_1 T_2$, where $H_1$ is the r.f. field at which the measurements were made, is approximately one, i.e., $\gamma^2 H_1^2 T_1 T_2$ is approximately zero. Independently, measurements were made using a spin-echo apparatus to determine $T_1$ so that the saturation factor could be calculated. The graph of $\log \left[M_\infty - M(t)\right]$ vs the polarizing time, Figure 20, from the spin-echo data appears as a straight line. The measurements were made at 60 megacycles, approximately 14,000 gauss, and 26°C. $T_1$ calculated from this data equals 770 msec.

$T_2$ was then recalculated including the saturation factor in the following manner. Beginning with the equation for the magnetic susceptibility due to absorption (8), an equation quadratic in $T_2$ can be derived:

$$\chi'' = \tfrac{1}{2} \chi_o w_o \frac{T_2}{1 + T_2^2 (w_o - w)^2 + \gamma^2 H_1^2 T_1 T_2}$$

at half maximum: $$\chi'' = \tfrac{1}{2}\left[\frac{\tfrac{1}{2}\chi_o w_o T_2}{1 + \gamma^2 H_1^2 T_1 T_2}\right]$$

and thus, $$\tfrac{1}{2}\left[\frac{\tfrac{1}{2}\chi_o w_o T_2}{1 + \gamma^2 H_1^2 T_1 T_2}\right] = \frac{\tfrac{1}{2}\chi_o w_o T_2}{1 + T_2^2(\Delta w_{\frac{1}{2}})^2 + \gamma^2 H_1^2 T_1 T_2},$$

which then yields,

$$T_2^2(\Delta w_{\frac{1}{2}})^2 - (\gamma^2 H_1^2 T_1) T_2 - 1 = 0.$$

Using the values,

gyromagnetic ratio, $\gamma = 2.70 \times 10^4 \ \frac{\text{rad/sec}}{\text{gauss}}$,

r.f. field, $H_1 = 0.2$ miligauss,

$T_1 = 0.770$ sec.,

and $\Delta w_{\frac{1}{2}} = \pi(13.5)$ rad/sec.,

$T_2$ was calculated to be 23.6 msec., the same value as had been previously calculated. Thus, the saturation factor must be considerably smaller than 1, which is actually the case. The saturation factor is calculated to be $5.29 \times 10^{-3}$ or 0.00529, a pure number.

Comparing this $T_2$ value with other values obtained previously for beef round it is seen that the 23.6 msec. from the absorption curve closely approximates ${}^{s}T_2$ values found.

Before a conclusion is reached, some data which adds confusion is submitted. $T_2$ measurements at 14,000 gauss and 26°C were also made on the spin-echo apparatus. These data are displayed in Figures 21a and 21b. The figures show that the decay of the transverse component of the

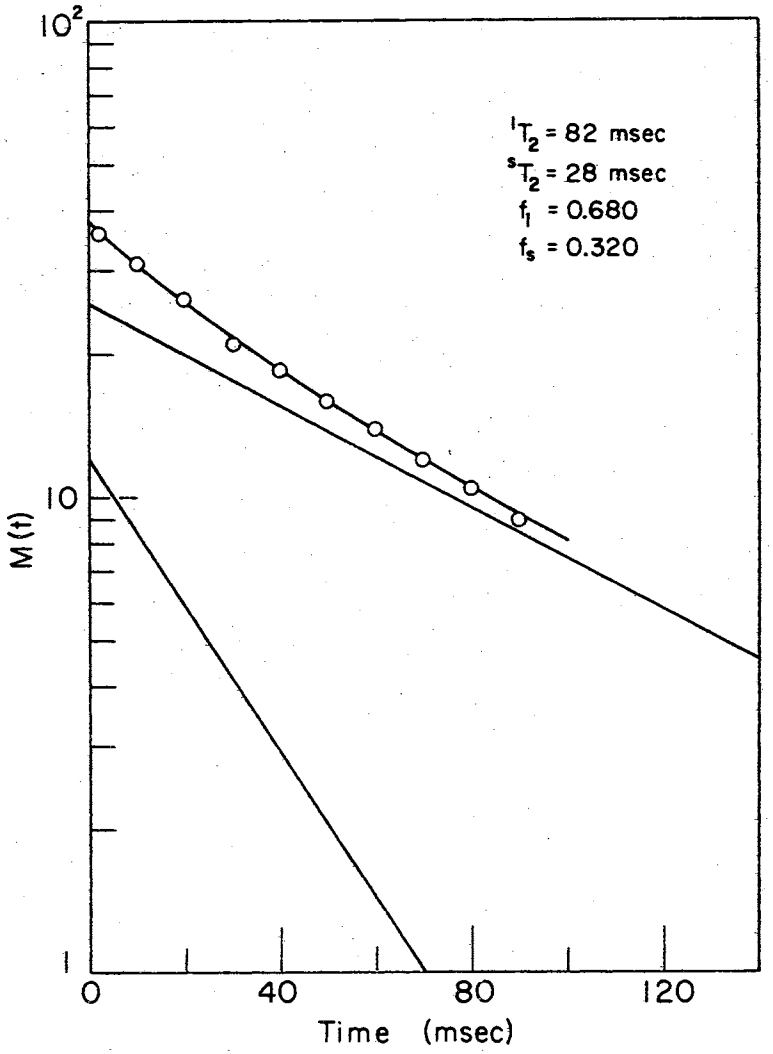


(a) First Measurement

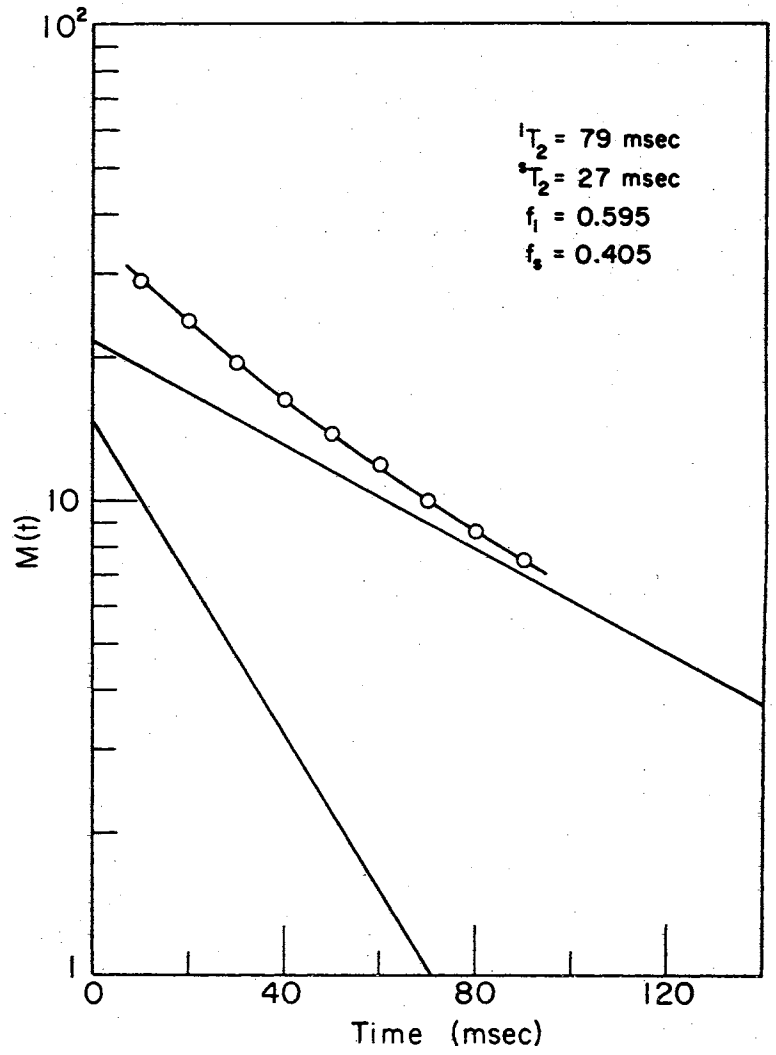


(b) Second Measurement

Figure 21. Spin-Echo Data for $T_2$ Determination of Beef Round

magnetization, is nearly exponential, but there is a slight curvature. It is not understood why the signal from the spin-echo apparatus is non-exponential while the signal from the A-60 is Lorentzian.

Applying the "best fit" technique to analyze the spin-echo data, the following sets of numbers were obtained:

For Figure 23a, $f_l = 0.680$ $\quad f_s = 0.320$

$^{l}T_2 = 82$ msec. $\quad ^{s}T_2 = 28$ msec.

For Figure 23b, $f_l = 0.595$ $\quad f_s = 0.405$

$^{l}T_2 = 79$ msec. $\quad ^{s}T_2 = 27$ msec.

The relaxation times for each figure are comparable, but the fractions of signal contributions deviate by about 15% from Figure 21a to Figure 21b. The fitting procedure can probably be blamed for the discrepency.

Regardless of the deviations in the $f_l$ values, the values obtained for $^{l}T_2$ and $^{s}T_2$ (at 14,000 gauss) are approximately equal to the values measured in the earth's field ($\approx 0.5$ gauss) using the EFP apparatus. This somewhat impressive result indicates that $T_2$ is independent of the field and agrees with the Bratton, Hopkins, and Weinberg model (5) for the $T_2$ relaxation (refer to Chapter I).

## Human Arm Experiments

Hope for explaining the data from human arms measurements has somewhat dwindled since the project was first begun. The reason for this is that the human arm system is so much more complex than, the beef round sample which has been studied. Data for the much simpler system, beef round, cannot be explained with much consistency.

The measurements of human arms were made with objectives in mind:

1) To confirm Ligon's observation of the non-exponential properties of the signal,

2) To obtain values of the fitting parameters for human forearms,

3) To determine the variance of these parameters from person to person, and

4) To compare the values obtained with the values of the parameters previously found by Ligon and the discussed beef measurements.

Possibly a general description of the forearms of subjects #1 and #9 is in order before the $T_1$ data for them is discussed. Subject #1 is a female, 20 years of age. Her muscle tone is thought to probably be representative for females of her age; although her forearm would be considered somewhat fattier than an average 20 year old male's forearm. Generally speaking, it is inherent that women have somewhat fattier tissue than men of the same age group. Subject #9 is a male, 20 years of age. His forearms were extremely hard and well-muscled, though they were not large.

The fitting parameters found from the $T_1$ field dependence measurements for subjects #1 and #9, Figures 22 and 23 and Tables VIII and IX, roughly show the same characteristics. $^{l}T_1$ and $^{s}T_1$ increase slightly with an increase in the field. $f_1$ seems to be fairly constant for subject #9 at a point somewhat above the value 0.5; for subject #1, $f_1$ has a greater amount of scatter, but it, too, has an average value of about 0.5. This value of 0.5 is just the value Ligon (4) found. But we know $f_1$ has no direct correlation with a single anatomical component as Ligon assumed. Also, it may be mentioned that the $f_1$ value of 0.5 is

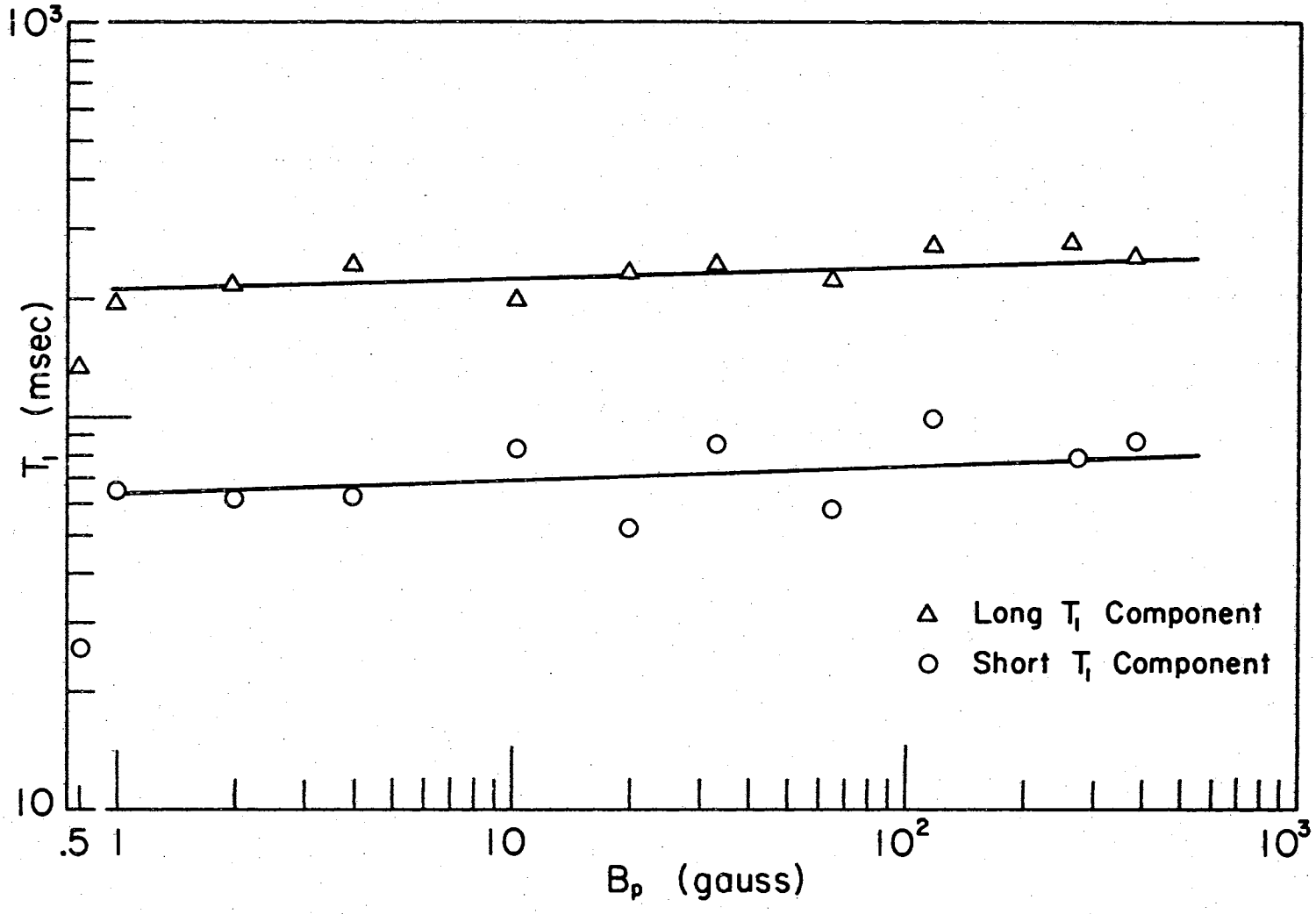


Figure 22. Log $T_{1,2}$ Versus Log B for Subject #1

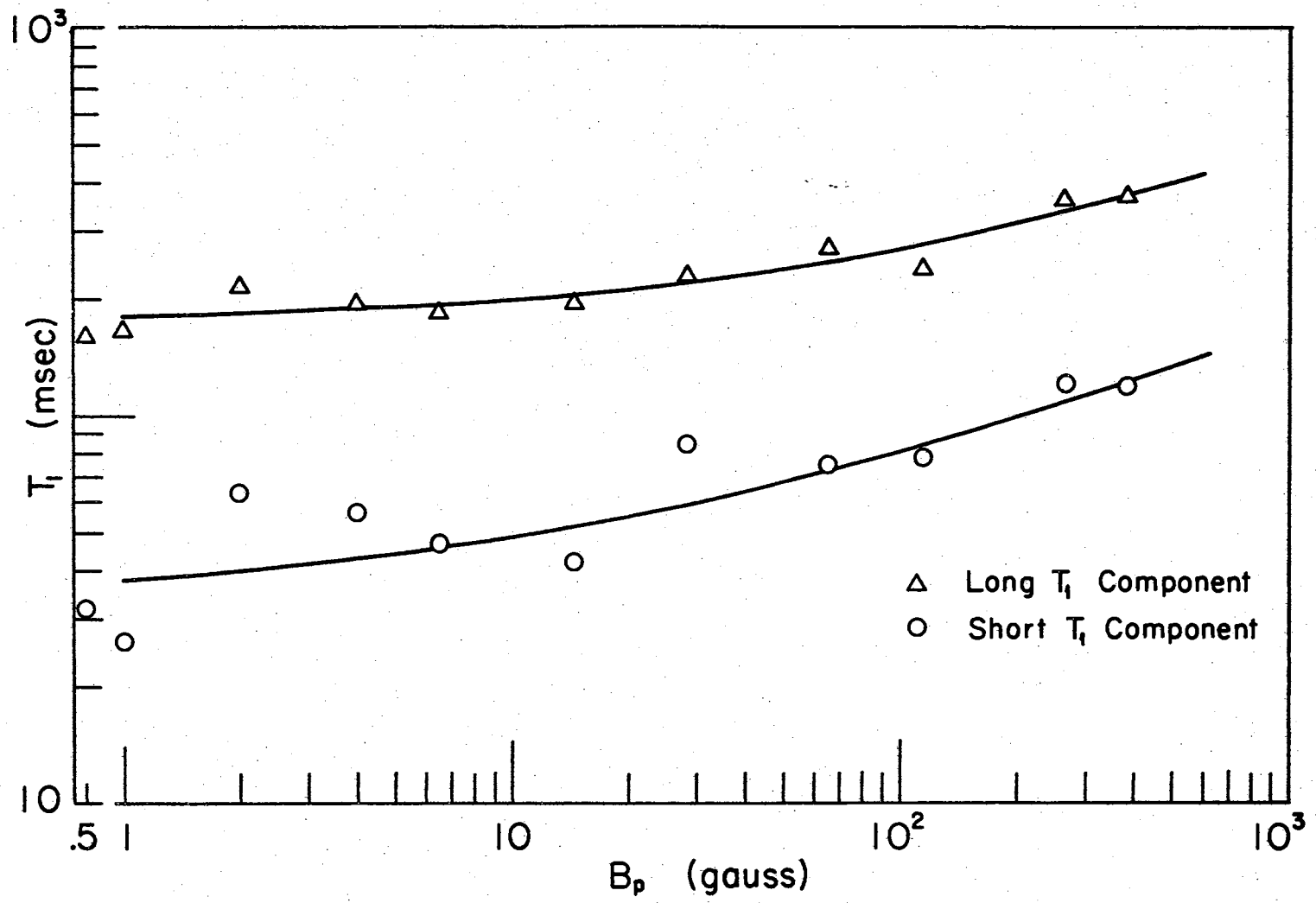


Figure 23. Log $T_{1,2}$ Versus Log B for Subject #9

approximately that obtained for beef round, and the $T_1$ values from the forearms are included within the range of values found for beef round and fat.

TABLE VIII

FITTING PARAMETER VALUES FOR SUBJECT #1

| Field (gauss) | $^{l}T_1$ (msec) | $^{s}T_1$ (msec) | $f_l$ | $f_s$ |
|---|---|---|---|---|
| 384 | 252 | 87 | 0.630 | 0.370 |
| 266 | 275 | 78 | 0.571 | 0.429 |
| 118 | 272 | 99 | 0.381 | 0.619 |
| 65 | 220 | 58 | 0.726 | 0.274 |
| 33 | 242 | 85 | 0.450 | 0.550 |
| 20 | 230 | 52 | 0.547 | 0.453 |
| 10 | 195 | 83 | 0.988 | 0.512 |
| 4 | 243 | 63 | 0.414 | 0.586 |
| 2 | 217 | 62 | 0.454 | 0.546 |
| 1 | 193 | 65 | 0.518 | 0.482 |
| ($T_2$ Data) @ ½ gauss | 137 | 26 | 0.295 | 0.705 |

The data obtained by the $T_2$ measurements are shown by the graphs of log M(t) vs decay time in Figures 24 through 26. Table X is a compilation of $^{l}T_2$, $^{s}T_2$, and $f_l$ values for all the subjects. The sex of the subject is also indicated. It is seen that the $^{l}T_2$ and $^{s}T_2$ values are all approximately the same from person to person, with no distinguishable differences of values for male subjects when compared to those

TABLE IX

FITTING PARAMETER VALUES FOR SUBJECT #9

| Field (gauss) | $^{l}T_1$ (msec) | $^{s}T_1$ (msec) | $f_l$ | $f_s$ |
|---|---|---|---|---|
| 383 | 365 | 120 | 0.509 | 0.491 |
| 266 | 360 | 120 | 0.490 | 0.510 |
| 115 | 238 | 78 | 0.557 | 0.443 |
| 65 | 268 | 75 | 0.468 | 0.532 |
| 28 | 230 | 85 | 0.493 | 0.507 |
| 14 | 195 | 42 | 0.519 | 0.481 |
| 6.5 | 183 | 47 | 0.599 | 0.401 |
| 4 | 192 | 56 | 0.566 | 0.434 |
| 2 | 215 | 63 | 0.525 | 0.475 |
| 1 | 165 | 26 | 0.594 | 0.406 |
| $T_2$ Measurements @ ½ gauss | 160 | 32 | 0.189 | 0.811 |

TABLE X

$^{l}T_2$, $^{s}T_2$, $f_l$ VALUES FROM THE HUMAN ARM MEASUREMENTS

| Subject | Sex | $^{l}T_2$ | $^{s}T_2$ | $f_l$ |
|---|---|---|---|---|
| #1 | F | 137 | 26 | 0.295 |
| #2 | F | 124 | 37 | 0.364 |
| #3 | F | 161 | 34 | 0.195 |
| #4 | M | 170 | 34 | 0.243 |
| #5 | F | 142 | 34 | 0.320 |
| #6 | M | 130 | 31 | 0.217 |
| #7 | F | 157 | 38 | 0.315 |
| #8 | F | 180 | 43 | 0.282 |
| #9 | M | 160 | 32 | 0.189 |

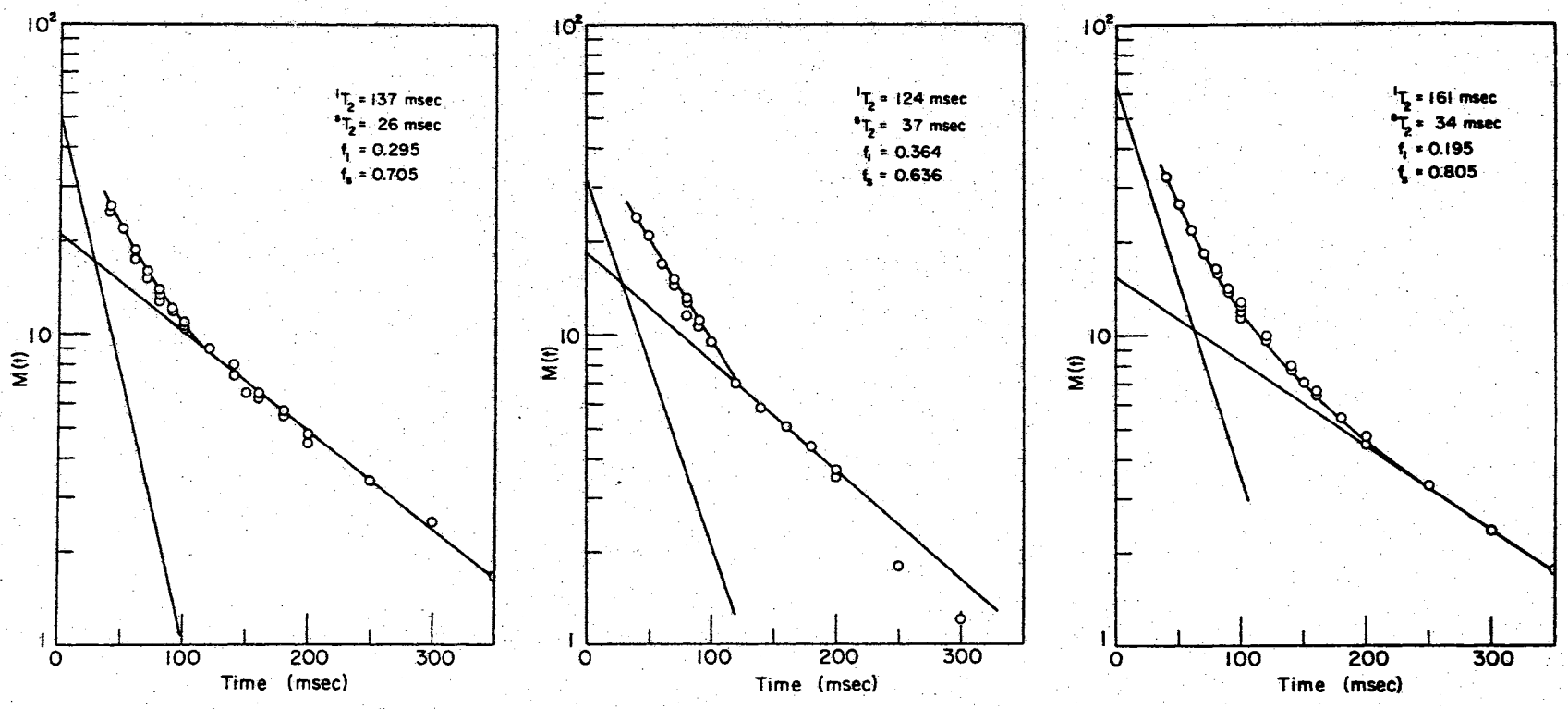


(a) Subject #1 (b) Subject #2 (c) Subject #3

Figure 24. $T_2$ Data Plots for Subjects #1, #2, #3

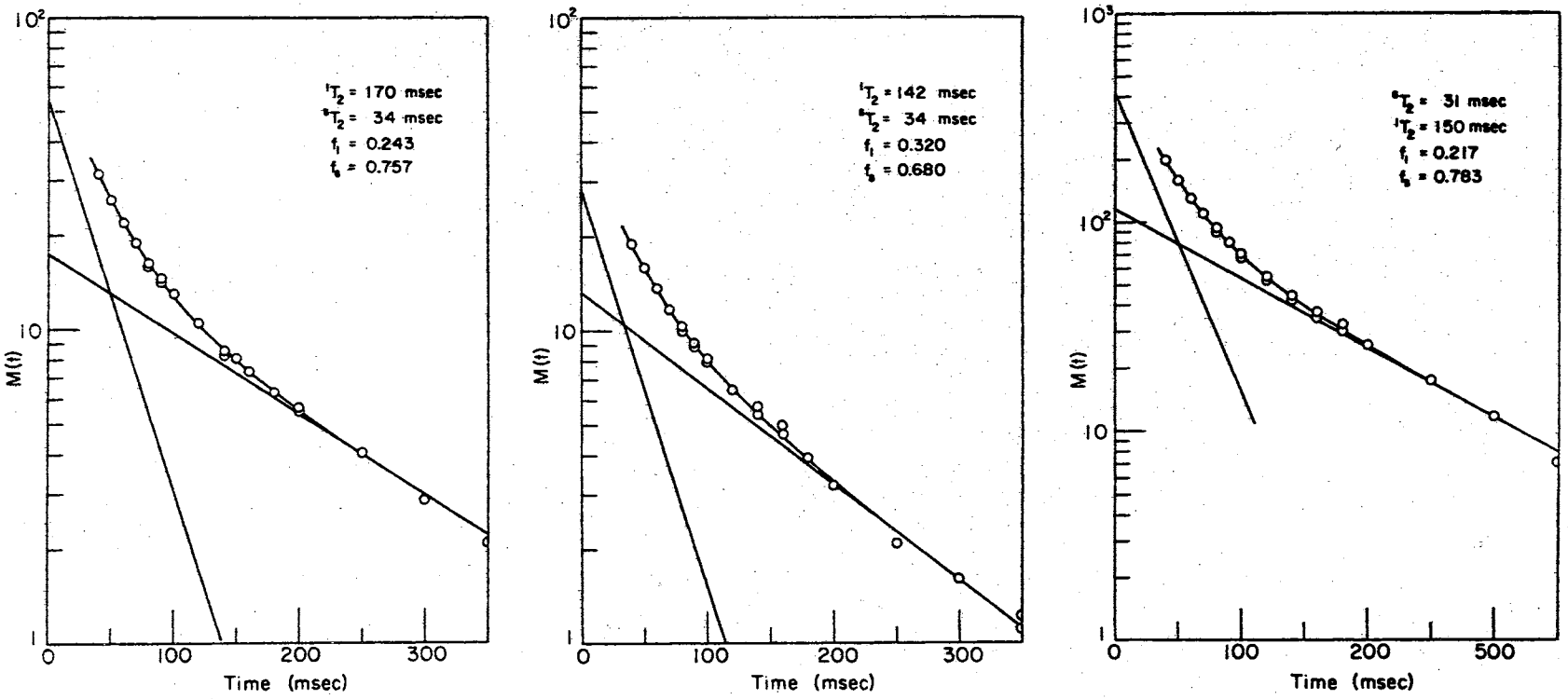


(a) Subject #4 (b) Subject #5 (c) Subject #6

Figure 25. $T_2$ Data Plots for Subjects #4, #5, #6

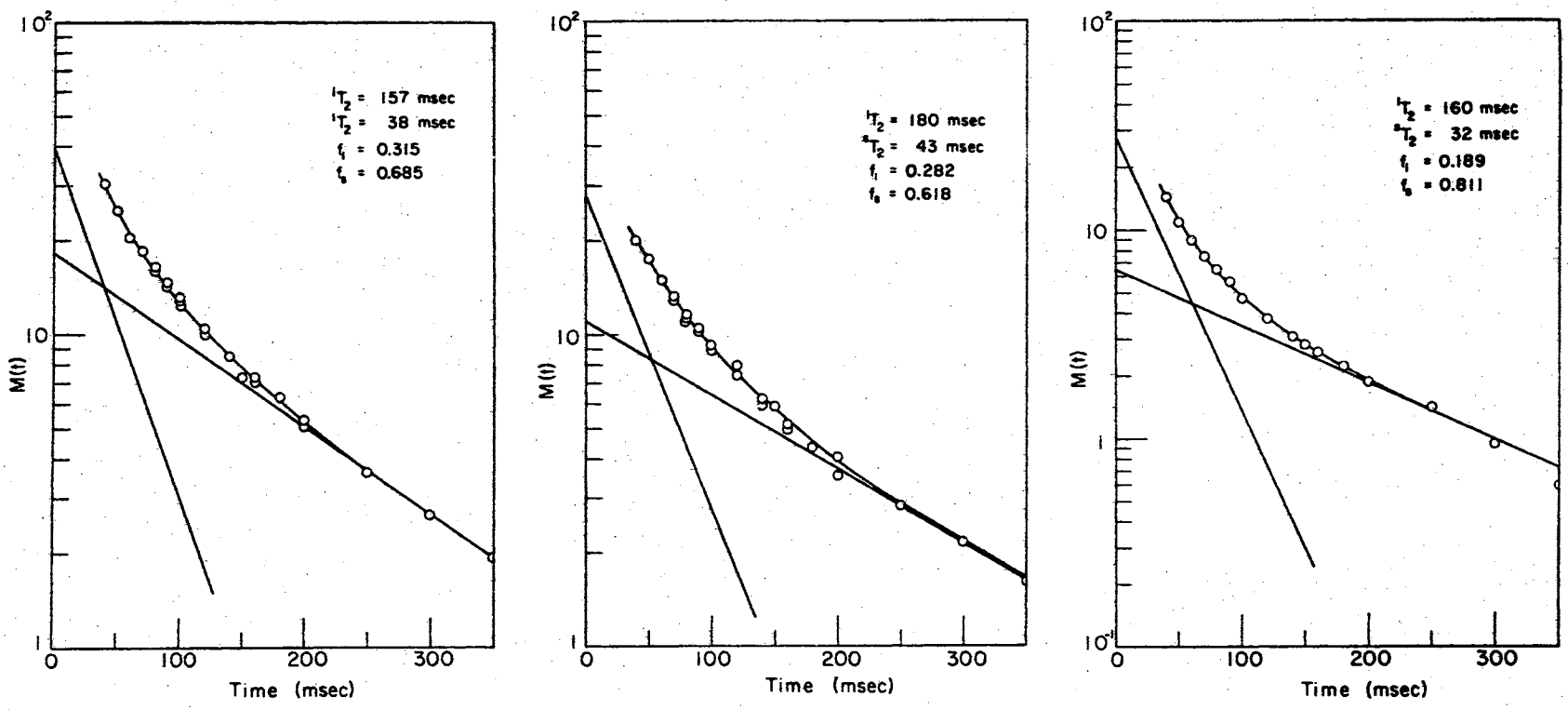


(a) Subject #7 (b) Subject #8 (c) Subject #9

Figure 26. $T_2$ Data Plots for Subjects #7, #8, #9

female subjects.

However, the $f_1$ values do seem to show some correlation with the characteristics of the subject. The $f_1$ values for males are all lower than the $f_1$ values for females, except for one, subject #3. Subject #3 is a very thin person and it could very well be that she is less fatty than the average female in this age group. A very good reason for this correlation of the $f_1$ values to the sex of the subject is that, in general, females have a heavier layer of adipose tissues than do males; and, thus it can be reasoned that $f_1$ values for males would be smaller.

This can probably be seen by the following hypothetical illustration. Let the $T_2$ decay signal from muscle be,

$$M(t) = Le^{-t/150} + Se^{-t/35},$$

and from fat be,

$$M(t) = Fe^{-t/80}.$$

where

L = the amount of signal contributed by the long relaxation time component of muscle.

S = the amount of signal contributed by the short relaxation time component of muscle.

F = the amount of signal contributed by the protons of fat.

Thus, the actual signal observed is,

$$M(t) = Le^{-t/150} + Se^{-t/35} + Fe^{-t/80}$$

Fitting this shape with the sum of two exponentials, the $f_1$ value will

be greater than it was for the pure muscle sample, and if the signal from fat becomes larger, $f_1$ will increase accordingly. This can be shown graphically.

## Other Experiments

A few other experiments are reported in this section[3]. These experiments were performed just as a matter of curiosity more than anything else.

Some measurements were taken on samples of chicken breasts and thighs. The data is presented in Figures 27a, 27b, and 27c. The $T_2$ graphs for chicken thighs are seen to be exponential for two temperatures, 5°C and ambient temperatures ($\approx$25°C). The values of $T_2$ for chicken thighs are seen to be within the same range of values obtained for beef round. The graph of the $T_2$ data at 5°C from the chicken breasts is non-exponential. The relaxation times $^{l}T_2$ = 40 msec. and $^{s}T_2$ = 10.5 msec. are much shorter than those obtained for any of the other experiments previously discussed. The $f_1$ value of 0.018 is much smaller than any $f_1$ value obtained previously; it is about one-tenth as large as that for lean beef.

$T_2$ experiments were also performed on samples from two varieties of fish: Sun Fish and Blue Gill. These fish were gutted and scaled before measurements were made. The data from these experiments is pre-

---

[3]Experiments much like these in this section are reported by J. A. Jackson and W. H. Langham (1). These workers use low field equipment, as we do, but they base an interpretation of the phenomenon upon the shape of the first derivative of the absorption rather than the relaxation of the proton signal.

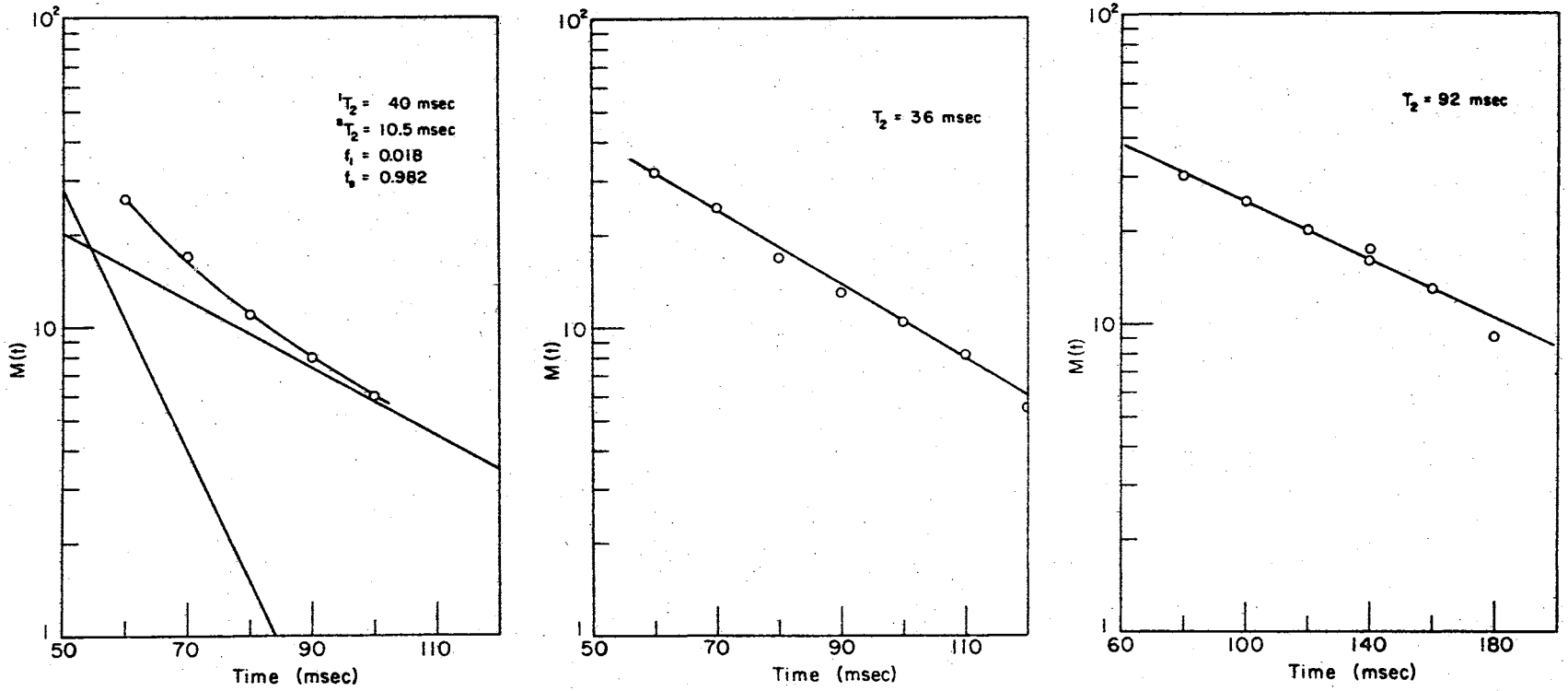


(a) Chicken Breast @ 5°C (b) Chicken Thighs @ 5°C (c) Chicken Thighs @ R.T.

Figure 27. $T_2$ Data Plots for Chicken Samples

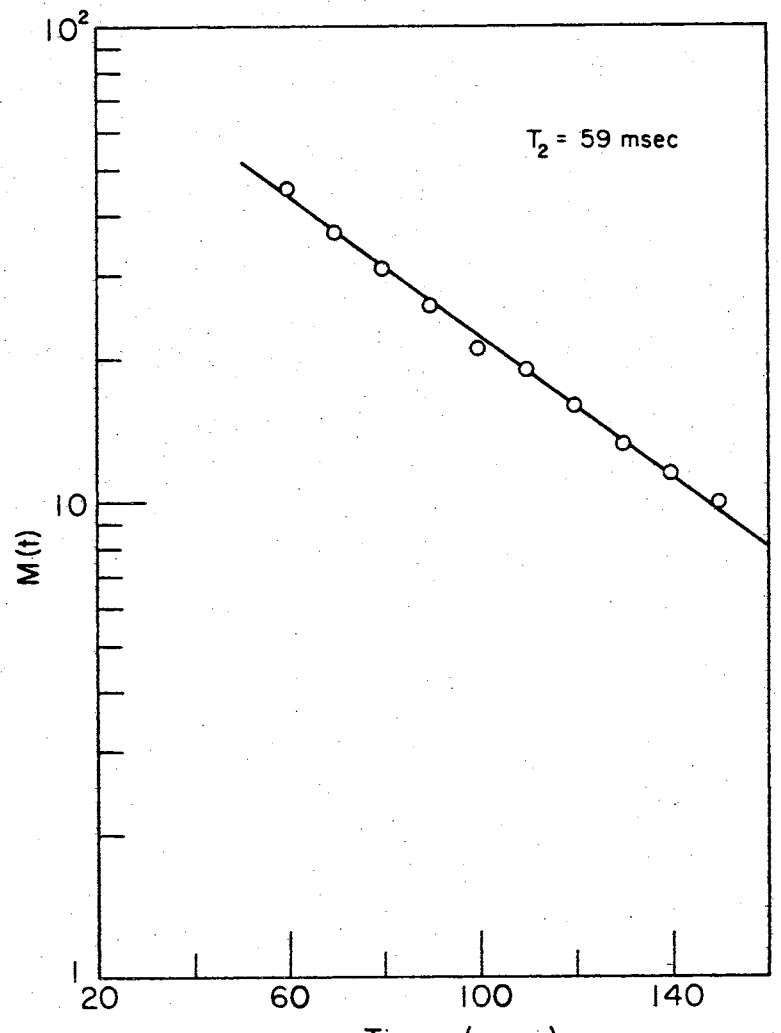


(a) Sun Fish @ 5°C

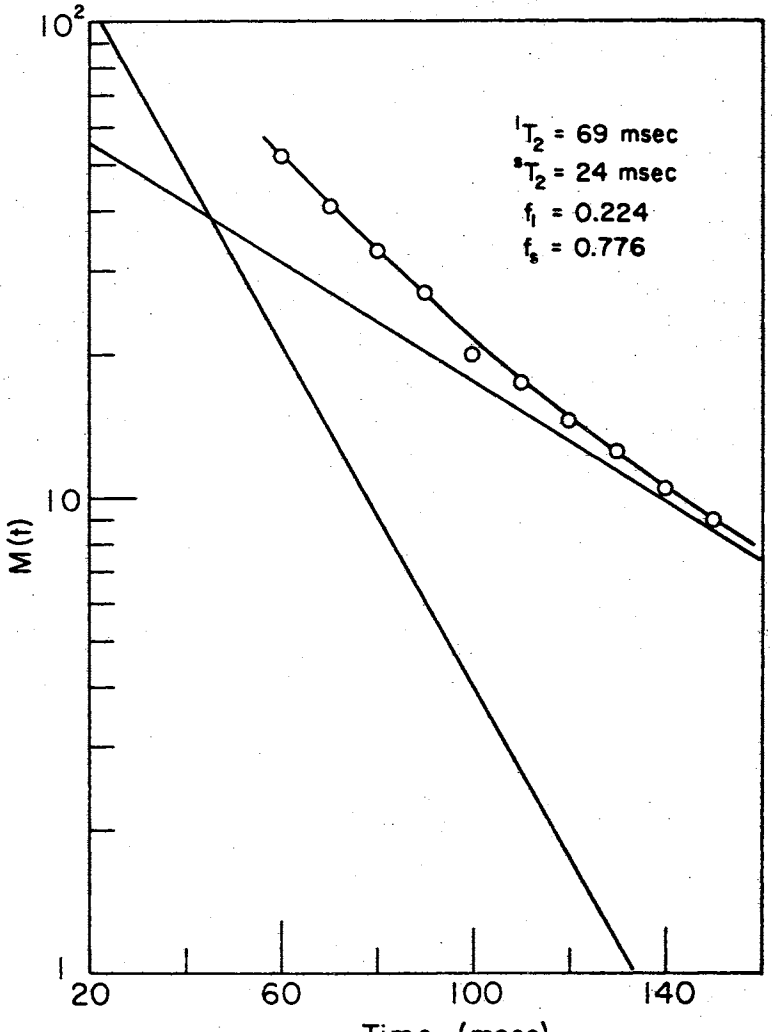


(b) Blue Gill @ 5°C

Figure 28. $T_2$ Data Plots for Fish Samples

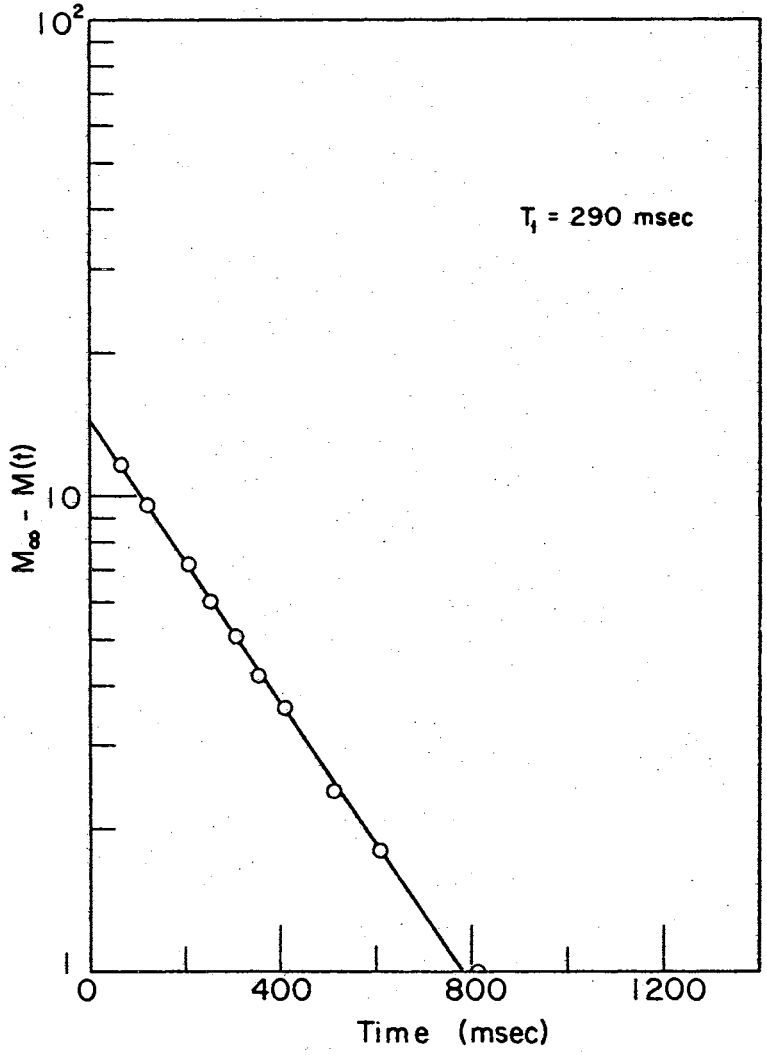


(a) $T_1$ Data @ 5°C

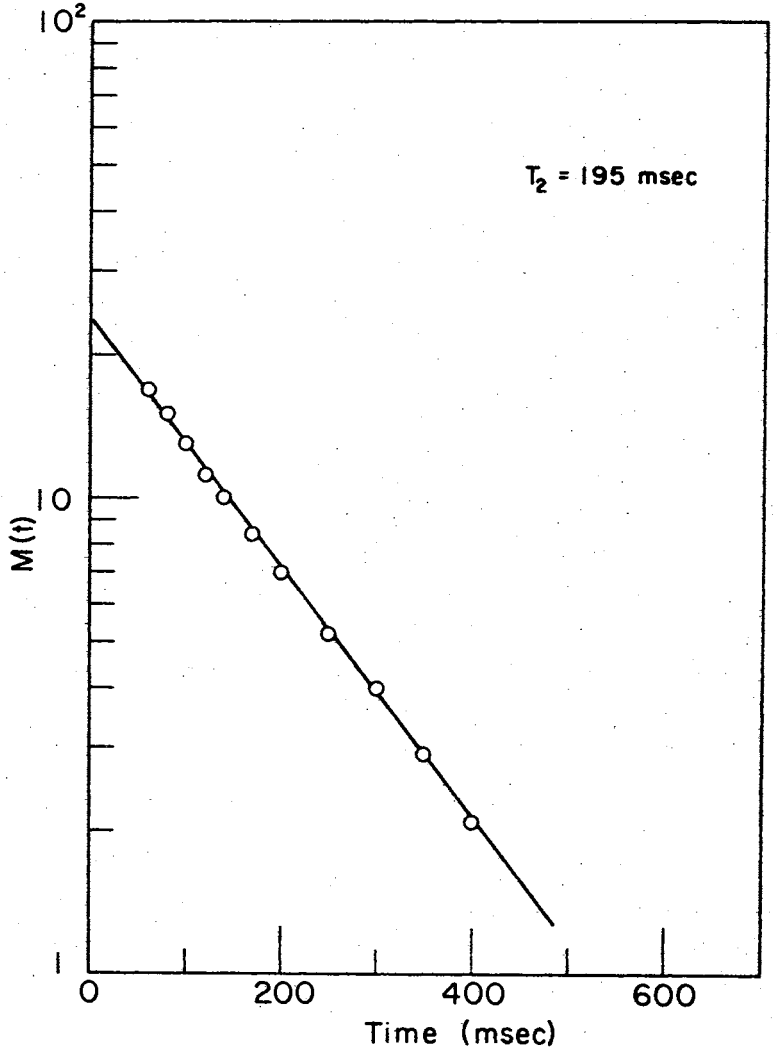


(b) $T_2$ Data @ 5°C

Figure 29. $T_1$ and $T_2$ Data Plots for Chicken Eggs at 5°C

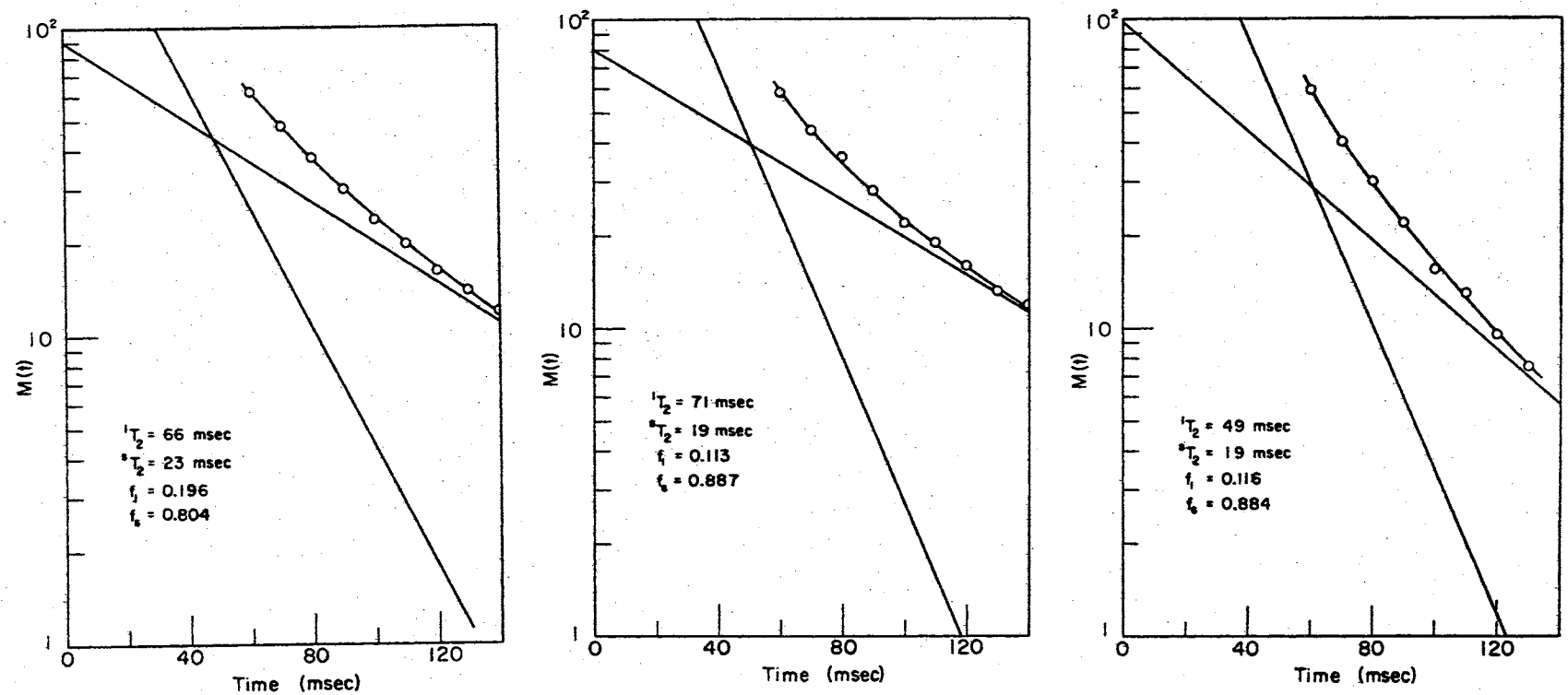


(a) Chunks @ R.T. (b) Ground @ R.T. (c) Emulsified @ R.T.

Figure 30. $T_2$ Data Plots for Chunks, Ground, and Emulsified Samples of Beef Round

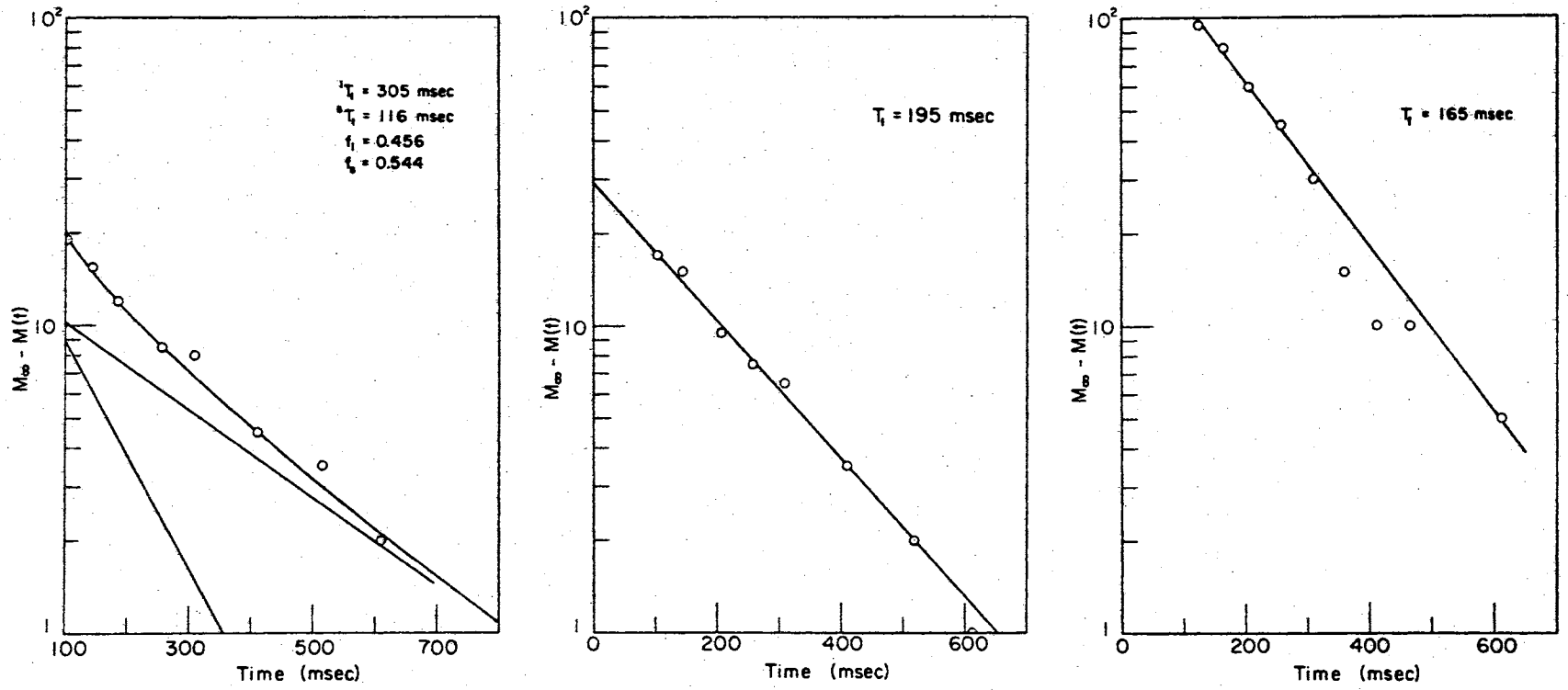


(a) Chunks @ R.T. (b) Ground @ R.T. (c) Emulsified @ R.T.

Figure 31. $T_1$ Data Plots for Chunks, Ground, and Emulsified Samples of Beef Round

sented in Figures 28a and 28b. The graph for the data obtained from the Sun Fish is seen to be exponential with a $T_2$ value of 59 msec. The graph for the Blue Gill is non-exponential with values of the fitting parameters comparing very well with those for beef round.

$T_1$ and $T_2$ measurements were made on a sample of chicken eggs. The eggs were put in a sample container with their yolks unbroken. The graphs of the $T_1$ data and the $T_2$ data displayed by Figures 29a and 29b, are both seen to be exponential over a fairly large range of polarizing and decay times. The $T_2$ value of 195 msec. is somewhat larger than that normally seen for the other kinds of samples treated.

The next set of experiments was to investigate the differences of the graphs of the data and the fitting parameters obtained from the graphs for chunks of beef round, ground beef round, and emulsified beef round. The results of the data are given by Figures 30 and 31. For the $T_2$ measurements, the fitting parameter values for the chunks compared to the ground sample are approximately the same. However, the $^1T_2$ value for the emulsified sample is about 20 msec. shorter than those values obtained for the ground and chunks samples.

Something unusual was seen for the $T_1$ data plots. The graph for the chunks sample is non-exponential while the graphs for the ground and emulsified samples are exponential. The overall relaxation rate for all three samples, however, is approximately the same.

The last experiments were to examine the effects of heating a sample of beef round for a period of 30 min. @ 70°C. $T_1$ and $T_2$ measurements were made before and after the sample had been heated, with the sample being allowed to cool down to room temperature after being heated. It

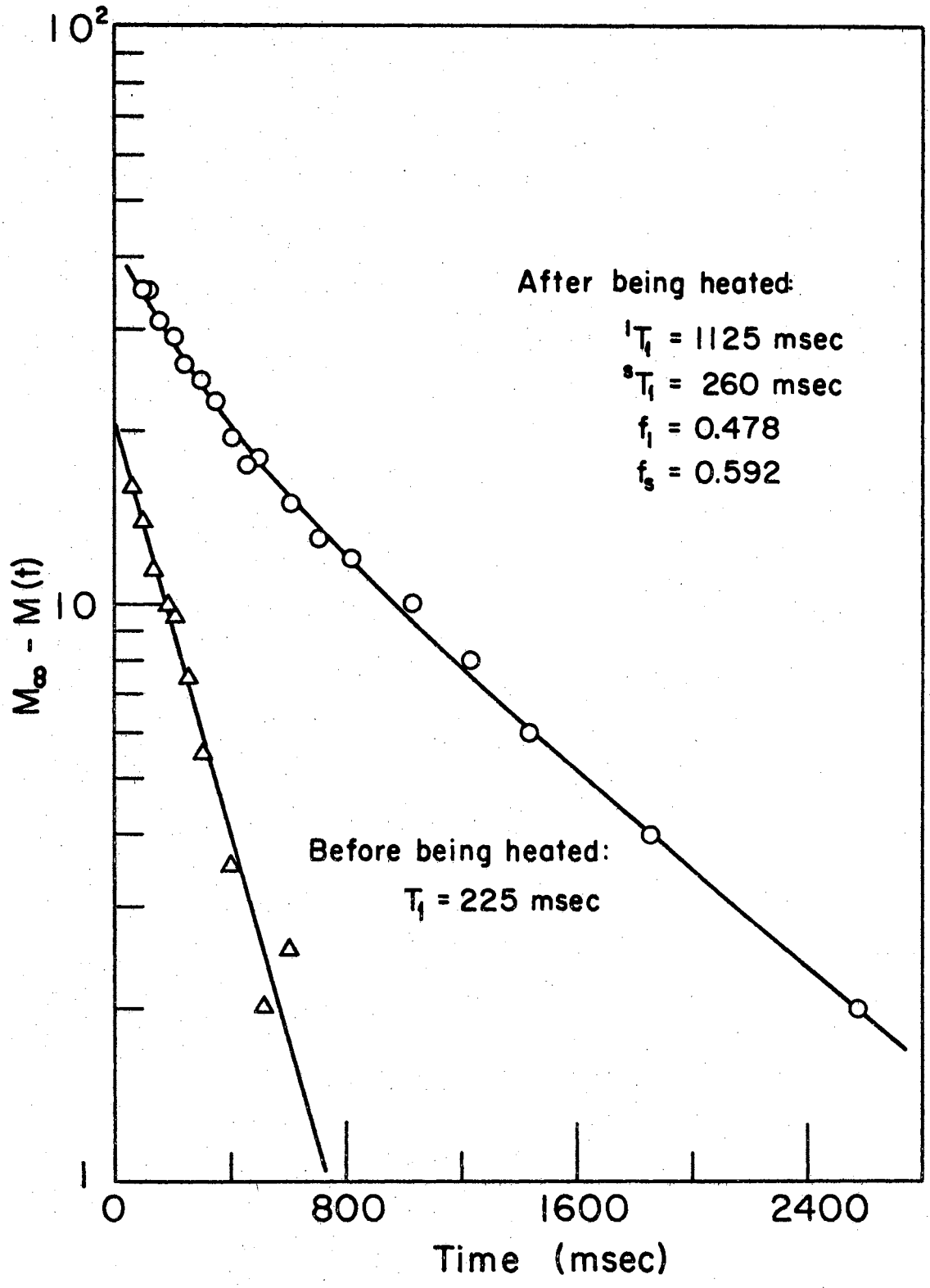


Figure 32. $T_1$ Data Plots for Beef Round Before and After Being Heated at 70°C.

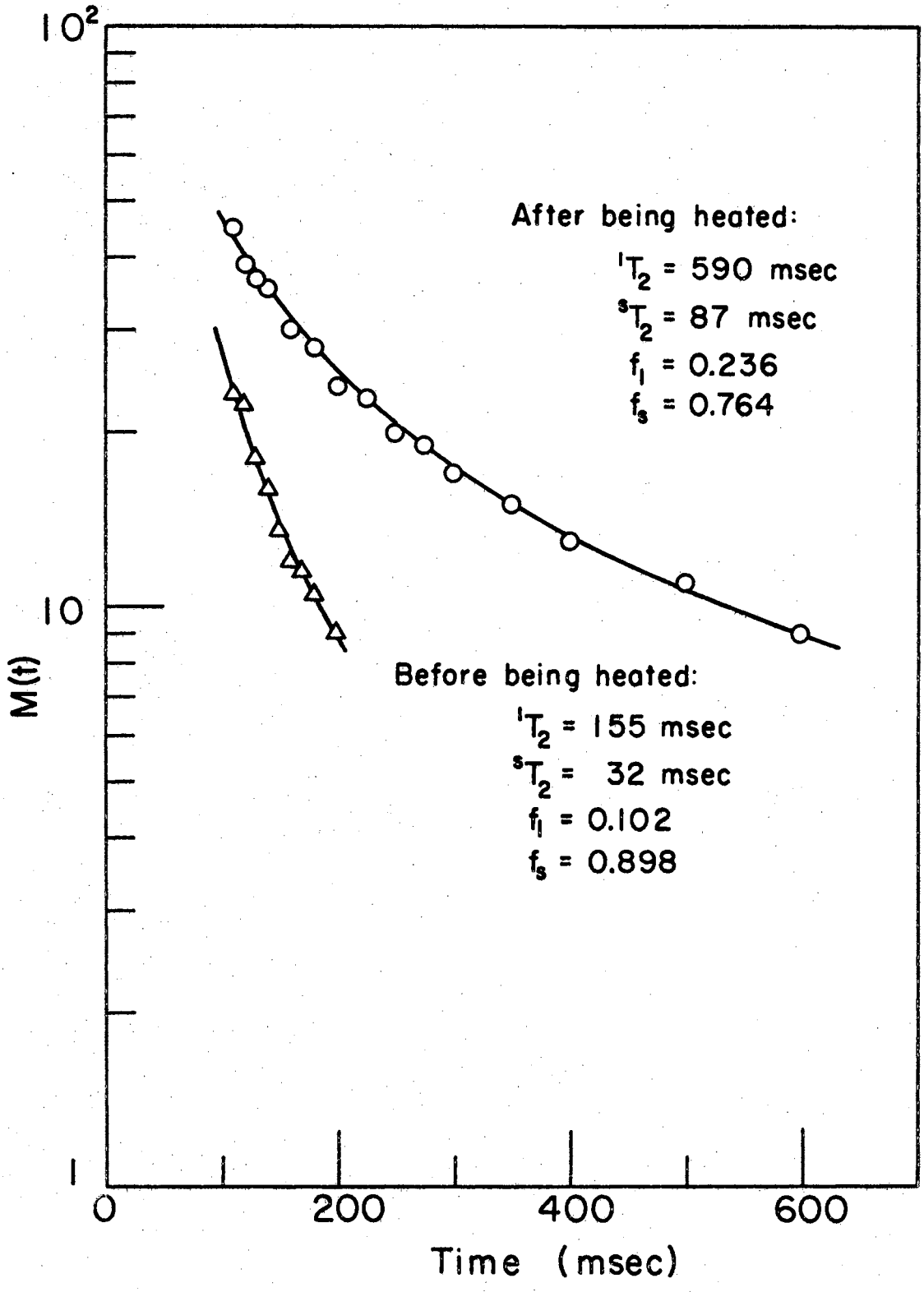


Figure 33. $T_2$ Data Plots for Beef Round Before and After Being Heated at 70°C.

is known that most of the water which is not hydrated to the proteins can be freed by this method (9). The results of the experiments are shown graphically by Figures 32 and 33. Figure 32 is the $T_1$ data for both the before and after states of the sample; and, likewise, Figure 35 is the $T_2$ data for both states of the beef sample. Simply put, the change seen for both graphs is the immense increase of the relaxation times after the sample has been heated.

# CHAPTER IV

## SUMMARY AND CONCLUSIONS

From the hypothesis by T. Ligon (4) that the sum of two exponentials describes the signal observed from human arms, one component corresponding to the fat tissue and the other to the muscle, arose the idea that possibly by making a survey study of a simpler system, such as beef round, some ideas could be found to help explain the human arm data. However, the observations on beef round, and likewise for beef liver and fat were not found to be simple.

Continuing to use the sum of two exponentials model to fit the data, even though the clarity regarding the nature of the components was missing, values for the fitting parameters were obtained. Sometimes the $T_1$ measurements yielded exponential graphs of the $\log \pm [M_\infty - M(t)]$ versus polarizing time, and sometimes the data graphed as non-exponentials. This seemed to occur only at fields of from 200 to 500 gauss. Nevertheless, it was seen from these measurements that Ligon's hypothesis was wrong because, in some cases, the graphs obtained from each fat and muscle tissue, were shown to be non-exponential. Also, this determination challenges Bratton, Hopkins, and Weinberg's model for the relaxation; their model will only explain exponentials.

The separation experiments, coupled with the results from the aging experiments and the analysis of the "best fit" method in Appendix B, were probably the experiments which showed the most promise for the sum

of two exponentials model. It will be recalled that the aging experiments showed the relaxation times increased with the aging of the sample. Appendix B showed that even if the signal is actually the sum of two exponentials,the relaxation times obtained using it will always be shorter than the true values. The comparison of the solid and liquid separation sample's field dependence curves with the corresponding plots of $T_1$ $^{l}T_1$, $^{s}T_1$, $^{l}T_2$, and $T_2$ vs B for the previously unseparated beef round sample was very favorable when allowing for the aging of the sample and the errors caused by the fitting technique. At this point the model, consisting of the sum of two exponentials, seemed fairly good except there still remained the problem of determining the nature of the two components of the signal. However, this certainly would not explain the erratic exponential behavior seen for the beef round sample

It was questioned if perhaps $f_1$ varied with the field. If $f_1$ does vary with the field strength in such a way that at high fields $f_1$ $f_s$, then this would explain why the exponential is seen for the $T_1$ measurement at high fields on the spin-echo equipment. But, for all of the field dependence measurements on the EFP apparatus, there was no clearly seen, orderly dependence of $f_1$ on B. At best, for the measurements using the EFP apparatus, the value of $f_1$ was estimated from the scattered values to be constant at the value 0.5. The $f_1$ values for $T_2$ measurements from the spin-echo and EFP apparatus show another anomoly. The $f_1$ value from the two spin-echo measurements was seen to be about 0.6 and for the numerous EFP measurements it is fairly well defined to be the value of 0.16. Thus, it would seem, in contrast to the $T_1$ measurements, that this would show a field depend-nce for the $f_1$

parameter.

The fact that the fitting parameters obtained from the EFP $T_2$ measurements were so repeatable enhanced the feeling that the sum of two exponentials is the model to use. It is also noted, as also mentioned by Ligon, that muscle tissue nominally has 80% of its water in intracellular fluid and 20% in extracellular fluids. These numbers so closely resemble the fractions of the signal components, that it was certainly thought that intracellular and extracellular water are, the contributors to the signal. They should be contributors. And, in the feeling of the author, they should be the major contributors.

A very appealing idea comes from a paper by H. J. C. Berendsen and C. Migchelsen (10). The article explains that water assumes an ordered structure near protein surfaces, and that water molecules adhere to each other and protein molecules in such a way so as to form a chain in the fiber direction of the protein. Because of this "ordering" of the protons, the protons have certain rotations which are hindered. The effect of "ordering" and the hindered rotations causes the signal shape (the first derivative of the absorption) to vary with the direction of the field relative to the fiber direction.

Information given the author by Dr. V. L. Pollak states that the anisotropy effect described by Berendsen and Migchelson has been investigated at Case-Western Researve University using frog muscle and collagen. For the frog muscle no anisotropy effect was observed, whereas for the collagen anisotropy was observed in agreement with Berendsen and Migchelsen's observations[10].

The above idea applied to our data would explain why exponential signals are obtained in some cases whereas in others non-exponentials

are seen. That is, for the specific comparison of the spin-echo $T_2$ data to the A-60 data the fibers in the sample tubes had, to a large extent, a particular orientation. This orientation was such that the field made the proper angle with the fiber orientation to obtain a Lorentzian line shape, indicative of a single exponential. And for the spin-echo sample the sample cored just happened to have its fibers oriented at a somewhat different angle to the equipment's field and this yielded a signal for the $T_2$ decay which was slightly non-exponential. These arguments can be extended to the $T_1$ measurements on the EFP apparatus.

However, the $T_2$ measurements at low fields seem insensitive to the above hypothesis. These troublesome data are certainly difficult to explain, but it is believed that, overall, this explanation relating the orientation of the fibers to the signal shape is better than any of the others.

Because the sum of two exponentials model doesn't seem to give results which show definite, realistic trends for the fitting parameters involved, a model for the signal shape is proposed which is the sum of three exponentials. The three contributing components of this model are the extracellular water, the intracellular water, and, as discussed above, the water hydrated onto the proteins. It is noted that Berendsen and Migchelsen (10) used the sum of three Lorentzians to analyze their data. However, they do not give the reasons for their using the sum of three Lorentzians and it is assumed that the components of the signal are as described previously.

There is a feeling that if the validity of the model proposed, or any models, is to be really tested, two things must be done:

1) A larger diameter coil with a higher Q value needs to be built

for the EFP equipment. This would greatly increase the accuracy of the data by being able to obtain a larger signal.

2) The fitting parameters for the model used need to be found by a computer fit of the data.

With these two innovations, and with additional measurements, it should be possible to obtain more reliable data. Moreover, the data acquired could be more accurately compared with a model especially if the data could be fitted by computer methods.

A SELECTED BIBLIOGRAPHY (Continued)

12. Pake, G. E. and E. M. Parcell. "Line Shapes in Nuclear Paramagnetism." Physical Review, Vol. 74, (1948), pp. 1184-1188.

13. Wolf, A. V. "Body Water." Scientific American, Vol. 199, (1958), pp. 125-132.

14. Wishnia, A. "Proton Relaxation Times in Protein Complexes of Paramagnetic Ions." Journal of Chemical Physics, Vol. 32, (1960), pp. 871-875.

# A P P E N D I C E S

## APPENDIX A

### BEST FIT ANALYSIS. METHOD FOR FITTING THE SUM OF TWO EXPONENTIALS TO A NON-EXPONENTIAL CURVE[1]

The forms for the sum of two exponentials which are possible are:

for the $T_2$ decay,

$$M(t) = L_2 e^{-t_d/{}^1T_2} + S_2 e^{-t_d/{}^sT_2} \tag{A.1}$$

and for the $T_1$ relaxation,

$$\pm \left[M_\infty - M(t)\right] = L_1 e^{-t_p/{}^1T_1} + S_1 e^{-t_p/{}^sT_1} \tag{A.2}$$

The definitions of the symbols in equation A.1 are:

$M(t)$ = the transverse component of the relaxing magnitization,

${}^1T_2$ = the longer of the two transverse relaxation times,

${}^sT_2$ = the shorter of the two transverse relaxation times,

$L_2$ = the initial value of the magnitization component corresponding to ${}^1T_2$,

$S_2$ = the initial value of the magnetization component corresponding to ${}^sT_2$.

The definitions of the symbols in equation A.2 are:

---

[1]This method may only be applied when either ${}^1T_2 \gg {}^sT_2$ or ${}^1T_1 \gg {}^sT_1$.

$M_\infty$ = the Curie value of the magnetization component parallel to the polarizing field,

$M(t)$ = the component of the relaxing magnetization parallel to the polarizing field,

${}^{l}T_1$ = the longer of the two longitudinal relaxation times,

${}^{s}T_1$ = the shorter of the two longitudinal relaxation times,

$L_1$ = the Curie value of the magnetization component corresponding to ${}^{l}T_1$.

$S_1$ = the Curie value of the magnetization component corresponding to ${}^{s}T_1$.

Each of the equations, A.1 and A.2, will now be normalized. Thus, equation A.1 becomes:

$$\text{A.3)} \qquad \frac{M(t)}{L_2 + S_2} = M_n(t) = f_l e^{-t_d/{}^{l}T_2} + f_s e^{-t_d/{}^{s}T_2}$$

where

$$f_l = \frac{L_2}{L_2 + S_2}$$

$$f_s = \frac{S_2}{L_2 + S_2} .$$

The equation A.2 becomes:

$$\text{A.4)} \qquad \frac{\pm\left[M_\infty - M(t)\right]}{L_1 + S_1} = \pm \left[M_\infty - M(t)\right]_n$$

$$\pm\left[M_\infty - M(t)\right]_n = f_l e^{-t_p/{}^l T_1} + f_s e^{-t_p/{}^s T_1}$$

where

$$f_l = \frac{L_1}{L_1 + S_1}$$

$$f_s = \frac{S_1}{L_1 + S_1}$$

The problem now is to determine graphically the four parameters which occur for each possible form. It may help to look at Figure 34 as the method is explained to help visualize the mechanics of the technique.

The initial trial is made by attempting to draw a line asymptotically to the "tail" portion of the curve; the "tail" being that portion of the graph for which the signal is small. This straight line is then subtracted from the data curve. If the technique is performed correctly the line which emerges from the subtraction should also be straight, as is seen from Figure 34.

Usually the first attempt will not yield the second line as straight, so the process is repeated by adjusting the "tail" line according to its placing and its slope until the "subtracted line" becomes straight. When this occurs, the slopes of the two lines correspond to the relaxation times of the two components and the extrapolations of the line $t = 0$ yields the relative amounts of signal from each of the components.

Without proof, it is thought that the relaxation times are found with more precision than the fractional values of the signal components.

It should be noted that the curve in Figure 34 is ideally suited

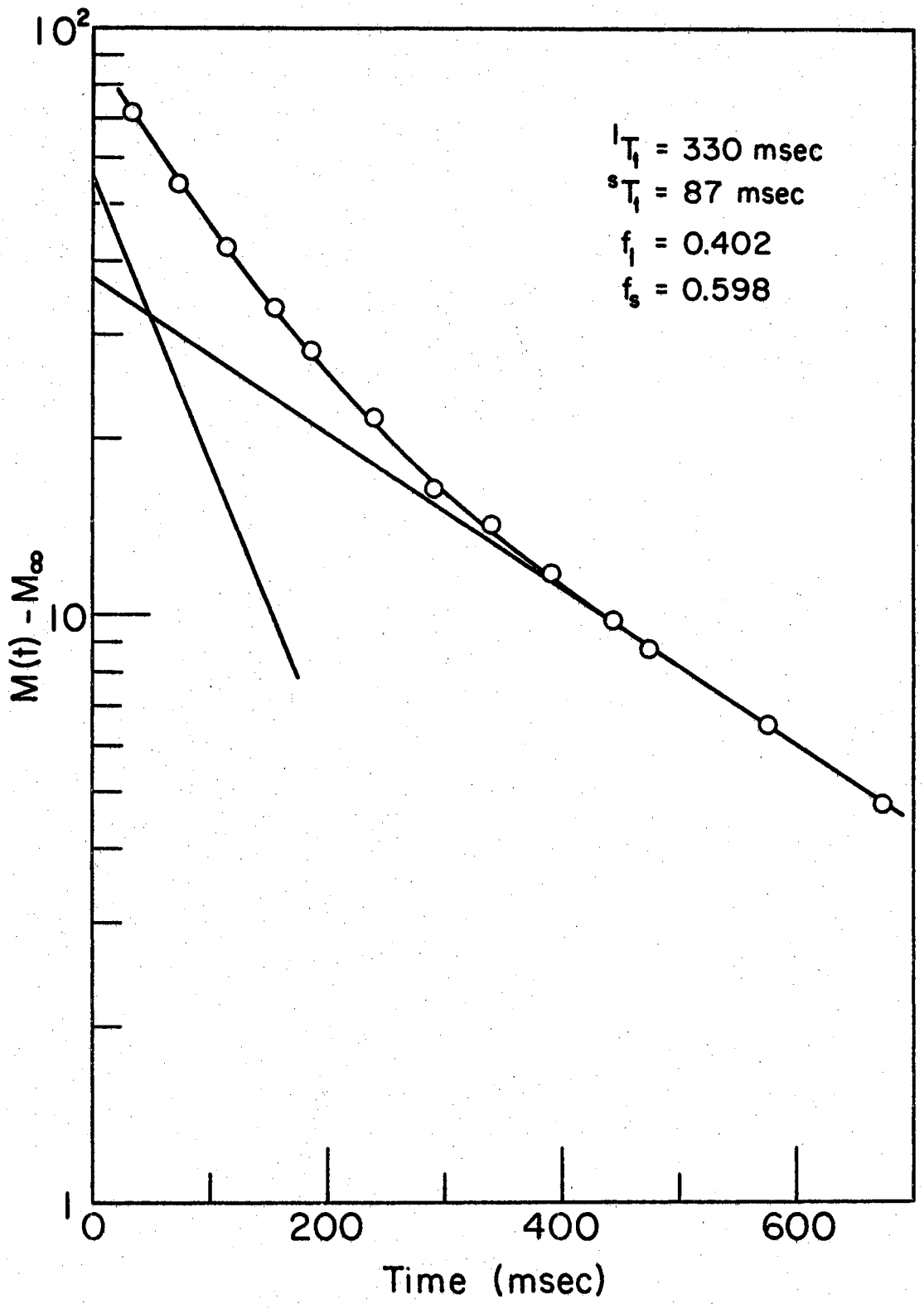


Figure 34. Graph of $T_1$ Data at B = 6.5 Gauss for Beef Fat

for this analysis because the "tail" portion is so well defined. However, for most of the data obtained the "tail" is still curving or not accurately determined because of the scatter of points. This adds more difficulty to the method and certainly more error to the results.

## APPENDIX B

### STUDY OF THE GRAPHICAL "BEST FIT" METHOD OF ANALYSIS

To determine what sort of errors in the fitting parameters ($f_l$,$f_s$, $^{l}T_1$, $^{s}T_1$, $^{l}T_2$, $^{s}T_2$) are caused by the application of the "best fit" method to the data, the following simple method was used: A curve which is actually the sum of two exponentials was constructed from a set of known values for the fitting parameters, then the "best fit" method was applied to determine them.

The values of $^{l}T_1$ and $^{s}T_1$ used in constructing the "known parameters" equations are ones which correspond somewhat to values which had been obtained for particular fields. In most cases, $f_l = 0.6$ and $f_s = 0.4$ were used.

A tabulation of the results are given in Table XI. The general trends shown by this analysis are:

1) $^{l}T_1$ and $^{s}T_1$ obtained graphically are found to be always shorter than the known values, with the $^{l}T_1$ value slightly more accurate;

2) $f_L$ is, generally, determined graphically to be larger than the known value (and thus $f_s$ is smaller.) In the one instance in which $f_L$ determined graphically was not greater than the known $f_L$ value, the two values were equal.

TABLE XI

EFFECTS OF BEST FIT ANALYSIS

| | Values of Known Parameters | Parameters Found By Best Fit Method | Difference Between Values (Known Minus Found) | % Deviation |
|---|---|---|---|---|
| $^{l}T_1$ = | 370 | 345 | + 30 | 8.1 |
| $^{s}T_1$ = | 125 | 115 | + 10 | 8.0 |
| $f_1$ = | 0.35 | 0.42 | - 0.07 | 20 |
| $^{l}T_1$ = | 240 | 182 | + 58 | 24.2 |
| $^{s}T_1$ = | 68 | 49 | + 19 | 28.0 |
| $f_1$ = | 0.6 | 0.8 | - 0.2 | 33.3 |
| $^{l}T_1$ = | 250 | 191 | + 59 | 23.6 |
| $^{s}T_1$ = | 78 | 55 | + 23 | 29.5 |
| $f_1$ = | 0.6 | 0.8 | - 0.2 | 33.3 |
| $^{l}T_1$ = | 590 | 590 | 0 | 0.0 |
| $^{s}T_1$ = | 215 | 205 | + 10 | 4.6 |
| $f_2$ = | 0.6 | 0.6 | 0 | 0.0 |
| $^{l}T_1$ = | 150 | 132 | + 18 | 12.0 |
| $^{s}T_1$ = | 42 | 34 | + 8 | 19.0 |
| $f_2$ = | 0.2 | 0.231 | - 0.031 | 15.5 |

## APPENDIX C

### METHOD FOR CORRELATING DATA FROM COILS #1 AND COILS #2

Beginning with the equations which have been hypothesized to describe the signal observed[1],

$$M(t)_H = A_H e^{-t/T_{2A}} + B_H e^{-t/T_{2B}}$$

and

$$M(t)_L = A_L e^{-t/T_{2A}} + B_L e^{-t/T_{2B}}$$

where the subscripts H and L refer, respectively, to a high Q set of coils and a low Q set of coils, and A and B are the initial values of the two components of the magnetization, it can be seen from Figure 35 that $\log M(t_i)_H - \log M(t_i)_L = \log C$ (the index i meaning for any value of t, and C is a constant). If this is true, then $M(t)_H$ equals $CM(t)_L$. In turn, this equation requires that $A_H/A_L = B_H/B_L = C$. Thus, the constant C may be evaluated by the ratio $A_H/A_L$. $A_H$ equals the gain of the system ($G_H$) times the magnetization of the A component of the sample ($A_{Hc}$); then $A_H = G_H A_{Hc}$. Further, $A_{Hc}$ is the Curie value and is proportional to the magnetizing field $B_H$ produced by the coil

---

[1]The shape of the signal is actually irrelevant to the matching procedure. However, the above equations for M(t) were used to make the method seem more closely related to the problem of fitting the sum of two exponentials to the data.

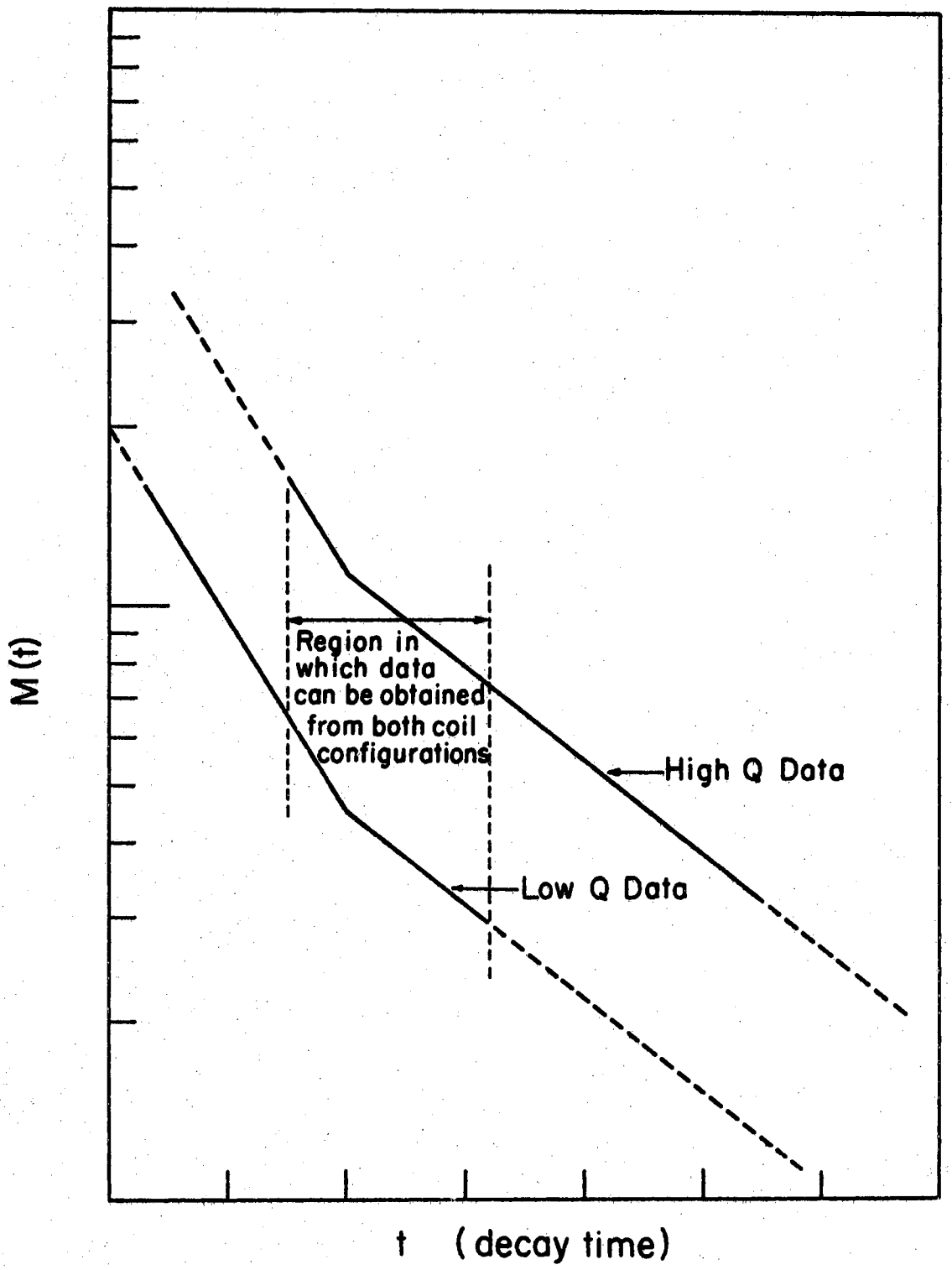


Figure 35. Hypothetical Graphs of Log M(t) Versus Time for High Q and Low Q Coils.

before the coil current is cut off, i.e., $A_{Hc} = pB_H$, where p is the constant of proportionality found from the Curie Law. By putting the value obtained for $A_{Hc}$ in the equation for $A_H$, the following equation is obtained:

$$A_H = pG_HB_H$$

Performing a similar analysis $A_L$ can be found to be: $A_L = pG_LB_L$. Thus, the value of C correlating the values obtained by one coil system with another can be calculated:

$$C = \frac{A_H}{A_L} = \frac{pG_HB_H}{pG_LB_L} = \frac{G_H}{G_L}\ \frac{B_H}{B_L}$$

Unfortunately, the factor C calculated in this way did not correctly match up the different parts of the decay. The reasons for this are not understood. Therefore, another method to calculate the correlation constant was sought.

Returning to Figure 35 and noting again that $\log M(t_i)_H - \log M(t_i)_L = \log C$; i.e., $M(t)_H = CM(t)_L$. It can also be seen that there is an overlapping region for which data is obtained using both the high Q and low Q coils. Thus, C, the correlating factor can be obtained by finding the ratios of $M(t)_H$ to $M(t)_L$ for the particular values of t which are in the region of overlap.

The accuracy of this method is determined by the variance of C's calculated for each of the corresponding points. When the C's were calculated the variance was found not to be large. So, this method was used to adjust the data.

## APPENDIX D

### METHOD FOR CONSTRUCTION OF A PROPER SIZED LORENTZIAN LINE SHAPE

To construct the proper sized Lorentzian line shape, a scale was arbitrarily assigned for the dimensions of the actual absorption curve. This was performed as seen in Figure 19. The following quantities were then measured:

amplitude at resonance frequency - - - - - - - - - - - - - - - 55.6

integral amplitude, measured using the same scale as the spectra amplitude- - - - - - - - - - - - - - - - - - - - - - - 81

$w'_o$ - w' in the abritrary unit scale at half maximum- - - - 3.5

Now, using the Lorentzian line shape,

$$F(w) = \frac{A}{B + C(w'_o - w')^2},$$

the parameters A, B, C, and w in some form, were evaluated using the measurements in the preceeding paragraph. Let F(w) be evaluated at $w_o$, the resonance frequency,

D.1) $$F(w)\Big|_{w = w_o} = A/B = H;$$

This is the quantity 55.6.

To evaluate the integral of the curve the line shape needs to be integrated over the whole spectrum of frequencies:

$$D.2) \qquad I = \int_{-\infty}^{\infty} F(w')dw' = \int_{-\infty}^{\infty} \frac{A/C}{B/C + (w_o' - w')^2}\, dw$$

$$= \pi \sqrt{\frac{A^2}{BC}}$$

This is the quantity 81.

Squaring both sides of equation D.2, the equation can be obtained:

$$I^2 = \pi 2 \frac{A^2}{BC} .$$

From this equation and equation D.1 an expression for A can be found to be:

$$D.3) \qquad A = \frac{I^2}{\pi^2 H} C,$$

and thus

$$\frac{A}{C} = \frac{I^2}{\pi^2 H} .$$

A/C may now be calculated from the measured quantities using the above equation:

$$\frac{A}{C} = \frac{(81)^2}{\pi^2 (55.6)} = 11.75.$$

From equations D.1 and D.3 an expression for B can be derived to be:

$$B = \frac{A}{H} = \left(\frac{I}{\pi H}\right)^2 C.$$

The quantity B/C may now be calculated form the preceeding equation and the known quantites as follows:

$$\frac{B}{C} = \left[\frac{81}{\pi(55.6)}\right]^2 = 0.215.$$

The last problem to consider is the proper scaling of the w units. For simplicity in notation the quantity $(w'_o - w')$ is redefined to be $\theta$. is then evaluated at the half maximum points by the following technique. The Lorentzian shape evaluated at half-maximum is written:

$$\tfrac{1}{2} F(w) \Big|_{w' = w'_o} = \frac{A}{B + C\theta^2} .$$

From equation D.1 it is thus seen that:

$$\tfrac{1}{2} \frac{A}{B} = \tfrac{1}{2}H = \frac{A}{B + C\theta^2} .$$

Dividing the right side of the above equation by C/C the equation

$$\tfrac{1}{2}H = \frac{A/C}{B/C + \theta^2}$$

can be obtained. This allows the mathematical expressions obtained previously for A/C and B/C to be substituted directly into the equation with the following result:

$$\tfrac{1}{2}H = \frac{(I^2/\pi^2 H)}{(I/\pi H)^2 + \theta^2} .$$

The above expression solved for $\theta$ is:

D.4) $$|\theta| = \frac{I}{\pi H} .$$

From the equation D.4 and the known quantities $|\theta|$ is then calculated at

the half-maximum points to be:

$$|\theta| = \frac{81}{(55.6)} = 0.464.$$

The arbitrary scale w's are then properly scaled when multiplied by the ratio

$$\frac{|\theta|}{(w'_o - w') @ \frac{1}{2} \text{ max.}} = \frac{0.464}{3.5} = 0.135.$$

The properly scaled Lorentzian curve for the absorption curve (Figure 19) has therefore been calculated to be:

$$F(w) = \frac{11.75}{0.215 + w^2}, \quad \text{where } w = (0.135)\, w'.$$

VITA

Walter Hayward Lipke

Candidate for the Degree of

Master of Science

Thesis: NMR STUDIES OF HUMAN AND BEEF TISSUES

Major Field: Physics

Biographical:

Personal Data: Born in Wichita, Kansas, September 10, 1942, the son of Mr. and Mrs. H. E. Lipke.

Education: Graduated from Will Rogers High School, Tulsa, Oklahoma, in May, 1960; attended University of Tulsa, 1960-1964; received Bachelor of Science degree in 1964 with a major in Physics.

Professional Experience: Project Engineer, O.C.A.M.A., Tinker A.F.B., 1964-1965 and Summer 1966; graduate teaching assistant, Physics Department 1965-1967; physics tutor for engineering tutoring service, Spring 1967; graduate research assistant, 1967-1968.

Organizations: Member of Sigma Pi Sigma.